I.O.S.

ASSESSMENT OF WAVE POWER AVAILABLE AT KEY UNITED KINGDOM SITES

BY

J.A. CRABB

REPORT NO. 186
1984

NATURAL ENVIRONMENT RESEARCH COUNCIL

INSTITUTE OF OCEANOGRAPHIC SCIENCES

INSTITUTE OF OCEANOGRAPHIC SCIENCES

Wormley, Godalming,
Surrey, GU8 5UB.
(0428 - 79 - 4141)

(Director: Dr. A.S. Laughton FRS)

Bidston Observatory,
Birkenhead,
Merseyside, L43 7RA.
(051 - 653 - 8633)

(Assistant Director: Dr D.E. Cartwright FRS)

Crossway,
Taunton,
Somerset, TA1 2DW.
(0823 - 86211)

(Assistant Director: M.J. Tucker)

When citing this document in a bibliography the reference should be given as follows:

CRABB, J.A. 1984 Assessment of wave power available at key United Kingdom sites: a description of work in the Department of Energy's Wave Energy Programme. *Institute of Oceanographic Sciences, Report*, No. 186, 113pp.

INSTITUTE OF OCEANOGRAPHIC SCIENCES

TAUNTON

Assessment of wave power available at key United Kingdom sites

A description of work undertaken in the Department of Energy's Wave Energy Programme

by

J.A. Crabb

I.O.S. Report No. 186

1984

Contents

INTRODUCTION

Early enthusiasm for the utilization of wave power for the generation of electricity centred largely on attractively high estimates of wave power availability in the mid-North Atlantic. These estimates (Salter (1974), Mollison et al (1976)) were based on wave data, in the form of significant wave heights and mean zero crossing periods, measured at OWS India; they were in the range 77-91 kW m^{-1} annual average power. These initial figures served to put some scale on the potential but they represented no more than an upper limit to the power available closer to the Scottish coast; more reliable information on power at coastal sites of particular interest was not available. A programme of wave measurement was initiated to fill this gap. Whilst, however, information on overall power could be obtained relatively readily by measurement, information on the directional distribution of the power could not - there being at that time no suitable ocean-going system for its routine measurement.

Directional information was recognized at the outset as being of importance, both for the accurate assessment of available power and for detailed design and determination of the forces experienced by devices. It was therefore necessary to make some estimate of this wave property prior to any measured data which might be collected becoming available.

Much of the work for providing information on wave climate was conducted by the Institute of Oceanographic Sciences under contract to the Department of Energy as part of the much larger Wave Energy Research Programme.

This report provides a succinct description of the work performed by IOS and a summary of results obtained. Also included is a description of new work in which all available information has been used to produce a final assessment of the wave power available at a number of key sites. Extensive use has been made of results from the Meteorological Office wind-wave model in this assessment.

The report has been structured in the following way. Descriptions of the various items of past work are given in subsections of the first part of the report, whilst the new work is reported in the second section. Most of the detailed descriptions of procedures employed appear in a series of appendices so as not to interrupt the flow of the general account.

Some use has been made of information resulting from measurement programmes sponsored by the United Kingdom Offshore Operators' Association; these data and results obtained from them have been presented together in a final appendix to which reference is made at appropriate points in the text.

1a The measurement programme

All of the wave measurements made specifically for the Wave Energy programme were obtained using Datawell Waverider buoys. Some use was also made of data from shipborne wave recorders installed on light vessels, as well as from other Waveriders installed for other programmes. The principle of operation of both these instruments is explained in Appendix A, and a full account of the analysis employed to obtain information on wave power from the data is given. It is sufficient to note here that both instruments give information only on the vertical displacement of the sea surface at a point, and yield no information on the direction of wave approach. The main products of the analysis are values of the significant wave height Hs, the mean zero-crossing period Tz, and the energy period Te. The spectrum of energy flux is also calculated, and this, when integrated over all wave frequencies, gives the average energy flux per unit length of wave crest. This is usually expressed in units of kW m^{-1} and is the power per metre of wave front. This quantity is referred to simply as power throughout this report.

The map of Figure 1 shows sites at which measurements have been made for the Wave Energy programme, as well as other sites from which data have also been used. Brief details of the measurement sites and the approximate durations of the measurements at each are shown in Table 1. The percentage of valid data obtained at each site is shown in Table 2a, and a general picture of data availability is presented in the bar chart of Table 2b. It is important to realize that this measurement programme was not planned in its entirety at the outset. It was initiated by the somewhat speculative deployment of the South Uist 45 m buoy and later augmented to provide more detailed information at this site, and to give some indication of wave power at other sites. In the light of experience, a more effective programme could now be designed for immediate implementation.

Site	Water depth	Instrument	Sponsor	Contractor	deployment start	deployment finish
Foula	160 m	WR	UKOOA	IOS/MAREX	Dec 76	Nov 79
S Uist	45 m	WR	PED	IOS	Mar 76	Apr 83
S Uist	100 m	WR	WESC	IOS	Aug 80	ongoing
S Uist	23 m	WR	WESC	IOS	Aug 79	July 82
S Uist	15 m	WR	WESC	IOS	Jun 78	Aug 79
Butt of Lewis	80 m	WR	WESC	NMI	Jan 79	May 80
St Gowan	49 m	SBWR	PED	IOS	Aug 74	ongoing
Sevenstones	60 m	SBWR	PED	IOS	Apr 75	ongoing
Scilly Isles	100 m	WR	WESC	IOS	Feb 80	ongoing
Berwick on T	80 m	WR	WESC	NMI	Jan 79	Mar 82
Kinnairds Hd	88 m	WR	WESC	IOS	Feb 80	Mar 82

Table 1 Site programme details

key

WR	Waverider buoy
SBWR	Shipborne wave recorder
IOS	Institute of Oceanographic Sciences
NMI	National Maritime Institute
PED	Petroleum Engineering Division, Department of Energy
UKOOA	United Kingdom Offshore Operations Association
WESC	Wave Energy Steering Committee

Site/Year	1976	1977	1978	1979	1980	1981	1982
Foula		65	32	21			
S Uist (45 m)	96	90	48	52	58	67	80
S Uist (100 m)					67	89	89
S Uist (15/23 m)				61	74	78	86
Butt of Lewis				6	5		
St Gowan	57	87	94	76	39	83	56
Sevenstones	98	99	66	94	99	74	97
Scilly Isles					70	77	95
Berwick on T				30			
Kinnairds Hd					32	77	31

Table 2a Percentage valid data returns

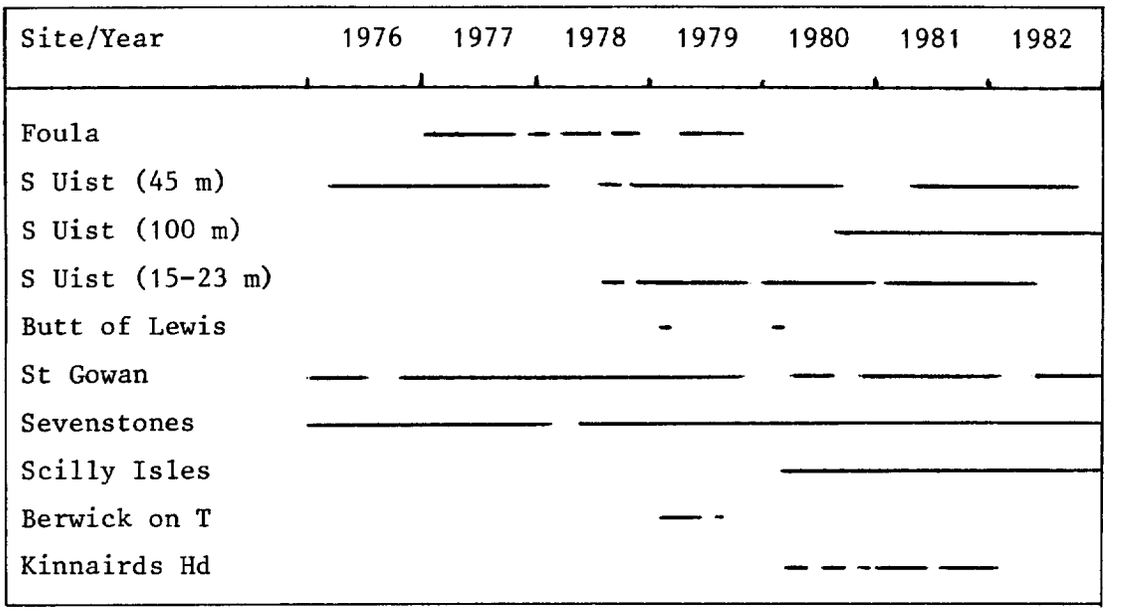

Table 2b Bar chart of valid data returns (approximate)

Most of the data sets obtained from the Waverider installations are disappointingly incomplete. A study has been made of the reasons for data loss at the S Uist 45 m site and the effect of the loss on measured average power has been assessed. This is reported on in Appendix B.

1b Prediction of annual average power

The potential wave energy resource is most readily summarized in a single figure for the annual average power to be expected over many years. This figure was obviously required early in the programme and, therefore, the majority of data now available could not be used in its estimation. Moreover, the fragmentary nature of the additional data series does not allow a meaningful direct calculation of the annual average power to be made; this problem is discussed in Appendix B and addressed in detail in Section 2.

It was necessary, therefore, to attempt a prediction of the long term annual average power on the basis of a relatively short time series of available data. This was first attempted for the South Uist 45 m site at a time when just one year's spectral data had been collected. This series covered the period March 1976 to February 1977, and was 94% complete. In addition to these wave data, wind data from two land-based stations were available.

A method was developed which avoided the bias inherent in just one year's wave recordings. Each wave record was associated with the values of wind speed and direction measured at the same time at a nearby meteorological station. A number of wave records was then chosen. The distribution of the wind speeds and directions associated with the chosen records was as close as possible to the distribution obtained from many years of wind recordings. A subset of wave recordings was compiled by this method within which, it was hoped, the distribution of locally generated seas has been adjusted directly towards the long term average, and the population of swell occurrences had been drawn at random from throughout the year. A detailed description of the procedure is given in Appendix C.

The 399 wave spectra selected by this procedure are taken as providing a summary of the characteristics of the long term average wave climate at the site. In particular, the average power of the subset spectra is taken as an estimate of the long term average annual power. At South Uist 45 m this figure is 47.8 kW m^{-1}

which compares with an average power of 35.6 kW m^{-1} for the year of data from which the selection was made. An adjustment in this direction was expected as the year March 1976 to February 1977 was a period of lower than average wind activity. The mean spectrum of power for both the selected set, and for the year's measured data are shown in Figure 2.

Mollison (1977, 1979) has made a separate attempt to predict the annual average power at this site. He uses the available wind data to establish the values of parameters in a model relating wind speed to wave power. The average annual wave power is then calculated from the long term wind data. The result for this method, and for a later modification, is very close to 50.0 kW m^{-1}.

The IOS method has been adapted and used on data from the St Gowan shipborne wave recorder (Crisp 1980) and the Foula waverider (Scott and Crabb 1981). Details of the modified procedure necessary to deal with the shipborne wave recorder at St Gowan are given in Appendix C.

The resulting prediction of annual average power at St Gowan was 15.7 kW m^{-1}. The corresponding value for Foula is reported in Appendix G.

1c Synthesis of directional properties

A full assessment of the available power cannot be made without regard to the directional distribution of power. Information on the directional composition of the sea is also important in that forces experienced by devices may depend critically upon its nature. Unfortunately, at the time such information was required, no measurements were available. In recognition of this lack of crucial information, an attempt was made to estimate the directional properties of waves at South Uist. It was expected that this interim information would be superseded by measured data. These data were, however, much delayed in coming and the estimated directional properties have been used throughout the wave power programme.

The basic data comprise the set of 399 selected spectra, to which has been added information on the directional properties of each spectrum. These were estimated from a consideration of the meteorological conditions pertaining at the time of each selected spectrum. As the directional properties of locally generated sea and swell waves are generally different, it was first necessary to divide each

spectrum into regions corresponding to these two wave types. Directional properties were then ascribed separately to each. In the case of the wind sea region this was accomplished by reference to an empirical formulation relating the directional characteristics of the waves to the local wind speed. In the case of swell waves, directional characteristics were determined from a consideration of the distance and size of the wind field responsible for their generation. The two regions of the spectrum were finally recombined to produce the estimated directional spectrum.

The procedure is described in detail in Appendix D.

The properties of the 399 directional spectra are taken as indicators of the main features of the directional wave climate. The mean directional power spectrum is shown in Figure 3; the peak frequency is 0.074 Hz and the peak direction 260°. The distribution of power with direction alone, shown in Figure 4, emphasizes the relative narrowness of the directional distribution at this site. Calculations of power separately for the wind sea and swell regions identified during the synthesis procedure indicated that greater than 60% of the energy arriving annually at the site is associated with swell - hence the low frequency peak and the narrow directional distribution.

The effect of the directional distribution on the power available to a line of seaward facing devices is summarized in the directionality factor. This indicates the proportion of the total power which is crossing the line and is thus defined

$$\text{directionality factor} = \frac{\int_{\theta = \bar{\theta} - \frac{\pi}{2}}^{\bar{\theta} + \frac{\pi}{2}} P(\theta)\, \cos(\theta - \bar{\theta}) d\theta}{\int_{0}^{2\pi} P(\theta)\, d\theta} \qquad (1)$$

where $P(\theta)$ is spectral density of power approaching from direction θ

$\bar{\theta}$ is direction towards which device faces

The directionality factor is thus a function of $P(\theta)$ and $\bar{\theta}$; the orientation of the device would normally be chosen such that the resulting value of $\bar{\theta}$ produced the maximum directionality factor. The product of directionality factor and total power gives the total power resolved in direction $\bar{\theta}$.

The directionality factor for the estimated South Uist (45 m) climate is 0.82, and the 'best' direction 260°.

Information on the directional properties of waves at other sites is also available from the archive of the Meteorological wave forecasting model results. These data are used extensively in Section 2. In addition the National Maritime Institute has developed a separate method for the synthesis of wave climate (Hogben 1978) and has produced predictions for Station Fitzroy.

1d Checking the directional synthesis

At the time that the need for information on wave direction was first identified, it was envisaged that quantities derived from the directional spectrum would be of primary interest. Chief amongst these was the mean crest length, that is to say the average distance between surface crossings of the mean water level along a line perpendicular to the principle wave direction. Much interest was expressed in this quantity by some device teams as it has implications on the expected value of bending moment experienced by long floating bodies. In the event it proved difficult to agree on a definition of this quantity which corresponded both to a statistically stable and meaningful parameter of sea state and embodied the necessary engineering information. It is inappropriate here to reproduce an account of the derivation of this quantity; this would not in any case approach the clarity of the original account given by Longuet-Higgins (1957). It is sufficient to note that the value of the mean crest length depends upon the second moment of the two dimensional wave number spectrum. This, since wave number is proportional to frequency squared, implies that the fourth moment of the frequency spectrum is involved which, for a spectrum decaying as f^{-5}, is not convergent. Consequently the value calculated for the mean crest length depends strongly on the choice of upper integration limit; this is at the heart of the definition difficulty mentioned above.

It was keenly realized that there could be little confidence in a process involving the estimation of directional wave properties and the calculation of derived properties without some evidence for its efficacy. An experiment was therefore conducted, the primary objective of which was to measure directly the mean crest length in a real sea, and compare this with a predicted value calculated using a directional spectrum synthesized for this purpose. Thus it was expected that, at one and the same time, the synthesis method and the theoretical derivation of the mean crest length could be checked. Meanwhile, however, priorities for the use of the directional spectrum were changing and, in retrospect, an experiment to test more directly the similarity between synthesized and measured

directional spectra would have been more appropriate.

The experiment actually conducted involved measurement of the sea surface elevation profile along a line flown by a fast moving aircraft trailing a radar altimeter in an aerodynamic body towed close to the sea surface. The finite speed of the waves meant that the mean crest length could not reliably be calculated from the recorded profile time history, as a reliable relationship between distance on the sea surface and elapsed time could not be established. This, combined with the difficulty mentioned above, lead to the abandonment of the mean crest length as the primary test quantity. Instead, the record of the rapid variations of sea surface elevation obtained during each aircraft run was Fourier transformed to produce the so-called encounter spectrum. These calculated spectra were then campared with the same quantity predicted from a transformation (Appendix E) of the directional spectrum synthesized for the time of the measurements. A Waverider, specially placed to the West of the Scilly Isles for the experiment, provided the source wave data for the directional spectrum synthesis.

A detailed description of the experiment and its results was produced at the time and this is reproduced in an abbreviated form as Appendix E. The main point to emerge was that the primary experiment did not effect satisfactory testing of the synthesis procedure. There were two main reasons for this: firstly the encounter spectrum did not prove to be very sensitive to changes in the form of the directional spectrum and, secondly, no significant swell energy was observed during the experiment, thus leaving the ability of the synthesis procedure to account accurately for swell untested. In addition the measurement method was not without problems as it transpired that spurious variations in sea surface elevation caused by fluctuations in the height of the altimeter could not be completely removed from the record.

The main conclusions on the reliability of the synthesis method were drawn from a comparison of the directional spectra synthesized for the Scilly Isles experiment with those measured at the DB1 location. This could not be entirely satisfactory since the two sites were separated by approximately 260 km. There existed a broad agreement between simple parameters of the directional spectra as synthesized and as measured. The best agreement was between the mean wave directions at each frequency, whilst the synthesized spectra tended to predict narrower directional distributions than those measured. It is not clear that this latter discrepancy

was solely a fault with the synthesis procedure.

The strongest reason for believing that the overall properties of the 399 synthesized directional spectra give a reasonably accurate picture of what might be expected to be the wave climate at the site lies in the restrictions built into the procedure. These include the facts that the spectra are based on actual measurements and that the whole thrust of the procedure was towards ensuring that the predicted wave conditions were in sensible conformity with the prevailing meteorological conditions. Whilst this may not have resulted in precise agreement between synthesized and measured spectra (had they been available) on each occasion, it appears unlikely that on average any seriously anomalous features could have been built into the picture by this process. Comparisons with the directional results of the Meteorological Office wave model conducted at the time, and since as reported in Section 2, show sufficiently close agreement to support this contention. It is very unfortunate that the measured directional spectra which it was always expected would supersede these estimates were never forthcoming.

1e Extracting a working set of spectra

Production of the set of 399 directional spectra was not, in itself, a solution to the problem of determining the productivity of wave power devices. The individual spectra departed significantly in form from that of the mean spectrum, being in general unimodal in neither frequency nordirection. In some cases devices were non-linear in that their response to changes in one aspect of sea state are not independent of the values adopted simultaneously by other parameters. The overall expected output could only, therefore, be determined in tank or numerical experiments by measuring the response of a device to each spectrum in turn and calculating an average output. This approach was impracticable with such a large number of spectra, especially as such a series of tests might have to be repeated many times to assess the effect of changes in design parameters. There was an urgent need for the essential information on the distribution of wave properties to be more succintly presented. This was attempted, and resulted in the selection of a smaller number of spectra which, in most important respects, summarized the properties of the 399.

The basic premise is that, in any large set of directional spectra, it should be possible to identify groups of spectra which, in a number of respects, are similar in form. It is then supposed that it is unnecessary to include all the members

of such a group in the final set, but that a group may be represented by just one of its members. The relative importance to be attached to such a spectrum is indicated by a weighting factor equal to the number of members in the group which it represents.

It was initially necessary to define a number of parameters which would allow concise characterization of each spectrum. These parameters were chosen both as summaries of spectral shape, and in the expectation that they described aspects of the sea state which could affect device performance. Definitions of the chosen parameters are given below.

P, total power - the total wave power integrated over all frequency and direction

Te, energy period - period defined as m_{-1}/m_o (see Equation A.15)

FW, frequency width - the frequency interval within which 80% of the total power is found; excludes the two 10% portions of power at the highest and lowest frequencies

DW, directional width - angular interval within which 80% of the power in the 80% frequency interval is found; excludes the two 10% portions of power found immediately north and south of due east

DP, peak direction - the direction associated with the peak of the directional power spectrum.

These parameters, especially those describing the spectral width, are simple and directly interpretable quantities. It would undoubtedly be possible to define other parameters which optimally summarized spectral properties for other applications.

The values of these parameters were determined for each of the 399 spectra and the spectra sorted into classes accordingly. A detailed description of the procedure employed is presented in Appendix F. It proved impossible to represent all occupied classes and at the same time effect a significant reduction in the number of spectra required to represent the wave climate. Attention was therefore focussed on the classes of spectra describing the conditions under which the majority of the energy was transported to the site. It was finally possible to produce a set of 46 spectra against which device productivity could

be determined.

The need to produce this 'working set' of spectra highlights the difficulties generally experienced in seeking to use measured wave data in engineering design. The raw data are too voluminous for direct application, but there are, as yet, no widely accepted procedures whereby the information may be condensed for effective application. The problem is most severe for measured (or estimated) directional spectra. The pragmatic approach adopted in this case may be capable of extension to more general use; the key to this would be a carefully devised set of parameter definitions to allow a succinct description of each directional spectrum. Any future measurement program would then be aimed at determining the joint statistics of occurrences of these parameters. This would allow the important features of the climate to be represented by a relatively small number of carefully chosen spectra, or allow reconstruction of model spectra to the same end.

1f Geographic variation of power near South Uist

The South Uist area, being the original focus of interest, was studied in much greater detail than other sites. In particular the question of the variability of the available wave power with distance from the shore, and thus with water depth, was addressed. The basic data necessary for this assessment were obtained by making relatively short series of measurements simultaneous with the continuing measurements at the 45 metre location. It was then possible to establish the relationship between the powers at each location and that at the 45 m buoy. Predictions for the long term average power at each site could then be made by appropriate scaling of the 47.8 kW m^{-1} figure predicted for the 45 m buoy. A detailed record of buoy deployments at the South Uist site is set out below.

Site	Depth	Deployment dates
Offshore	45 m	March 1976 to April 1983
Nearshore 1	15	June 1978 to August 1979
Nearshore 2	23	August 1979 to January 1981
Nearshore 3	25	March 1981 to July 1982
Deepwater	100	August 1980 - ongoing at December 1983

The position of each site is shown on the map of Figure 11.

Relationships between the site powers were determined by regression analysis in the manner appropriate to allow scaling of the 45 m buoy result. The results of these analyses, based on all available data up to December 1982, are set out below.

Site	No of data points	Slope	Intercept (kW/m)	Correlation coefficient	Std error of slope	Std error of intercept
Nearshore 1	1051	0.27	2.38	0.910	0.004	0.18
Nearshore 2	1993	0.70	0.92	0.943	0.006	0.28
Nearshore 3	2858	0.71	-0.11	0.922	0.006	0.36
Deepwater	4012	1.41	-2.46	0.944	0.008	0.52

These figures, when applied to the predicted average power at the offshore site of 47.8 kW m^{-1}, result in the following predictions of long term average annual power at the other sites.

Nearshore 1 15.29 kW m^{-1}
Nearshore 2 34.38 kW m^{-1}
Nearshore 3 33.83 kW m^{-1}
Deepwater 64.94 kW m^{-1}

Standard errors due to the regression are very small (< 0.5 kW m^{-1}); it would be misleading to quote just these as the major uncertainty lies in the value of 47.8 kW m^{-1} from which the predictions are made. This uncertainty is not directly quantifiable.

The powers quoted are as derived from the directionally insensitive measurements and as such are misleading on their own. Waves approaching the shallower water of the coastal region suffer refraction which tends to turn their direction to be more normal to the beach. This in itself leads to a reduction in the overall measured power, but without there being any reduction in the shoreward component of energy flux. This phenomenon is illustrated in Figure 5, which shows the abrupt refraction of two wave normals at a contour line. The energy transported between normals is constant; prior to refraction this energy is distributed along the line AB, after refraction along CD. Since CD is longer than AB ($AB = CD \cos(\theta - \phi)$) the energy density, and thus the power per unit wavefront, decreases. The flux resolved in the shoreward direction remains constant as, both before and after refraction, the energy is distributed along AD.

This simple figure illustrates the mechanism, but in practice to predict the diminution of measured energy to be expected from this cause is very difficult. The refraction of a real directionally distributed sea over an uneven sea bed is complicated. Attempts have been made however, notably by Brampton and Bellamy (1982) of the Hydraulics Research Station, to reproduce the observed variations in power at the different locations by modelling the refraction of realistic seas over a sampled version of the actual contours. The main interest is in whether refraction alone can explain the observed variation, in which case no loss of shoreward power is implied, or whether a power loss mechanism such as friction must be supposed to be operating.

The general conclusion of the HRS study, although not subscribed to by all interested parties, is that for depths over approximately 25 m refraction is the chief cause of the observed power differences. At depths less than this a further mechanism of actual power loss becomes important. This conclusion is supported by results of some directional measurements presented by Ewing and Pitt (1982).

The picture could have been further clarified by directional wave measurements at the various sites. Knowledge of the directional distribution of power allows direct calculation of shoreward flux and the extent of actual power loss could be seen. There is a complicating factor, however, which is the alongshore variability of power due to the tendency of the local topography to focus or defocus energy; an average of conditions along a contour should ideally be considered.

A useful concept, already introduced in Section 1c, is that of the directionality factor which arises as follows.

If P_θ is the power, integrated over all frequency, which approaches from direction θ, then the shoreward component of flux is

$$P'_\theta = P_\theta \cos(\theta - \psi) \qquad (2)$$

where ψ is the bearing of the beach normal.

The total shoreward flux is obtained by summing components from all incident directions

$$P' = \sum_{\theta=-\frac{\pi}{2}}^{\frac{\pi}{2}} P_\theta \cos(\theta-\psi) \qquad (3)$$

when expressed as a fraction of the total power, P, it indicates the proportion of power available to a single-sided device placed parallel to the coast. Instead of the coast normal, a reference direction which maximizes this fraction may be calculated. This is the direction of the vector sum resultant of the individual P_θ's; it may be defined

$$\tan \phi = \frac{\sum_{\theta=0}^{2\pi} P_\theta \sin \theta}{\sum_{\theta=0}^{2\pi} P_\theta \cos \theta} \qquad (4)$$

Although the HRS study into power variability at the South Uist site has been the most extensive, other attempts have been made to shed light on the situation. It had been postulated that, in view of the very rugged and somewhat periodic nature of the sea bed, Figure 6, some coherent interference between the incoming waves and the bottom structure could be causing a backscattering of energy. An attempt was made to test this hypothesis (Ewing and Pitt 1982) by making a number of measurements with a directionally sensitive clover-leaf buoy. It was expected that the measurements would enable the presence of any backscattered energy to be revealed. Conditions at the time of the experiment saw a westerly swell of amplitude 2.5-3.0 m; no conclusive evidence for the presence of backscattered energy was obtained. As a separate point, the authors claimed that the measurements supported the view that most wave energy loss occurs in depths less than 24 m.

Pitt and Scott (1982) noted the variability in the ratio of instantaneous powers at the nearshore and offshore sites and postulated that this might be matched by a sensitivity in the measured power ratios to the direction of wave approach. Using the results of the Meteorological Office wave model to ascribe directions to the measured offshore waves, they plotted the dependency of power ratio on incident direction using ten weeks of data. The relationship obtained in this way did not agree with predictions made by refraction calculations over real (sampled) nor assumed parallel bathymetry; the measured power attenuation being always greater than that predicted by the latter.

Mollison (1982) seriously questions the conclusion, drawn from the HRS study, that negligible power loss occurs in water deeper than 23 m. He argues that reasonable assumptions of frictional loss coefficients would point to power losses of approximately 15% between water depths of 42 and 23 m. These levels of loss, he argues, are consistent with the measurements when the probable directional distribution of energy is taken into account. In particular Mollison rejects the HRS argument that the "total internal reflection" back to seaward of some incident energy may account for some of the observed discrepancies in power; he questions their methodology and considers frictional loss to be a more probable cause.

It will be clear from the foregoing that the question of the locational variability of wave power at South Uist was, at the time the argument was truncated by external circumstances, a matter of continuing debate. The issue is an important one for it has implications for the predicted yield of devices in all water depths.

One new complicating factor not known at the time of the original debate is the fact that, on latest predictions, power at the deepwater location is higher by 10% than had previously been supposed. The disparity between power at this site and that at 42 m requires an explanation.

Although it is not possible to resolve the argument here, it would appear that Mollison's contention that frictional loss must play a role at this site carries considerable force. The probability is, therefore, that further study would allow the discrepancies between gross powers at the various sites to be explained by a combination of refraction and frictional loss.

2a Final assessment of annual average power at key sites

Section 1b and Appendix C describe attempts to predict the long term annual average power at three sites - South Uist (45 m), Foula and St Gowan. The predictions were, of necessity, made on the basis of rather short measured time series and there must be uncertainty regarding their accuracy. Since these early predictions, however, further data have accumulated at each of the measurement sites and it is clearly desirable that these be used as a basis for more reliable estimates. This might be attempted in at least two ways. Firstly, a direct calculation of the measured annual average power may be attempted at sites where a sufficiently long and continuous time series of data has been accumulated. Secondly, the data may be used to establish the relationship between measurements and the results

of a wind-wave model: this approach is of value if the measured time series is short or fragmentary, and a long and continuous series of archived model results is available. Both methods are attempted in this section. Direct calculations of annual average power (adjusted for seasonal bias) have been attempted for the South Uist (45 m) and Sevenstones sites; whilst data from the Kinnairds Head, South Uist deepwater, Scilly Isles and DB1 sites have been correlated with the results of the Meteorological Office wind-wave model and used to scale the annual average power calculated from a complete four year time series of model results. Additionally the model results for the Foula site have also been averaged, but scaling by the measured results was not possible owing to there being insufficient overlap between the measured and model data series.

This is the first time that all measured data have been used to extend and improve on the original attempts to predict annual average power. The results are still, however, only based on four years model data for each site. Comparisons with the previous predictions are presented where possible.

Average of measured powers

The longest measured time series of waves has been that obtained at the original offshore (45 m) South Uist location where, by the end of 1982, the installation had been maintained for almost seven years. Unfortunately this series is far from complete as shown in the data return bar chart of Table 2b. A simple average of the power measured would be biased due to the apparent tendency to lose most data during the winter months. The data returns from the other sites are also shown in Table 2. In the case of the South Uist deepwater and Scilly Isles sites, the measurement series are more complete but shorter than that at the offshore buoy. Those at Kinnairds Head and Foula are both short and fragmentary.

In view of the length of the measured time series and of the importance of the site, an attempt has been made to average the data from the South Uist offshore buoy in a manner which avoids the most obvious bias due to missing data. All the data for each month of the year were averaged to produce twelve mean monthly power figures. The relative paucity of data for the winter months means that the averages for these months are based on fewer data and are thus less reliable than the others. Later in this section the annual average power calculated from these twelve monthly means is compared with the final estimated value for the location, thus allowing the magnitude of the bias inherent in the measured data to be estimated.

The monthly and annual averages presented in Table 3 have been calculated using different portions of the data series from March 1976 to December 1982 as follows:-

a) Using data from all months for which the valid data return was greater than 60%, but excluding the first year (March 1976 to February 1977)

b) As a) but including the first year

c) Using all the data without regard to data return

	a) mean power kW m^{-1}	b) mean power kW m^{-1}	c) mean power kW m^{-1}
January	55.2 (4)	53.3 (5)	58.0 (6)
February	56.4 (4)	50.9 (5)	59.7 (6)
March	65.5 (3)	73.0 (4)	73.4 (5)
April	34.6 (4)	36.2 (5)	35.2 (6)
May	15.0 (5)	16.9 (6)	16.9 (6)
June	13.8 (5)	15.9 (6)	15.2 (7)
July	12.8 (5)	12.3 (6)	12.6 (7)
August	18.2 (5)	16.7 (6)	16.7 (6)
September	41.9 (5)	37.1 (6)	34.5 (7)
October	61.6 (3)	55.6 (4)	56.4 (6)
November	87.7 (2)	82.1 (3)	90.0 (5)
December	39.4 (3)	39.5 (4)	51.8 (5)
ANNUAL MEAN	41.8	40.8	43.4

Table 3 South Uist offshore buoy

March 1976 - December 1982, means of monthly average wave power densities. Figures in brackets indicate the number of monthly means averaged to produce the tabulated figure.

It has been recognised that the year March 1976 to February 1977 was anomalously low in wind and wave energy, the table therefore offers the option of excluding it from consideration. Such anomalous years, both high and low in energy, contribute to the long term average of power, but it is perhaps not fair to include them in averages made over a few years only.

The credence to be placed on the annual mean figures as estimates of long term average power is difficult to assess in view of the unknown effect of missing data. This, combined with the fact that averages of the shorter data series from the other sites are not in any case reliable indicators of long term average conditions,

has led to a different approach to the use of the measured data.

The Meteorological Office wave model data has already played a part in climate assessment (Golding 1978). Its wide area coverage and almost 100% 'data return' have been attractive features, whilst the wave directional information which it produces is not available from any other source. However, the results of the model have yet to be fully checked against measurements at each site, and conclusions based on the model results alone are thus unreliable. The next section describes how all the measured data at each site have been correlated with the simultaneous model results at a nearby location. These comparisons allow the model data to be scaled and used as a more accurate indicator of actual conditions.

Correlation of measured and Meteorological Office model powers

The Meteorological Office wave model data cover the period 1 October 1978 to 26 September 1982. Data were obtained for grid points as close as possible to the Foula, South Uist deepwater, Kinnairds Head, Scilly Isles and DB1 wave measurement sites. The data were supplied in the form of directional energy (variance) spectra at 12 hour intervals throughout the period. In order to calculate the overall wave power on each occasion, the spectra were converted to spectra of energy flux density using the relationship of Equation A.8, and integrated over all frequency and direction.

A major drawback of the archived Meteorological Office data is the 12 hour sampling interval. This is too coarse to reproduce all the important features of the wave power time series. However, the precise effect on the average power calculated is not predictable.

In making the comparison between measured and model data considerable care was taken to ensure that the final set of power values for each site were truly simultaneous pairs (within ±2 hours), and included only measured data classed as valid by the IOS routine validation procedure. A regression analysis was performed on the data set from each site; the model powers were taken as the independent variable and the measured values as the dependent. The resultant regression curves may thus be used to predict from the average of the model powers, the average value of the measured power had the measured time series been as complete as that from the model. The regression results are shown in Table 4.

Site	No of data points	Slope b	intercept a kW m^{-1}	correlation coefficient r	Standard error in b	Standard error in a kW m^{-1}
Scilly Isles	1542	.868	5.95	.664	.025	1.33
S Uist (deep)	1297	.929	7.13	.673	.028	2.15
Kinnairds Head	832	.751	4.86	.757	.023	0.67
DB1	(Comparison reported in Appendix E)					

Table 4

There are several things to note. The regression curves have significant intercepts on the 'measured' axes. This is a consequence of the scatter in the data indicated by the low correlation coefficients. An analysis of variance, however, shows the regressions to be statistically highly significant. Thus the average properties of the model data may be used as indicators of average measured conditions (standard error of predictions made on this basis are stated in Table 5 below). However, scatter diagrams and distributions of the model data are not so reliable as indicators since they display the full scatter evident in the relationship between the data sets.

It is difficult, from the regression results presented, to draw general conclusions on the utility of the Meteorological Office model as an estimator of wave power at sites where no measurements exist for comparison. In the next section however, the final estimates of average power are obtained for the listed sites by applying the regression formulae to the average of the model powers. It will be seen that the magnitude of the resulting adjustment in the mean values is not large. To this extent, one may expect that the uncorrected average power derived for any chosen model location constitutes a fairly reliable estimate of the mean power which might have been measured there.

Average of the model wave powers

The model data were supplied by the Meteorological Office in three separate files covering the period 1 October 1978 to 23 September 1982 and comprised directional wave energy (variance) spectra presented at twelve hour intervals. Spectral density estimates were presented at 30° intervals in direction and, for the second and third files only, at eleven unequally spaced frequencies. The spectra contained in the first file covered six frequency bands differently spaced from those in the second and third files. It thus proved impracticable to present an

averaged directional spectrum drawing on the data from all three files, only those in the second and third being directly combinable. Overall averages of the integrated power have, however, been calculated using all the data. These average powers are presented in column one of Table 5 below.

Site	Average of model powers kW m^{-1}	Adjusted average model powers kW m^{-1}	Standard error of adjusted value kW m^{-1}
Scilly Isles	45.16	45.15	1.53
S Uist (deep)	62.95	65.61	1.68
Kinnairds Head	15.02	16.14	0.57
Foula	54.89	54.89*	--
DB1	56.92	(adjusted values reported in Appendix E)	
*No regression results available for Foula as measured and model time series do not overlap significantly.			

Table 5

Average Meteorological Office model power over the four year period 1 October 1978 to 23 September 1982, with values also adjusted by regression formulae of Table 2.

Applying the regression results of Table 2 to the average power presented in column one of Table 5 produces, finally, the required scaled results. These are estimates of the four year measured averages which would have resulted if the measured series had been complete; they are presented in column two of Table 5 with the corresponding standard errors on the estimates in column three.

Comparisons with other predictions of annual average power

Predictions of the long term average powers to be expected at the South Uist offshore and Foula sites have already been made by the procedure detailed in Section 1b. The prediction for Foula was based on measured data confidential to the UKOOA and discussion of the result is therefore conducted in Appendix G. This result, along with others in this report based on UKOOA data, will not be generally available until the confidentiality restrictions expire.

In the case of the South Uist offshore (45 m) site the predicted long term power average is 47.8 kW m^{-1}. In order to obtain a figure with which this value may be compared, we must take the scaled four year model average for the deepwater South Uist site, and re-scale it according to the appropriate regression curve describing

its relationship to the offshore site. The appropriate regression result has been calculated from the simultaneous power measurements at the offshore and deepwater sites, but has not previously been quoted. It is:-

$$\text{Offshore power} = \text{deepwater power} \times 0.632 + 5.76 \text{ kW m}^{-1}$$

Applying this to the adjusted deepwater power in Table 5 results in a prediction of 47.2 ± 2 kW m^{-1} for the four year average measured power at the offshore site. This is in almost exact agreement with the 47.8 kW m^{-1} previously predicted as the long term average at the site from the procedure described in Section 1b. Whilst the excellence of agreement is perhaps fortuitous in view of the relative brevity of the model data series, it suffices to show that the effect of missing data on the measured average power of 41.8 kW m^{-1} presented in column one of Table 3 has been to produce a significant underestimate of power.

In addition to the average of model powers just discussed, it is interesting also to look at the distribution of power as a function of frequency of occurrence. It must be remembered however, that these distributions are somewhat distorted due to the scatter in the relationship between the measured and model powers. Figures 7a to 7d present, for each site, the percentage cumulative distributions of power. They show the percentage of the overall annual average power figures achieved by averaging occurrences with powers up to the stated thresholds. In the case of the curves marked (a), occurrences above the thresholds are totally excluded from the cumulative sum (equivalent to a device switching off when a threshold is exceeded). In curves (b), occurrences above the threshold are ascribed a power equal to the threshold level and incorporated in the sum (equivalent to a device yielding constant power once a threshold is exceeded).

The basic frequency distributions from which the cumulative versions were compiled are shown in Figures 8a to 8d. The results presented are based in all cases on the unadjusted model results.

Directional aspects

For the reasons previously stated only model data for two of the data files, covering the period 23 October 1979 to 26 September 1982, could be combined to form a mean directional power spectrum at each site. The mean is thus slightly biased by virtue of the exclusion of one October in the three year period. Nevertheless, the mean distribution of power with direction obtained from these results provides, in relative terms, the best available estimate of this quantity. These

distributions are presented in Figures 9a to 9e. In the case of the South Uist site, the Meteorological Office directional results are plotted along with the directional distribution of power previously estimated for the 399 synthesized directional spectra. The directionality factor of these synthesized data is 0.82.

Directionality factors have also been calculated for each model site. These indicate the proportion of the total power, tabulated in Table 5, crossing a line perpendicular to the peak direction in a shoreward direction. This proportion of the total power is, subject to the directional response of the device, available to an energy convertor facing the direction from which most of the power approaches. The directionality factors appear in Table 6.

Direct comparison of the model directional distributions with measured directional data have only been possible at the DB1 site. Again, for reasons of confidentiality, this comparison is presented in Appendix G.

Site	Directionality factor	Best direction
Scilly Isles	0.80	265°
South Uist (deepwater)	0.71	260°
Kinnairds Head	0.43	033°
Foula	0.63	248°
DB1	0.74	272°

Table 6 Directionality factors

2b Survey of results at other sites

There are two further sites shown in Table 1 at which considerable effort has been expended in accumulating wave climate information: these are the shipborne wave recorder equipped light vessels at Sevenstones and St Gowan. Owing to the uncertainties in the Meteorological Office wave model results for the more sheltered coastal locations, it has not been possible effectively to relate these measured data to the model results as was done for the sites covered in the previous section. These data have, however, been used in a number of ways and are presented here as indicators of the likely long term average power at these sites. Additionally,

at St Gowan, some information on the probable distribution of power with direction has been deduced.

St Gowan

It was previously mentioned in 1b that wave data from the St Gowan shipborne wave recorder have been processed (Crisp 1980) to yield a figure for the expected long term annual average power. This exercise, which closely followed that used on the South Uist data and involved the selection of a set of 401 spectra, resulted in a figure of 15.7 kW m^{-1}. The previous discussion is extended here to include directional aspects of the wave climate. Average directional characteristics of the climate were estimated using the measured spectra in conjunction with meteorological data. As was the case at South Uist, it was necessary to distinguish between swell and wind sea regions of each spectrum, and to ascribe directional characteristics separately to each. In general, the properties of any wind sea are rather broad with energy propagating over a range of directions either side of the mean wind direction. In this work it was assumed for simplicity that, for each spectrum, the wind sea energy propagates in the same direction as the generating wind. It is expected that any tendency for the average distribution of power to be too narrow will be minimized by the decision to present the angular power distribution smoothed over 30° sectors.

The energy contained in the swell portion of the spectrum was assumed to have been generated by distant wind fields located in the open Atlantic. As the recording site is exposed to the Atlantic over a relatively narrow range of angles from 210° to 270°, this condition defines the directional properties of the swell energy within reasonably close limits. For the purpose of calculating the average power as a function of direction no attempt was made to establish the form of the swell distribution with angle within the allowed range of directions. Instead it has been assumed that the swell energy is evenly distributed over angles from 210°-270°.

The separation of each spectrum into wind-sea and swell regions revealed that, of the total average annual power of 15.7 kW m^{-1}, 7.4 kW m^{-1} was contained in the wind-sea portion and 8.3 kW m^{-1} in the swell. The average directional distribution of power calculated for the St Gowan selected spectra is shown in Figure 10.

The average power fluxes reported here are approximately one third of the energy

flux for measurements made at the South Uist offshore buoy. Such a difference in the wave climate at that location and at St Gowan, is thought to arise as a result of a number of factors:

1. St Gowan is exposed to the open Atlantic over a smaller range of angles than is South Uist, so that it would be expected to receive less swell energy.

2. The fetch available for wind-sea generation is restricted over a larger range of angles than at South Uist so that the energy in the wind-sea portion of the St Gowan spectra is reduced.

3. The average wind speeds at the two sites, calculated from long term wind speed and direction data are 14 knots at South Uist and 10.5 knots at St Gowan.

Sevenstones

The value of the data gathered at this site lies in the length and completeness of the measured time series. Accurate calculations of power are not, however, possible as the effort required to render the chart data into spectral form is prohibitive. An approximate estimate of the power available at this site has been made using Hs and Tz values derived from five years of measurements - January 1968 to December 1969 and July 1971 to June 1974 (all inclusive). These calculations use Equation A.17 of Appendix A where Te has been taken as

$$Te = 1.14\ Tz$$

This is correct on the assumption that each spectrum has the Pierson-Moskowitz form.

The resulting annual average power is 34.7 kW m^{-1}, which compares with 45.15 kW m^{-1} for the Scilly Isles Waverider site. It must be assumed that the difference is a manifestation of the sheltering effect of the Scilly Isles on the light ship location.

2c Tabulated summary of important results

Site	best estimate of		
	Annual average power kW m^{-1}	directionality factor	best direction degrees
Scilly Isles	45.2	0.80	265
South Uist Deep	65.6	0.71	260
South Uist 45 m	47.8	-	-
Kinnairds Head	16.1	0.43	033
St Gowan	15.7	-	240
Sevenstones	34.7	-	-
Foula	54.9	0.63	248
DB1 (model) (see Appendix G for adjusted value)	56.9	0.74	272

ACKNOWLEDGEMENTS

The work described in this report was conducted over many years and thanks are due to numerous colleagues at IOS Taunton for their invaluable assistance, either directly with the work reported, or through their involvement with the wave measurement programme which provided the data.

The work was funded by the Department of Energy through the Energy Technology Support Unit at Harwell. I am grateful to the staff, past and present, of that Unit for the support and interest they have consistently provided.

Thanks are due to the United Kingdom Offshore Operators Association, Oceanographic Committee for their permission to include the data from Foula and DB1 which are included in Appendix G.

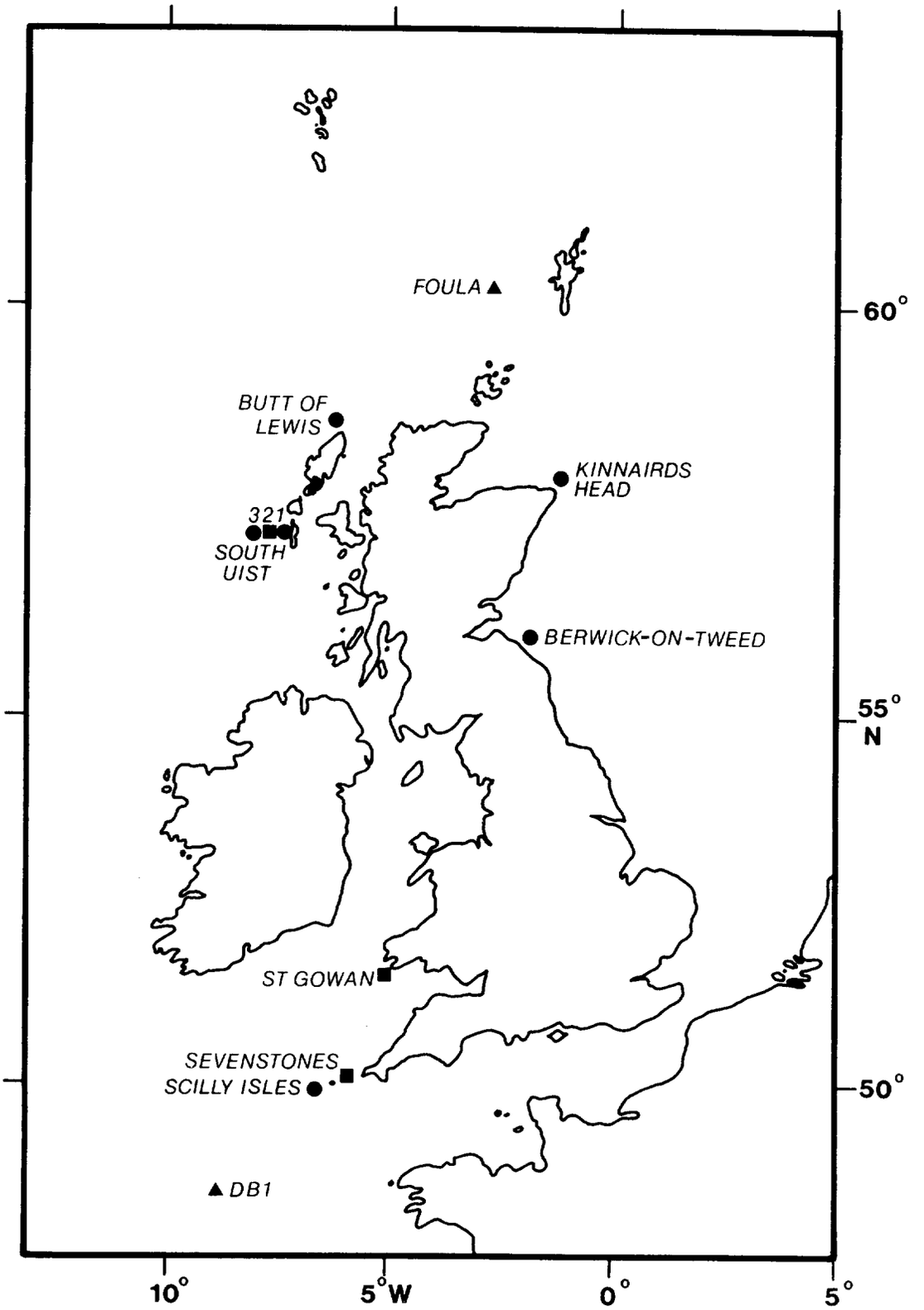

▲ United Kingdom Offshore Operators Association

■ Department of Energy, Petroleum Engineering Division

● Wave Energy Steering Committee

Figure 1 Locations of wave measurement sites

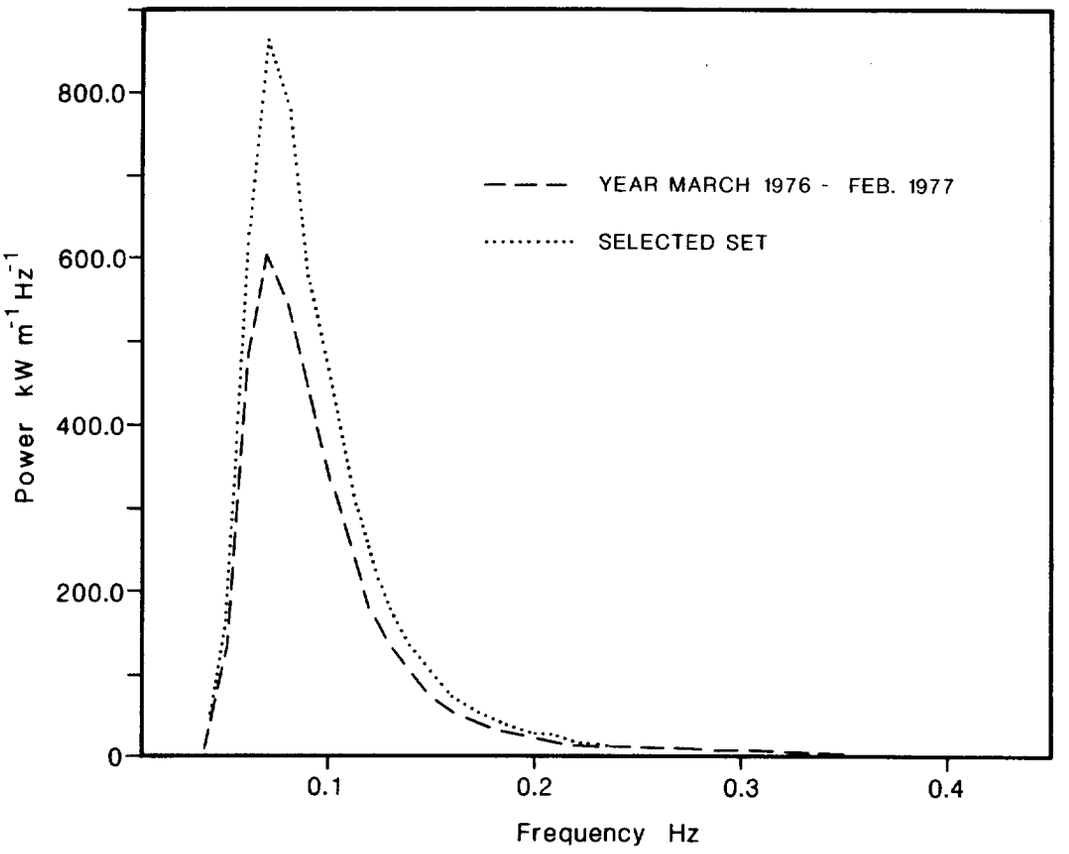

Figure 2 South Uist offshore (45 m). Mean distribution of power with frequency.

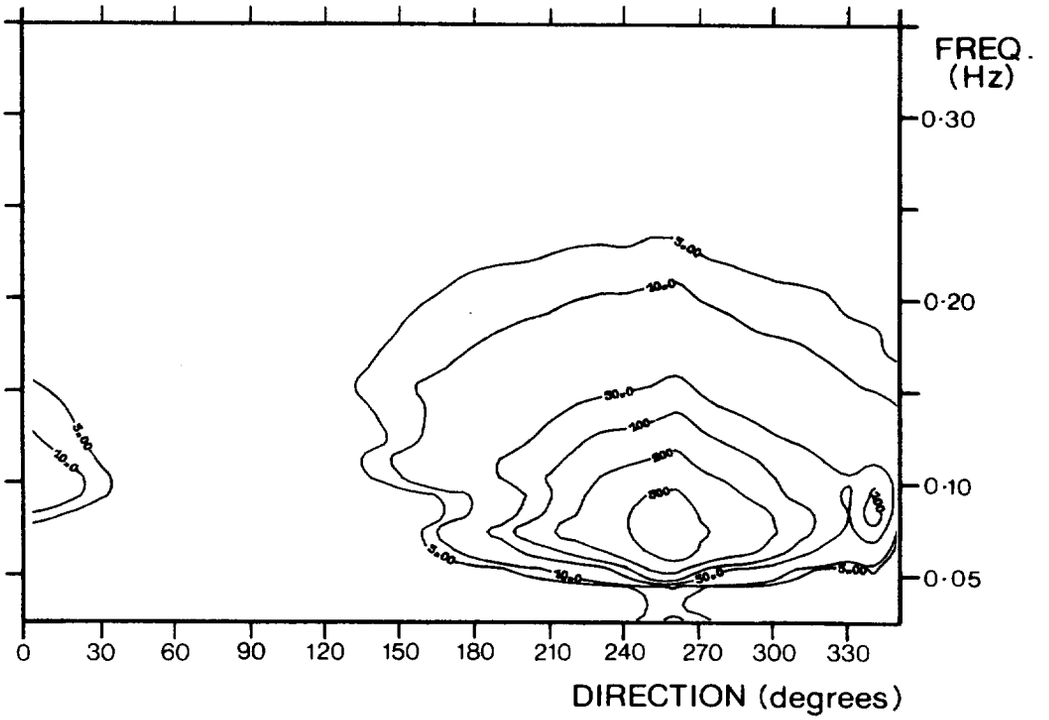

Figure 3 South Uist offshore (45 m). Selected set. Mean distribution of power with frequency and direction. Contours of power density in kW m^{-1} Hz^{-1} rad^{-1}

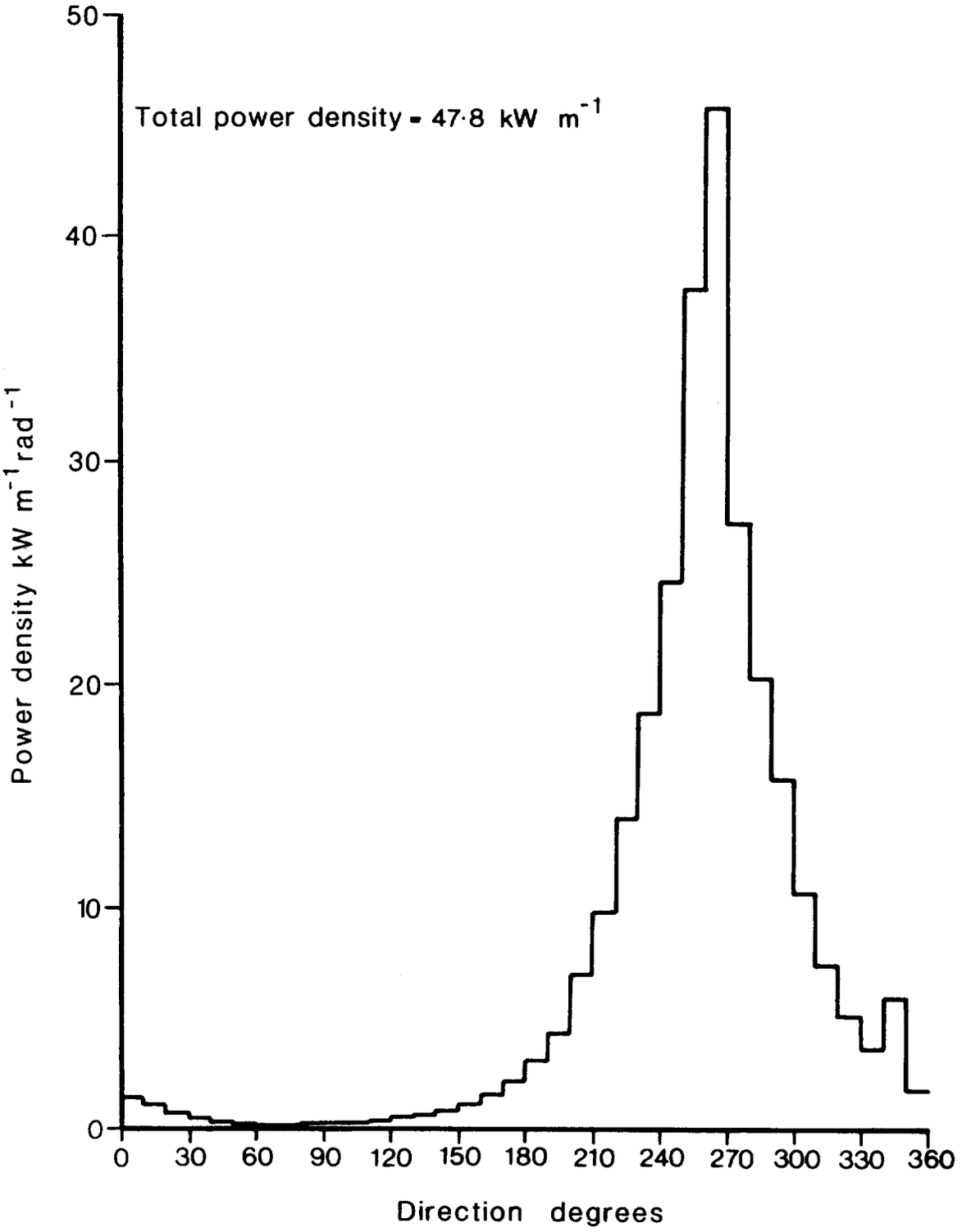

Figure 4 South Uist offshore (45 m) selected set. Mean distribution of power with direction

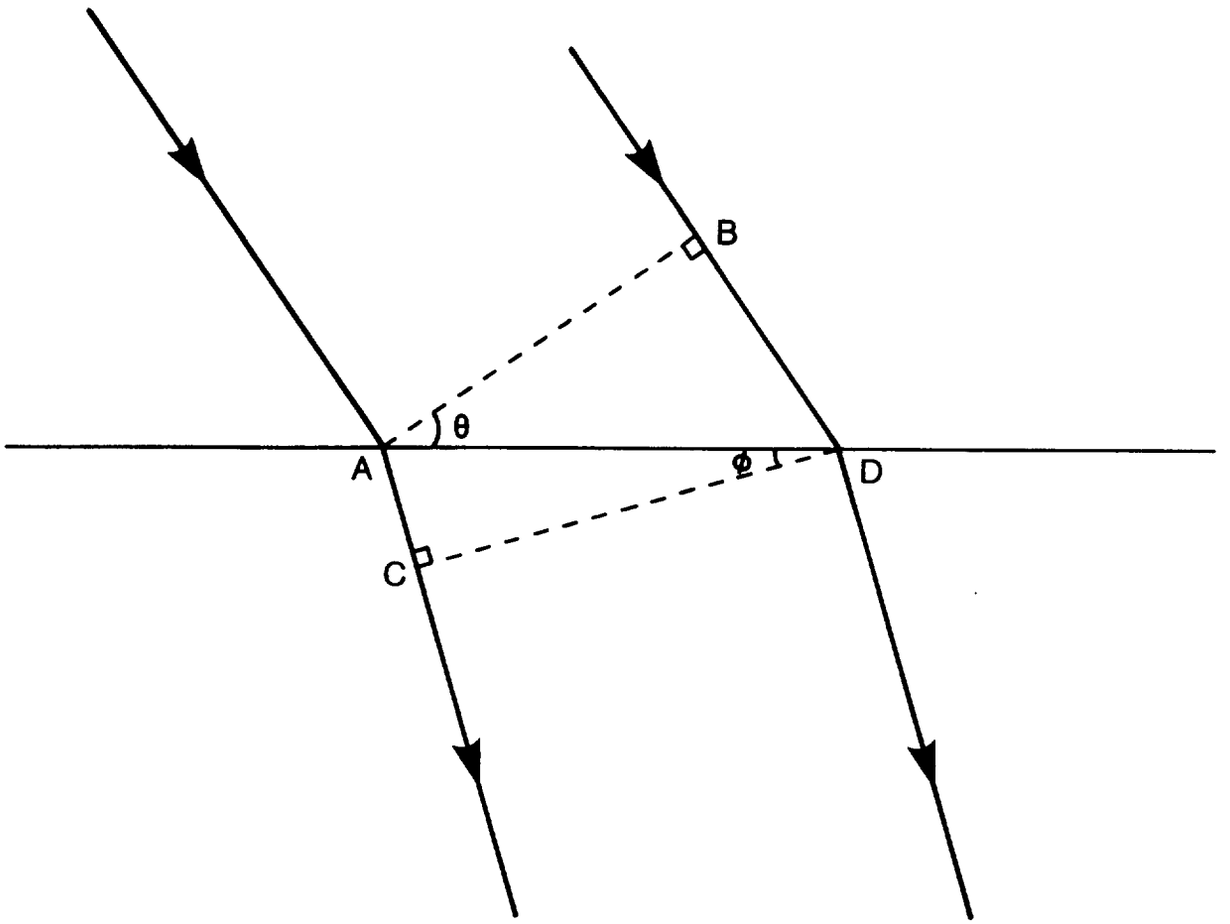

Figure 5 Reduction of wave energy flux per unit crest length due to refraction

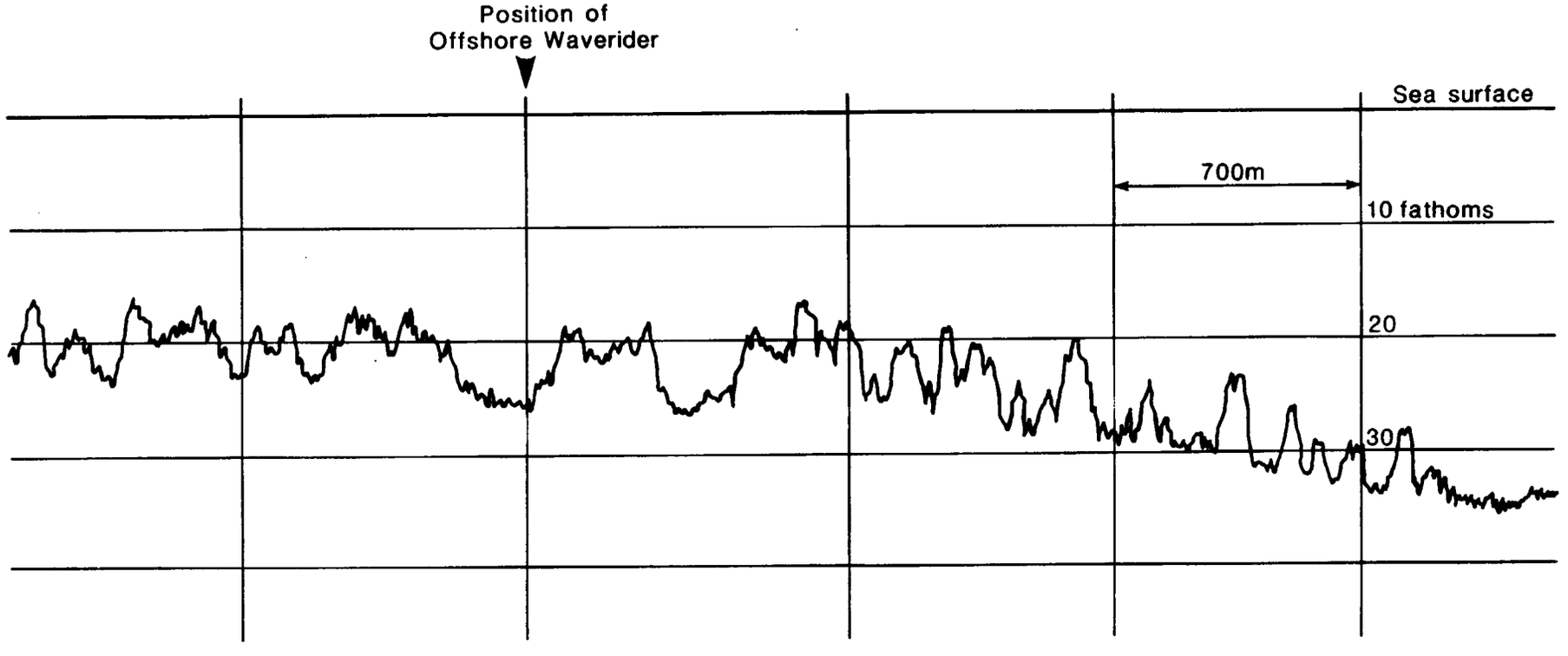

Figure 6 Section of seabed profile along a line passing through South Uist offshore (45 m) and deepwater buoy positions

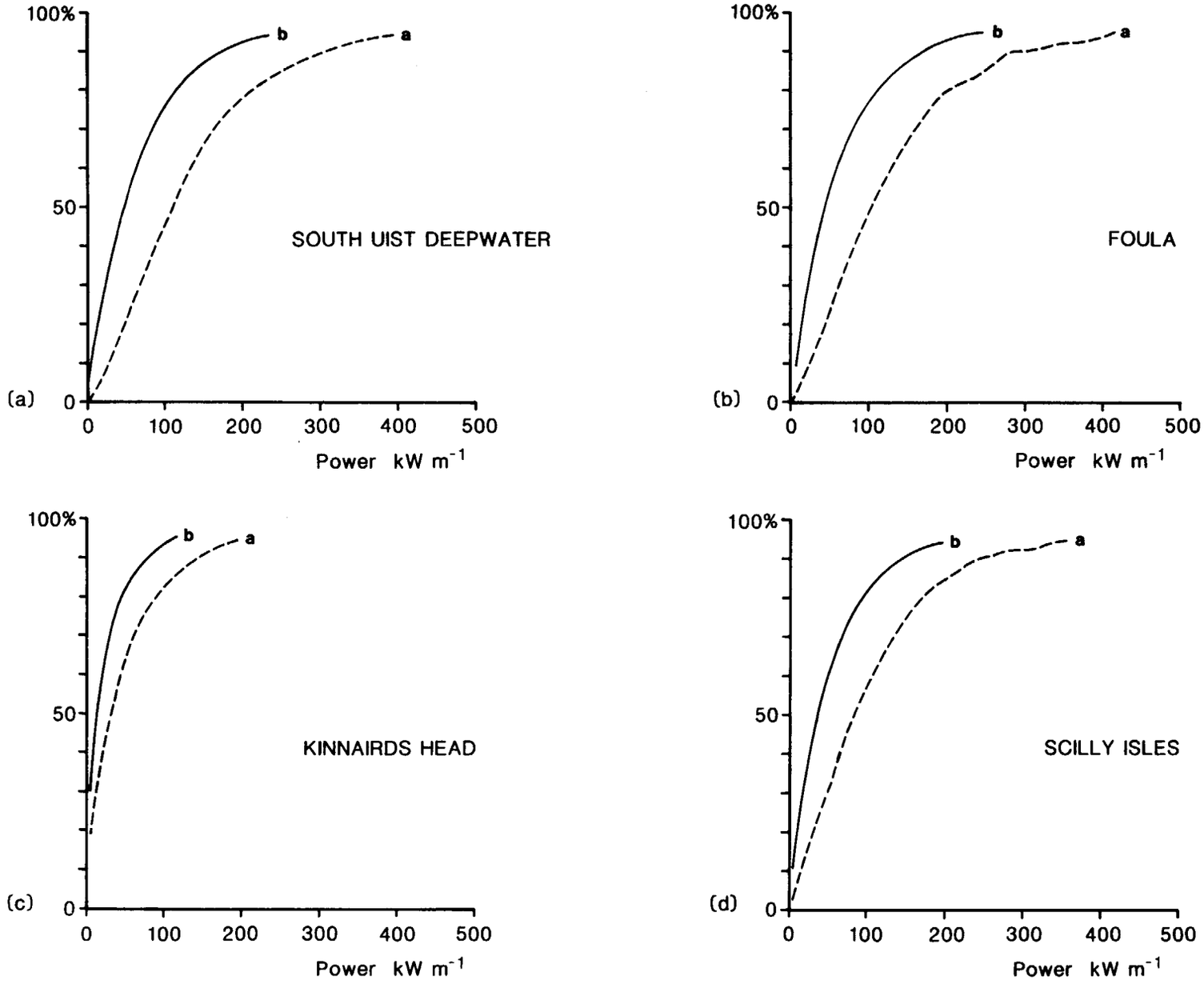

Figure 7 Meteorological Office wave model results. Cumulative distribution of power as percentage of average annual power.

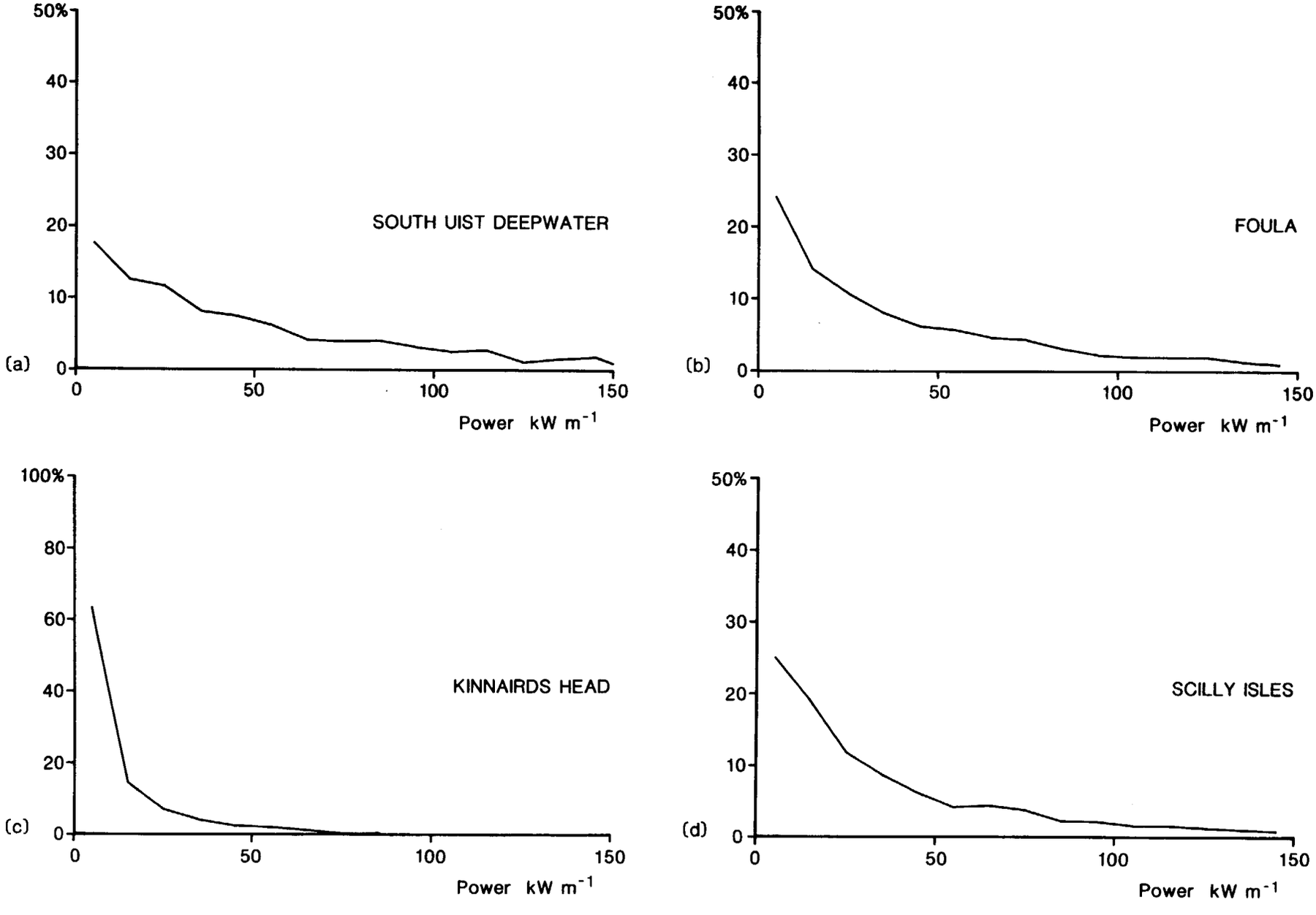

Figure 8 Meteorological Office wave model results. Distribution of power, percentage occurrence.

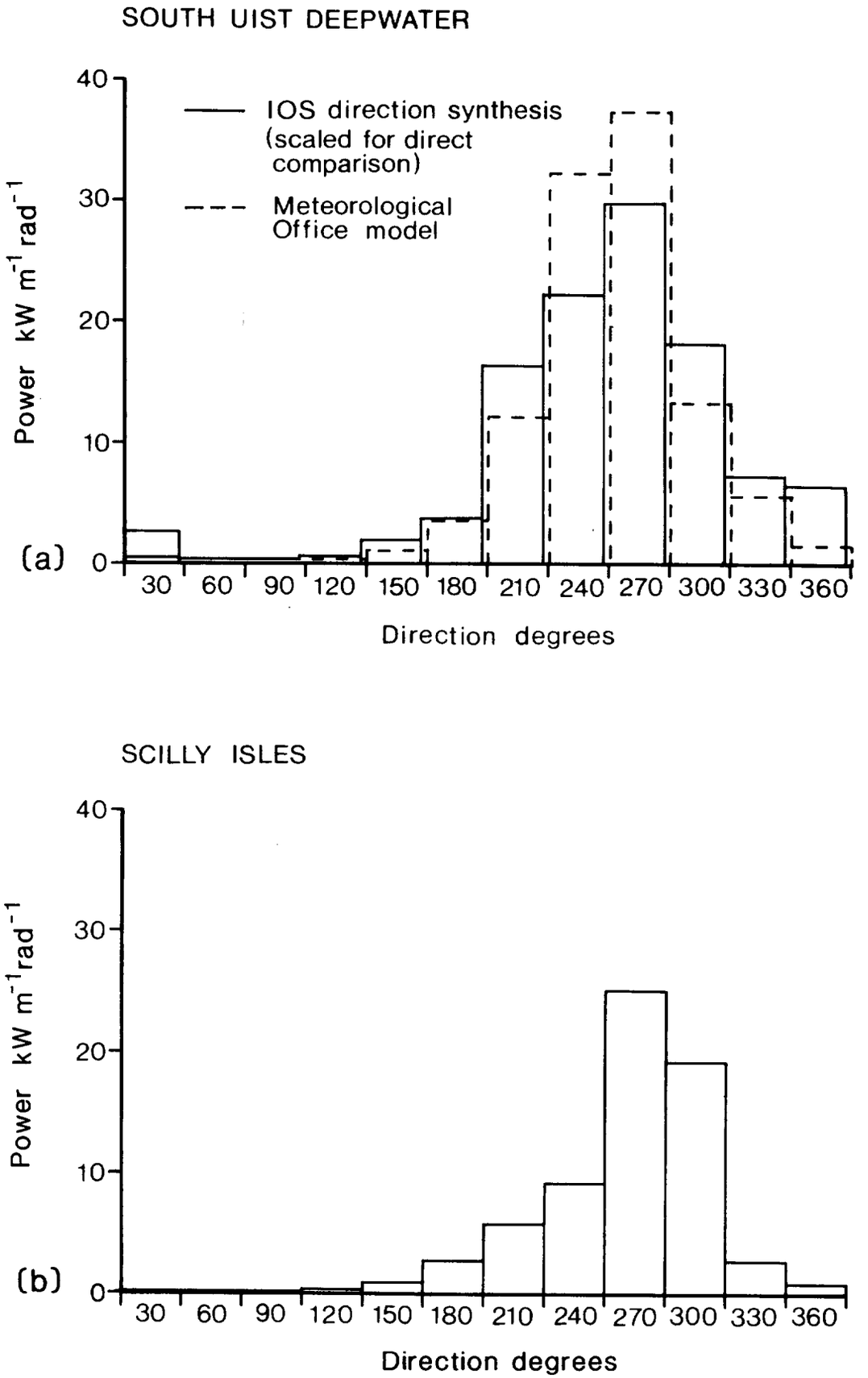

Figure 9 Meteorological Office wave model results. Distribution of power with direction.

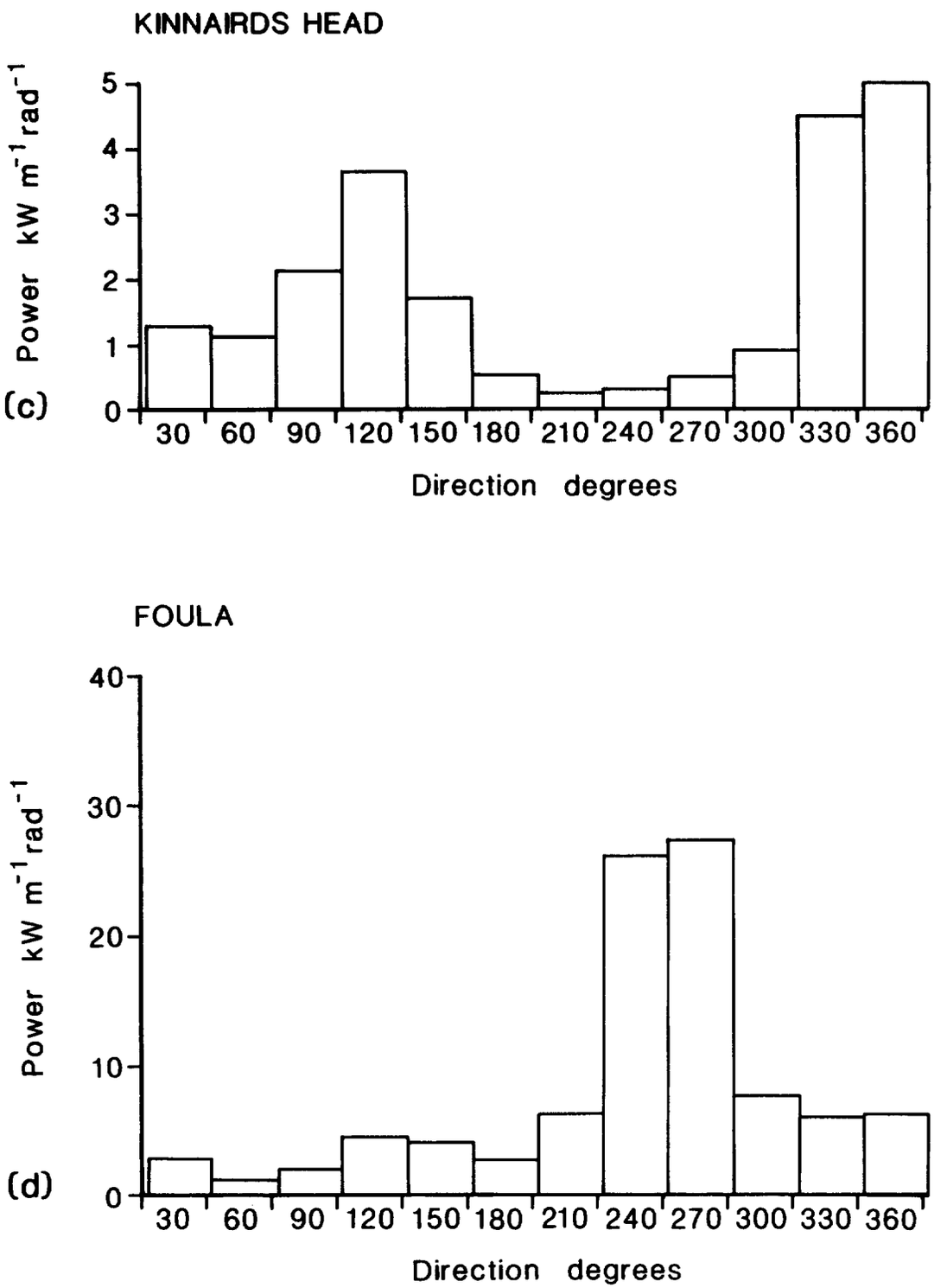

Figure 9 Meteorological Office wave model results. Distribution of power with direction.

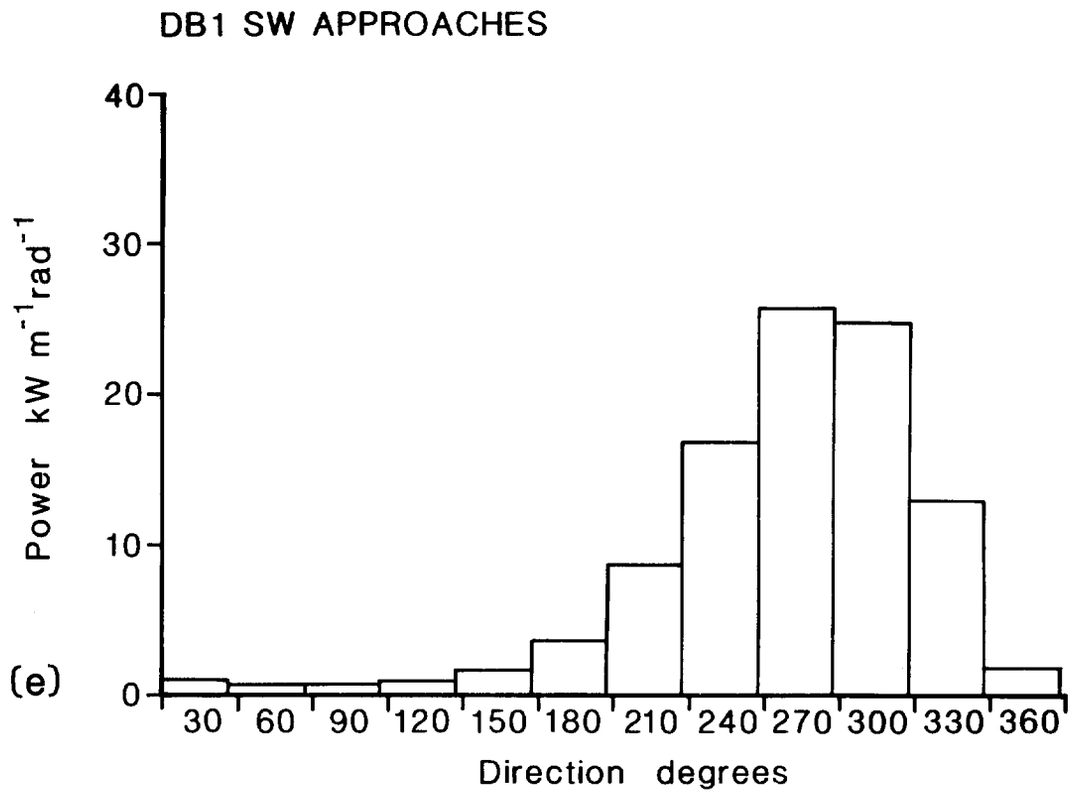

Figure 9 Meteorological Office wave model results. Distribution of power with direction.

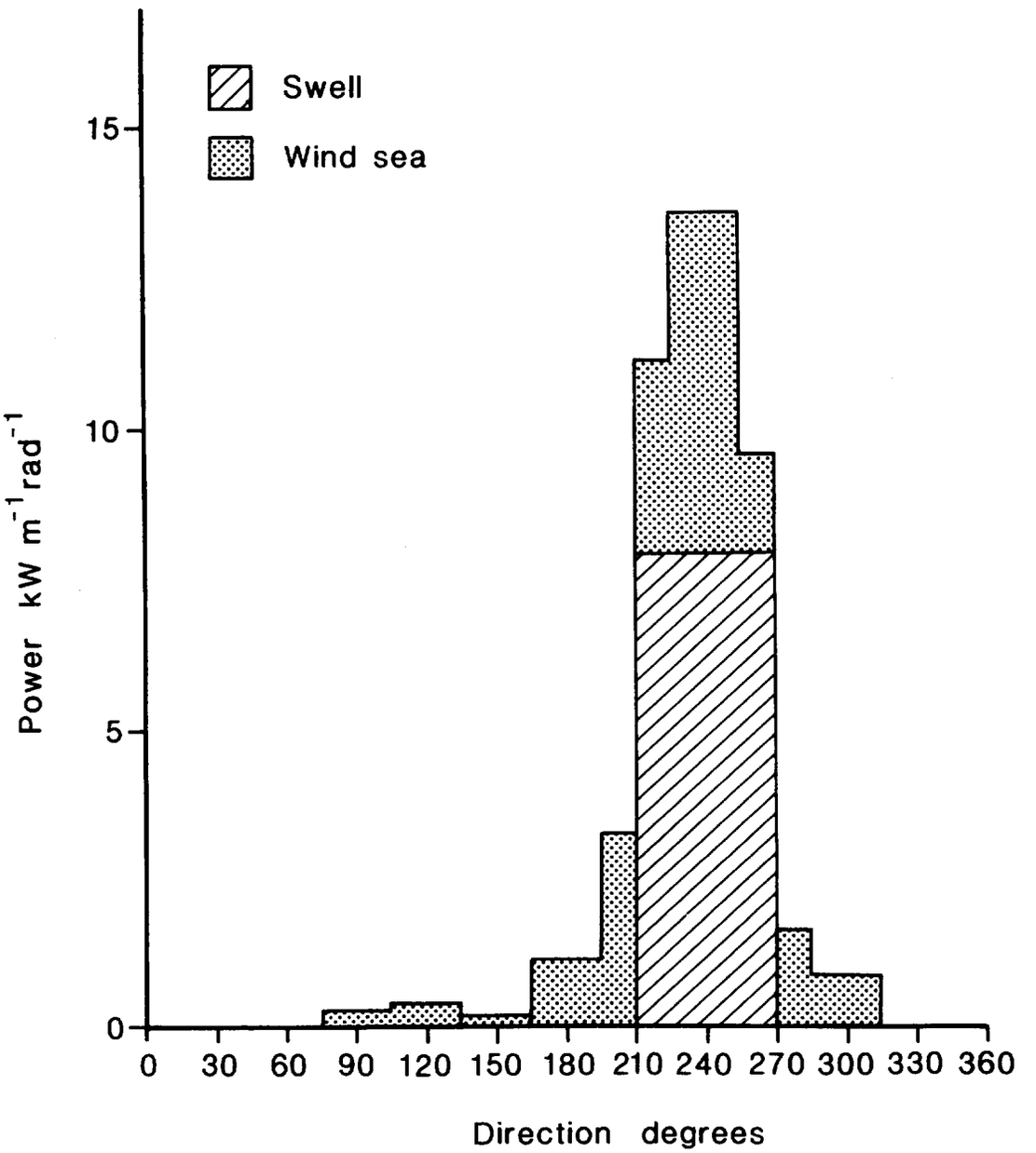

Figure 10 St Gowan selected set. Distribution of power with direction.

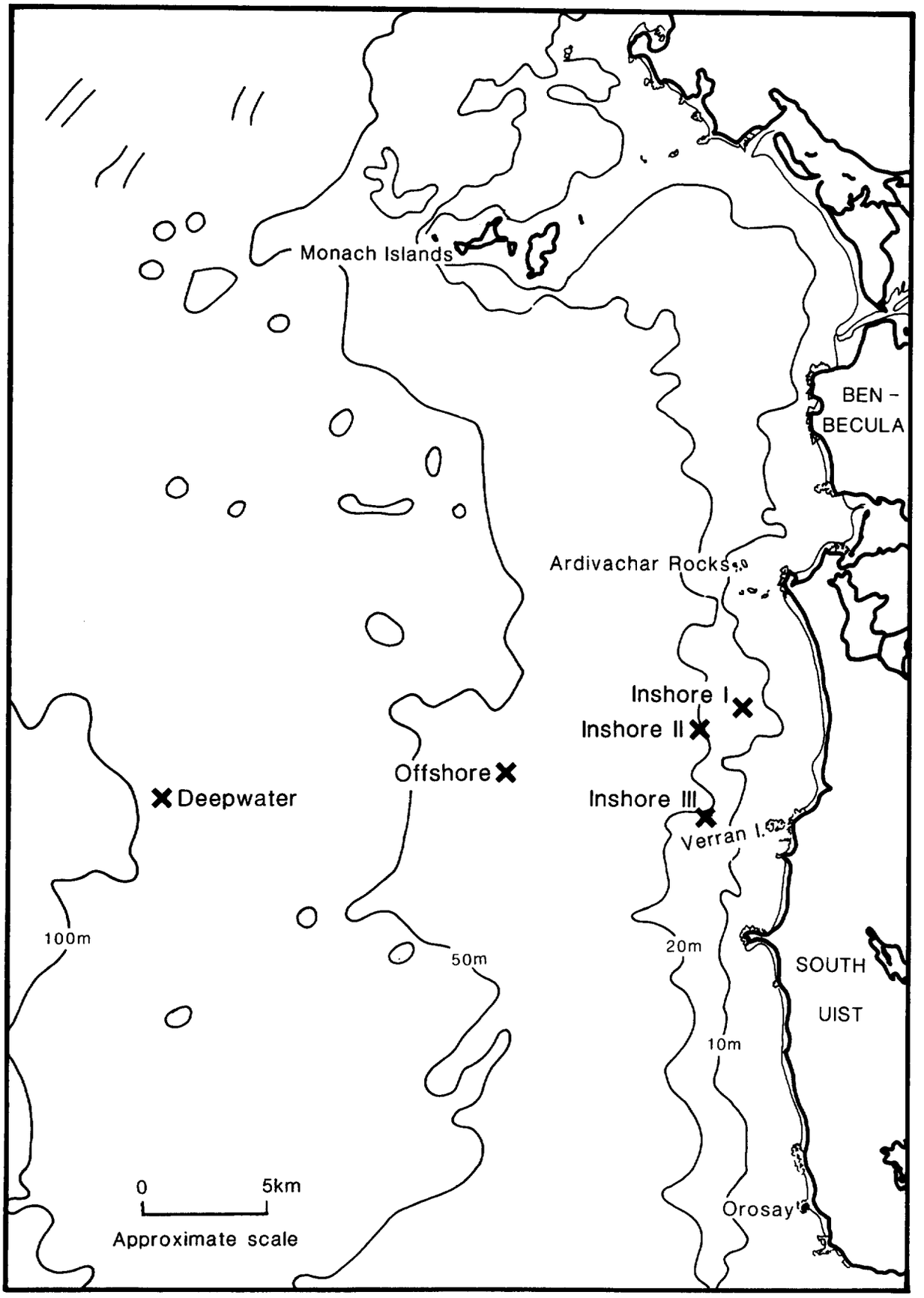

Figure 11 Relative positions of South Uist Waveriders.

APPENDIX A - Wave measurement and the processing of wave data

It was clear that, for ecomony and ease of landing electrical power, wave energy convertors would be stationed in relatively close proximity to the shore. Measurements of waves were therefore required at locations generally within 30 km of land. It was thus possible for the Institute of Oceanographic Sciences to make these measurements using the system then recently developed for wave measurement in coastal waters. This comprised a Datawell Waverider buoy stationed offshore and transmitting heave displacement data to a shore based radio receiving station. Data were logged in digital form.

The sensing mechanism and battery power supply of the Waverider are encased in a stainless steel spherical shell 0.7 m in diameter. This is sealed except for a small access hatch on the top. Attached to the hatch on the outside is a navigation warning light and radio aerial and, on the inside, the radio transmitter electronics. The sensing element, positioned centrally and towards the bottom of the hull, is an accelerometer comprising a fine wire bristle cantilevered to lie between two electrodes, one above and one below. The whole arrangement is mounted on a fully gimballed platform motion damped by total immersion in an electrolytic fluid and contained in a Perspex sphere. The whole support forms in effect a long period pendulum which serves to ensure that, at wave frequencies, the sensing element measures only the vertical component of acceleration suffered by the buoy. The wire element responds to acceleration by changing its position relative to the two surrounding electrodes and thereby affects the balance of impedances in two legs of an AC capacitance bridge. The out-of-balance voltage is rectified and twice integrated to yield a voltage proportional to vertical displacement. This voltage is used to modulate the frequency of an audio frequency sub-carrier on the RF carrier.

In this way, information on the changing vertical displacement is transmitted ashore; here the signal is decoded and presented as a voltage closely proportional to displacement over most of the frequency range covered by ocean gravity waves. This signal is passed to a digital recorder within which it is sampled every 0.5 seconds for a total period of 1024 seconds; the digital values are recorded on magnetic tape. This recording cycle is repeated every 3 hours.

The effective range of the Waverider transmitter is approximately 30 km, although

this is capable of extension to about 50 km by the use of more elaborate and sensitive receiving antennae.

The mooring system used to restrain the buoy on location is chosen to suit the nature of the sea bed, the speed of the current and the water depth. All configurations, however, have one element in common; a length of compliant rubber cord is included to allow the buoy to follow the surface motions without undue restraint.

Processing

Data tapes are returned regularly to the laboratory by a local site agent. On receipt the tapes are transcribed to a disk file and subjected to an automatic validation procedure. This validation is conducted in three stages. The first task is to check the data record character by character to identify badly recorded characters, or format slippages due to missing characters. Data values corrupted by occurrences of this kind are replaced by a very high value; this both preserves the sequence of values, and allows the presence of an error to be recognized during the second stage. At this first stage also the data record timing headers are inspected to identify the limits of each recorded data sample.

In the second stage the time series of data values is subjected to a series of tests designed to detect features inconsistent with the expected behaviour of a valid wave record. There are tests to check for certain common faults known to be characteristic of the particular measurement system, and others to check the time series for reasonableness. The criteria for reasonableness are based loosely on the assumption that the sampled water surface elevation is a Guassian process with the additional constraint that a well established steepness criterion may not be violated. The characteristics tested for are listed below, the program counts the number of failures of each test.

Test 1 scans the data for the high values inserted at Stage 1 to replace uninterpretable data points.

Test 2 tests for failures of Test 1 on adjacent data points.

The mean and standard deviation of the data record are calculated at this point, and the criterion value for Test 5 calculated.

Test 3 checks for the occurrence of ten consecutive data points having the same value. This is a fault condition arising from equipment failure

or under conditions of severe interference.

Test 4 checks that the time interval between successive up-crossings of the record mean line does not exceed 25 seconds. This is an attempt to detect severe wander in the record mean line.

Test 5 compares the difference between adjacent data values with a maximum allowed value. The criterion value is calculated separately for each record.

Test 6 tests for failure of Test 5 on consecutive data points.

Test 7 determines whether the magnitude of each data point exceeds four times the record standard deviation.

Test 8 tests for failures of Test 7 on consecutive data points.

The actions taken on failures of the above tests are as follows:

Test 1 - Faulty values replaced by average of preceding and following data values (ie single point linear interpolation). Failure noted for stage 3.

Test 2 - Failure noted for stage 3.

Test 3 - Failure notes for stage 3.

Test 4 - Failure noted for stage 3.

Test 5 - Replacement of faulty value by single point linear interpolation.

Test 6 - Failure noted for stage 3.

Test 7 - Failure noted for stage 3.

Test 8 - Failure noted for stage 3.

At the third stage the test results are assessed by comparing the recorded number of failures of each with a figure for the maximum number of failures allowed. The numbers of failures allowed for each test (for a 2048 point record) are

Test	1	2	3	4	5	6	7	8
Allowed failures	36	0	0	0	5	0	6	3

If the number of recorded failures exceeds those allowed for any test, or if the total number of test failures exceeds forty-four, the record is flagged invalid.

The level at which each of these criterion values is set was determined after an

extended period of testing. The performance of the automatic procedure in distinguishing between wave records which, in the judgement of an experienced analyst, are either valid or faulty, is well established. The performance of the program is, however, continuously monitored in an effort to detect failures of the procedure under changed circumstances.

Finally the validated wave records are written to computer compatible magnetic tape. Each valid record so obtained is Fourier analysed and scaled to yield an estimate of the variance spectrum of the sea surface elevation. (In this application there is no need to preserve the distinction between the true elevation spectrum and this estimate of it.)

The spectrum S(f) is defined as follows

$$S(f)\delta f = \sum_{f_n = f - \frac{\delta f}{2}}^{f + \frac{\delta f}{2}} \tfrac{1}{2} C_n^2 \qquad \text{A.1}$$

where the time series of displacement, h(t), is represented as the linear superpostion of an infinite number of sinusoids of small amplitudes, C_n, and frequencies, $f_n = n/T$; T being the time series length.

$$h(t) = \sum_{n=1}^{\infty} C_n \cos(2\pi f_n t + \theta_n) \qquad \text{A.2}$$

The phases θ_n are randomly distributed in the range 0 to 2π. Thus $S(f)\delta f$ specifies the total variance in a frequency band of width δf centred on f.

The 2048 point sampled time series is cosine tapered over 256 points at each end of the series; this permits a more precise determination of the energy associated with each frequency by limiting the amount of energy leaking from one spectral estimate to the others. The transform is performed on the entire series and the resulting raw spectral estimates averaged in groups of ten to produce a final spectrum with a frequency resolution of approximately 0.01 Hz. Prior to averaging, each spectral estimate is multiplied by a factor compensating for the response of the buoy and receiving system which are not precisely unity over the whole range of interest. A small amount of the total variance is lost during the tapering process and this also is compensated for at this stage.

Other data sources

Although most of the data collected specifically for the wave energy programme were obtained using systems similar to that described above, some use was made of data gathered at shipborne wave recorder stations. The principle of operation of this instrument is similar to that of the Waverider only in so far as both rely on measuring vertical acceleration. A ship, however, does not follow surface motions as well as a small buoy, and further refinements are necessary to produce a workable instrument. A sensor package comprising a gimballed accelerometer and a pressure unit is installed inboard and amidships on each side of the ship's hull; a small hole connects the pressure sensing diaphragm to the outside water. The combined pressure and doubly integrated acceleration signal, averaged from the two packages, gives the vertical displacement of the water surface above an arbitrary datum. Variations in the surface displacement are recorded by a pen and paper chart recorder.

Whilst giving reliable measurements of average wave height, it is not a simple matter to obtain an accurate estimate of the sea state spectrum with this instrument. Apart from the inconvenience of digitizing the analogue pen chart signal, there is uncertainty regarding the precise form of the function which should be used to correct the pressure signal for attenuation with depth. Despite these difficulties the data from this instrument are, with care, usable in this application. Data from shipborne wave recorders situated at Sevenstones, St Gowan and OWS India have been used.

Calculation of wave power

Some useful relationships are stated but not derived in this section.

The total energy associated with each metre of wavefront of a long-crested sinusoidal wave of wavelength λ and amplitude a is, for one complete wavelength,

$$\tfrac{1}{2}\rho g a^2 \lambda \qquad \text{A.3}$$

where ρ = density of water

g = gravitational acceleration

Averaged over one wavelength to give the energy per unit area of sea surface it is

$$E' = \tfrac{1}{2}\rho g a^2 \qquad \text{A.4}$$

The total energy density of a number of superposed waves is obtained by adding their individual energy densities. Thus the total energy per unit area of all

waves having frequencies in the interval between $f - \frac{\delta f}{2}$ and $f + \frac{\delta f}{2}$

is

$$E(f) = \sum_{f_n=f-\frac{\delta f}{2}}^{f+\frac{\delta f}{2}} \tfrac{1}{2}\rho g a_n^2 = \rho g\, S(f)\delta f \qquad A.5$$

The area under the variance spectrum is therefore proportional to the total wave energy density

$$E = \rho g \int_0^\infty S(f)df \qquad A.6$$

Energy flux is defined as the time rate of change of energy per unit area normal to the wave direction. When integrated over depth and averaged over one wave period, the average energy flux per unit length of wave crest P(f) is

$$= \frac{\rho g a^2}{2} Cg = E(f).Cg \qquad A.7$$

where Cg is the wave group velocity at frequency f

and so

$$P(f) = \rho g S(f).\delta f.Cg \qquad A.8$$

The variance spectrum may thus be converted to a spectrum of depth integrated average energy flux by multiplying each S(f) by the constant ρg and the group velocity appropriate to the wave frequency and the water depth.

The total depth integrated energy flux for the whole spectrum is

$$P = \rho g \int_0^\infty S(f).Cg.df \qquad A.9$$

This is the time rate of change of energy per unit length normal to the wave direction. It is usually expressed in units of kW m^{-1} and is the power per metre of wavefront. This quantity is referred to simply as power throughout this report.

Now $$Cg = \tfrac{1}{2}\left[\frac{g}{k}\tanh(kh)\right]^{\frac{1}{2}}\left[1 + \frac{2kh}{\sinh(2kh)}\right] \qquad A.10$$

where h is water depth

k is wave number

but in deepwater this becomes

$$Cg = \frac{g}{4\pi f} \qquad A.11$$

thus

$$P = \frac{\rho g^2}{4\pi} \int_0^\infty \frac{1}{f}.S(f).df \qquad A.12$$

Moments of the variance spectrum are defined

$$m_n = \int_0^\infty f^n \, S(f).df \qquad A.13$$

So $$P = \frac{\rho g^2}{4\pi} \, m_{-1} \qquad A.14$$

It is convenient to define the quantity, Te, which has dimensions of time and is called the energy period

$$Te = \frac{m_{-1}}{m_o} \qquad A.15$$

whence

$$P = \frac{\rho g^2}{4\pi} \, m_o \, Te \qquad A.16$$

or, since significant wave height, H_s, is defined as $4\sqrt{m_o}$

$$P = \frac{\rho g^2}{64\pi} Hs^2 Te \qquad A.17$$

which is a useful deepwater approximation to total power. (At the South Uist 45 m site this expression underestimates power on average by approximately 12%.)

Since the directions of waves in the real sea are widely distributed with direction, the expressions for P given above describe the total power crossing a unit diameter circle.

APPENDIX B - The effect of lost data

Using data collected at the South Uist 45 m site over the period March 1976 to August 1981, five main causes of data loss were identified. The amount of data lost due to each was determined from a careful study of the validation results and of the documentation associated with the data. The percentage of data lost due to each cause is shown in the table below:

Cause	% of lost data
Logger malfunction	25
Buoy faulty	38
Buoy missing	34
Radio interference	1
Servicing	.5
Unexplained	2

These figures were derived from an analysis of data losses exceeding one day in duration. Consequently, the amount of data lost to intermittent occurrences of radio interference is seriously underestimated in the table. Confining attention to periods greater than one day accounts for only approximately 73% of all data lost. The overall valid data return for the period was 67% of that which might have been collected.

Lessons may be drawn from these figures on the operational priorities in future measurement programmes.

An attempt has been made to assess the effect of the missing 33% of data on the calculated average wave power. Data from the Meteorological Office wave model for a grid point close to the South Uist deepwater site were used in this exercise; the data covered the period October 1979 to December 1981. The frequency distributions of 'observed' model powers were compiled for both the whole period considered and, separately, using only model data coinciding with valid data being collected at the South Uist 45 m site. These show, Figure B.1, that conditions at the time of successful measurements included fewer high sea states and more low sea states than was on average the case over the whole period. The average power at these times was 27% lower than that for the complete series.

Annual average wave powers are not, however, calculated as the straight average of all available results. An average power is calculated for each calendar month of the year using all available data for that month from throughout the series; eg an average power for January is calculated using all available January data. This avoids bias due to disparities in the amounts of data for each month. In Section 2 it is shown that the average power calculated in this way from five years of measured data, falls short of the average power derived from a complete four year time series of wave model results by 11%. The model results had been corrected for disagreement with simultaneous measured powers prior to averaging, and the observed shortfall thus indicates the approximate effect of the missing data on the calculation of measured annual average power.

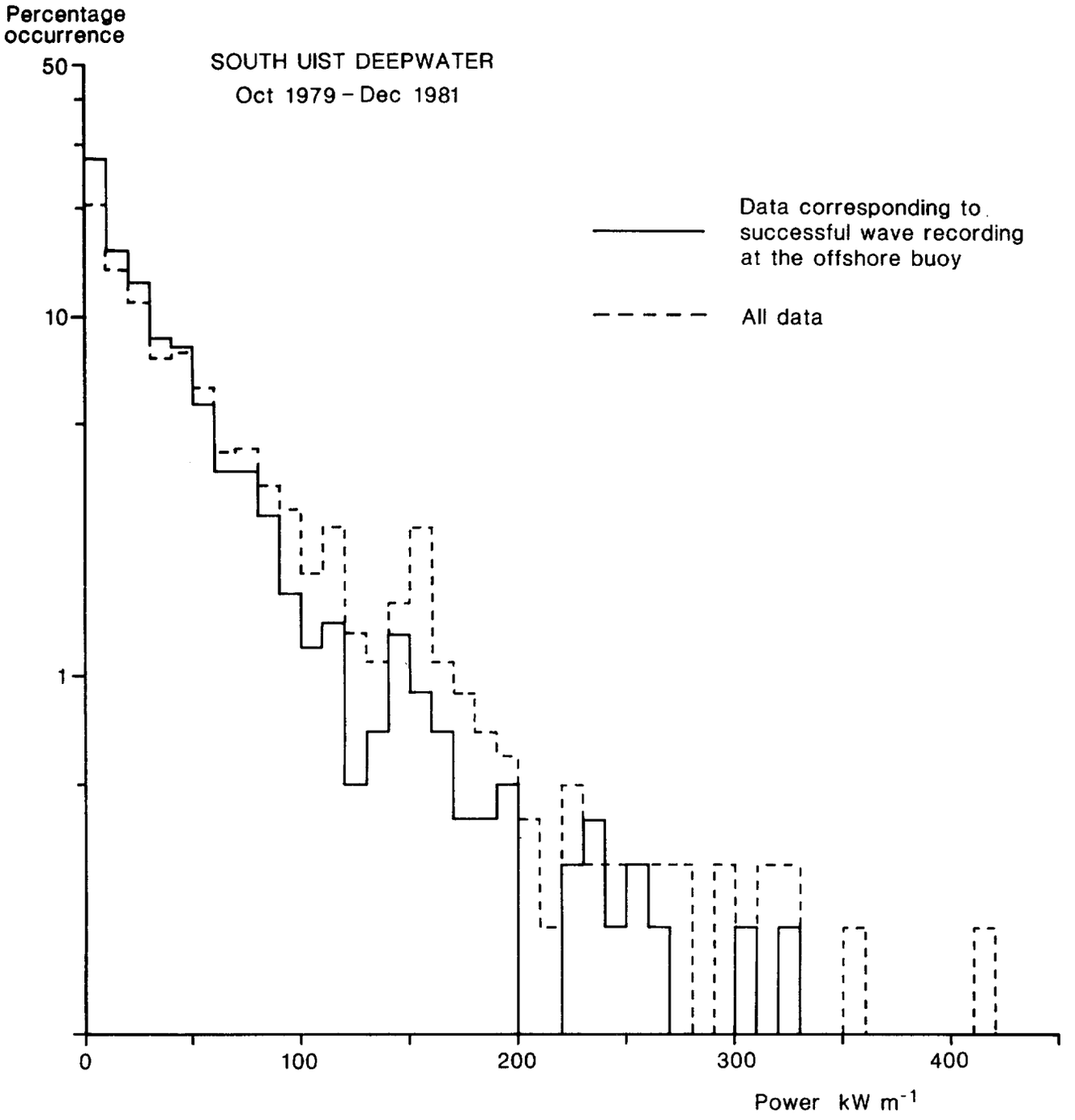

Figure B.1 Distribution of Meteorological Office model wave power results

APPENDIX C - Selection of wave record subsets

South Uist 45 m site

Listings of the hourly mean wind speed and direction measured at Benbecula airport (1 km inland, a total of 25 km from the buoy) covering the period of the first years wave recordings were obtained. This allowed each wave record to be associated with the average value of wind speed and direction measured over the hour preceding each wave recording. In addition to these hourly data, long term bivariate histograms describing the distribution of hourly mean speeds and directions were obtained. The histograms supplied had been compiled on both an annual and a monthly basis and were derived from measurements made over the following periods at the Tiree and Benbecula anemograph stations.

Tiree	1950-1959	(10 years)
Benbecula	1957-1960	(4 years)
Benbecula	1960-1969	(10 years)

All three annual distributions were combined to produce a distribution representative of the general area to the west of the Hebrides. This is shown in Figure C.1. A similar procedure was employed with the monthly distributions to produce four long term seasonal distributions. Seasons were taken to be 3 months long; winter being December, January and February, and so on.

Although the objective was to select a subset of wave records, it was more convenient initially to refer only to the wind records associated with each wave record. Viewed in this way, the task was to select a subset of wind records which conform as closely as possible to the derived long term distributions.

In preparation for the task of selection, the hourly mean speed and direction observations for the year were sorted by computer to produce tabulations of the observations by classes of direction and speed for each month of the year. Each wind observation was identified by the time and date of its collection. These monthly tabulations were collected together to form seasonal groups. It should be clear that, whilst approximately 8760 wind recordings were made at Benbecula during the year, all of which were tabulated as described, only those pertaining to the hour immediately preceding a wave recording were eligible for selection.

It had previously been decided to produce a subset of 400 records. The number of records required in each speed and direction class was thus calculated by multiplying by 4 the corresponding percentage of occurrence figure in the derived annual distribution of Figure C.1. The records required to complete a class were drawn from the individual seasons in proportions which reflected the relative likelihood of recording winds of that class in each season.

The precise procedure employed in selecting records is best illustrated by means of an example illustrating the selection of records for a particular distribution class.

Example Selection of records for the class:

wind speed	11-16 knots
wind direction	50-70 degrees

The frequency of occurrence figure for this class, taken from the table of Figure C.1, was 1.65%. Multiplying by four and rounding indicates that seven records should be included in the subset from this class. The percentage frequency of occurrence figures listed in the seasonal distributions for this class (not reproduced here) were:

Winter	1.30%
Spring	2.22%
Summer	1.85%
Autumn	1.24%

The nearest one can get to a whole-number choice is two drawn from the winter months, two from the spring, two from the summer and one from the autumn, so as best to reflect the relative seasonal frequencies. It will be recognised that the precision to which the seasonal distributions could be matched was severely limited by the small number of observations involved (approximately 100) for each season. It was felt, nevertheless, that attempting to do so was an important aspect of the method in so far as it ensured that records were drawn from throughout the year in a realistic manner. This was particularly important to ensure that a representative sample of swell conditions was taken.

To select the two winter observations required for this class the previously

compiled wind tabulations for a winter month, say December 1976, would first be consulted. It is found that 35 observations fall into this class of speed and direction, of which 12 pertain to hours immediately preceding a wave recording period. Each of these would be allocated a serial number from 1 to 12 and a table of random digits consulted to decide which of them should be included in the subset. The second winter observation would then be selected in the same manner from the tabulations for January 1977; all subsequent selections for the winter season being taken from each of the 3 winter months in rotation.

A similar procedure was used to select records from the other seasons.

A wind observation was only finally included in the subset if reference to the results of the wave record validation for the month indicated that a valid associated wave record existed.

The distribution of all the winds measured at Benbecula during the year was such that it was generally possible to find sufficient wind observations to complete each class. Difficulty was, however, experienced at the upper end of the speed range (> 28 knots), since there were relatively few such observations in the year. It is also apparent that, since one observation in a set of 400 represents a frequency of occurrence of 0.25%, it was not possible to reproduce accurately the tail of the annual distribution. Both of these factors necessitated some departure from the distribution of Figure C.1. The final distribution of the subset winds is tabulated in Figure C.2. Rounding errors in seeking to match the distributions resulted in 399 rather than 400 records being selected.

The wave spectra observed at the same time as the selected wind records constitute the descriptive subset of wave conditions. Full details of these spectra may be found in Crabb (1978).

St Gowan

As mentioned in Section 1b, a similar procedure to that just described was used to extract a subset of records from the data recorded at the St Gowan light vessel. Certain detail changes in the procedure were necessitated by the fact that the shipborne wave recorder returns data in the form of a pen trace on a paper chart roll; these had to be rendered into digital form to allow calculations of the Fourier transform. The selected records were digitised by the image

analysis group in the Department of Nuclear Physics at Oxford University. Each record was photographed on to 70 mm film and the photographic copy digitised using 'PEPR', a computer-controlled, semi-automatic, optical digitising system. The very high resolution of this machine enabled digitisation with an accuracy somewhat better than half the width of the original pen trace. The optical scanning system used had, however, to distinguish the required pen trace from a background grid printed on each chart. This was achieved successfully for approximately 80% of the records, in the remaining 20% of the records there were small regions of the digital record which corresponded to lines in the background grid, rather than the required pen trace.

Each of the digital records was plotted to the same scale as the original chart, and the two were compared by superimposing the plot upon the original. Where the two did not match, the digital record was edited and the procedure repeated until a good match was achieved. The records were digitised at equal increments along the time axis, corresponding to a sample rate of 2 Hz. The vertical resolution of the digital records corresponded to approximately 1 cm elevation of the sea surface. (This is roughly in accordance with the variance of the calmest record in the set which in all probability is dominated by instrumental noise originating from the digitisation process.)

Each of the digital wave records was converted into a corresponding spectrum using a standard Fast Fourier Transform algorithm applied to the whole digital time series. No window function was applied to the time series. The spectral estimates were averaged 7 at a time, rendering smoothed spectra with a frequency resolution of 0.0097 Hz.

Each spectrum was then corrected for the instrument response using the formula

$$S'(f) = S(f).\left(0.83\left[1 + \frac{(2\pi f)^2}{77.44}\right]^{3/2} e^{(2\pi f)^2 d/g}\right)^2$$

where d was the depth of the pressure unit used in the recorder, S'(f) the corrected spectral estimate and S(f) the uncorrected spectral estimate. The correction formula results in large corrections at high frequency, and inspection of the corrected spectra revealed an unreasonable increase in S'(f) at high frequencies, presumably originating from instrumental noise. As, at high frequencies, the form of the spectrum is expected to tend to $S'(f) \propto f^{-5}$ each spectrum was plotted logarithmically and a straight line of slope -5 fitted to the spectrum at a frequency

below that at which unreasonable behaviour was displayed. The higher frequency spectral estimates were then replaced by the value obtained from the extrapolated straight line. This procedure is illustrated in Figures C.3a and C.3b. The frequency at which the f^{-5} 'tail' was spliced onto the original spectrum was chosen by eye so as to obtain as good a fit as possible to the original spectrum.

A full description of the resulting spectra and of the methods used in selecting them is presented in Crisp (1980).

Direction degrees / Speed knots	350–10	20–40	50–70	80–100	110–130	140–160	170–190	200–220	230–250	260–280	290–310	320–340	Totals
0													2.28
1–3	.47	.74	.75	.61	.58	.69	.54	.44	.35	.32	.39	.38	6.26
4–6	.97	.80	.80	.74	.74	.84	.89	.67	.66	.61	.67	.65	9.04
7–10	1.98	1.41	1.30	1.24	1.48	1.88	1.95	1.62	1.61	1.38	1.41	1.35	18.61
11–16	2.95	1.44	1.65	1.26	1.96	3.07	3.50	3.61	3.27	2.59	2.18	2.22	29.70
17–21	1.48	.57	.76	.51	1.05	2.04	2.32	2.29	1.84	1.69	1.25	1.11	16.91
22–27	.83	.30	.35	.21	.71	1.61	1.78	1.41	1.26	1.15	.96	.73	11.30
28–33	.22	.10	.09	.06	.24	.70	.59	.46	.38	.43	.38	.30	3.95
34–40	.06	.02	.01		.01	.27	.21	.17	.13	.20	.15	.10	1.42
41–47	.02					.03	.04	.02	.02	.06	.05	.03	.27
48–55							.01			.01	.01		.03
56–63													
Totals	8.98	5.38	5.71	4.63	6.86	11.13	11.83	10.69	9.52	8.44	7.45	6.87	99.77

Figure C.1 Distribution of observed hourly mean wind speeds and directions compiled for the area west of the Outer Hebrides

Direction degrees / Speed Knots	350-10	20-40	50-70	80-100	110-130	140-160	170-190	200-220	230-250	260-280	290-310	320-340	Totals
0													2.25
1-3	.50	.75	.75	.50	.50	.75	.50	.50	.25	.25	.50	.50	6.25
4-6	1.00	.75	.75	.75	.75	.75	1.00	.75	.75	.50	.75	.75	9.25
7-10	2.00	1.50	1.25	1.25	1.50	2.00	2.00	1.50	1.50	1.50	1.50	1.25	18.75
11-16	3.00	1.50	1.75	1.25	2.00	3.00	3.50	3.50	3.25	2.50	2.25	2.25	29.75
17-21	1.50	.50	.75	.50	1.00	2.00	2.25	2.25	1.75	1.75	1.25	1.00	16.50
22-27	.75	.25	.25	.25	.75	1.50	1.75	1.50	1.25	1.25	1.00	.75	11.25
28-33	.50				.25	.75	.50	.50	.50	.50	.25	.25	4.00
34-40						.25	.25	.50	.50		.25		1.75
41-47													
48-55													
56-63													
Totals	9.25	5.25	5.50	4.50	6.75	11.00	11.75	11.00	9.75	8.25	7.75	6.75	99.75

Figure C.2 Distribution of hourly mean wind speeds and directions associated with the selected set

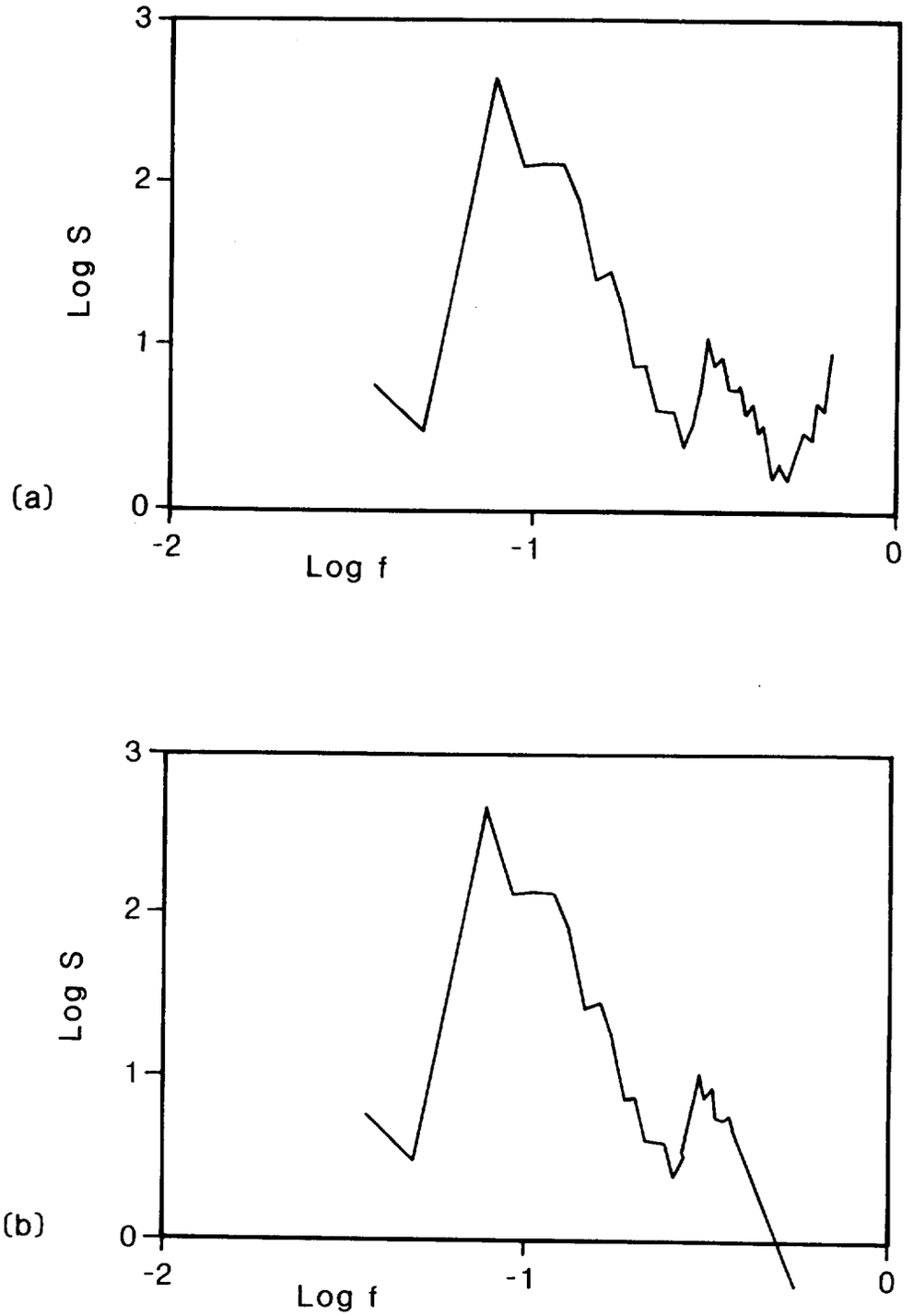

Figure C.3 a) Corrected SBWR spectrum showing the presence of high frequency noise.
b) The same spectrum fitted with a high frequency tail proportional f^{-5}.

APPENDIX D - Ascribing directional properties

At each component frequency of the wave spectrum the directional distribution of energy is assumed to be unimodal and symmetric about a mean direction $\bar{\theta}$, except for swell waves where a bimodal distribution is allowed if the meteorological conditions justify it. The form adopted to describe the distribution is that suggested by Longuet-Higgins et al (1963)

$$|\cos\tfrac{1}{2}(\theta - \bar{\theta})|^{2s}$$

where s may be a constant or a function of one or more variables. In cases where two swells occur at the same frequency, each peak of the distribution has this form.

The directional spectrum is viewed as the product of the one-dimensional frequency spectrum with a directional distribution (or spreading function) according to the following scheme:-

$$S(f,\theta) = S(f).G(s).|\cos\tfrac{1}{2}(\theta - \bar{\theta})|^{2s} \qquad (D.1)$$

where G(s) is a normalising function such that

$$\int_0^{2\pi} G(s).|\cos\tfrac{1}{2}(\theta - \bar{\theta})|^{2s} d\theta = 1 \qquad (D.2)$$

The allocation of directional characteristics to each of the 399 spectra amounts to determining suitable values for the spreading parameter, s, at each wave frequency. The various steps are described in the following sections.

Distinguishing between wind sea and swell

A simple model of the one-dimensional spectrum was adopted in which the local wind is assumed to be capable of generating waves with frequencies extending down to a certain lower limit, depending upon its strength and the fetch over which it blows. The remainder of the energy in the spectrum occurring at frequencies below this cut-off frequency was regarded as being due to swell advected from a non-local source.

The value of the cut-off frequency was estimated initially by attempting to predict, from a consideration of local meteorological conditions, the lowest frequency which could be present in the wind sea. Various empirical formulae and charts are

available which purport to relate the peak frequency of the spectrum to the wind speed, fetch and duration, and one such was selected and adapted for the purpose of predicting the cut-off frequency.

Although there was in general no clear visual distinction in the plotted spectra between the sea and swell regions, there were among the 399 selected spectra, 56 of a clearly bimodal form (Figure D.1 is an example), suggesting that in these cases the position of the lower frequency cut-off could be estimated directly. These cases were helpful in selecting a method to use on the other spectra, the choice from the various formulae being made by testing their ability to predict consistently the cut-off frequency in those 56 cases where an independent estimate could be made.

The estimates of the cut-off frequencies were finalised at a later stage after several opportunities to adjust the initial values had occurred. During the first pass through the data, therefore, the simplifying assumption that the development of a sea was limited only by virtue of inadequate fetch was made (the effect of limited duration being estimated later). Furthermore, the fetches used in the chosen procedure were "potential" fetches limited by the geometrically determined distance to the nearest coastline for each wind direction, rather than by the scale of the wind fields involved.

A procedure for predicting the cut-off frequency was chosed from those formulae considered by using each in turn to predict the frequency of the wind sea peak in each of the 56 test cases. The ratio of the observed cut-off frequency to the predicted peak frequency was then calculated in each case and the mean and standard deviation of this ratio over the 56 cases were calculated for each of the prediction methods. The method giving the smallest standard deviation about the mean ratio was selected and was used to compile a "forecasting" table relating cut-off frequency to wind speed and fetch.

The expression chosen was based on work by Inoue (1967), as reported by Silvester (1974), in which the development of the wave spectrum with increasing fetch was modelled by allowing the fetch to modify the values of the constants α and β in the Pierson-Moskowitz spectrum

$$S(f) = \frac{\alpha g^2}{(2\pi)^4 f^5} \exp -\beta\left(\frac{g}{2\pi U f}\right)^4 \qquad (D.3)$$

for fully developed seas

$$\alpha = 0.0081 \qquad (D.4)$$

$$\beta = 0.74 \qquad (D.5)$$

for seas where the actual fetch, F, is less than the fetch F_{FDS}, consistent with fully developed conditions at windspeed U

$$\alpha = 0.0081 (F/F_{FDS})^{-0.194} \qquad (D.6)$$

$$\beta = 0.1 \exp[(\ln 7.4)(F/F_{FDS})^{-0.284}] \qquad (D.7)$$

and differentiating gives for the spectral peak frequency

$$f_m = (0.8\beta)^{\frac{1}{4}} \frac{g}{2\pi U} \qquad (D.8)$$

Equations (D.7) and (D.8) constitute the model by which the spectrum peak frequency may be estimated using the values of wind speed and fetch. The value of F_{FDS} was calculated using a further empirical relationship

$$F_{FDS} = 3.19 U^{1.5} \qquad (D.9)$$

with F_{FDS} in nautical miles and U in knots.

It was found that this expression when given a wind speed equal to the mean speed during the 12 hours preceding the wave recording period, and a fetch equal to the fetch obtaining during the hour immediately prior to the period, gave the most consistent predictions of the cut-off frequency in the 56 test cases.

The procedure was then modified for use on the complete subset of spectra to allow a more detailed consideration of the meteorological circumstances in each case. To this end computer files of mean wind speed and direction for each hour of the year were compiled and a computer program used to list the values of wind speed,

direction and associated fetch for each of the 24 hours preceding the time of each selected spectrum.

This procedure revealed the way in which the wind speed and fetch fluctuated prior to each spectral observation and permitted more realistic choices of speed and fetch than those initially used. These values were then used in conjunction with the previously compiled forecasting table to make individual predictions of the cut-off frequency for each of the selected spectra. The duration of wind conditions also became apparent and allowance for any effect on the cut-off frequency was made by determining what reduced value of fetch was equivalent to that wind duration, and then entering the forecasting table with this value.

The effectiveness of this more detailed procedure was apparent on reinspection of the 56 test cases, where it reduced from 23% to 11% the standard deviation of the ratios formerly obtained in the simple prediction model.

Old Wind Sea

During this procedure it became apparent that in addition to wind sea and swell, a further wave category was justified. This arose when the 24 hour wind speed and fetch listing showed that a significant change in wind speed or fetch length had occurred shortly before the wave measurement in question was made. Under these circumstances the sea generated prior to the change in conditions could still be propagating past the recorder from further up the original fetch, whilst the current (changed) wind conditions would have started to generate a second wind sea. Energy in the former category was called "old wind sea". The upper frequency limit of this category was taken to be the lowest frequency which the most recent wind was capable of generating under the fetch and duration conditions pertaining. The lower frequency limit was less straightforward and depended on circumstances; it could not be lower than the lowest frequency which the former wind conditions were capable of generating, but it could be considerably higher. In the interval following the change in conditions the waves generated over the previous fetch will propagate past the recorder, the faster lower frequency waves clearing the area first. The lowest frequency in this category still present at the time of the wave observation depends, then, on the previous fetch length and on the time elapsed since the change in conditions. A value for the lower frequency limit was calculated from these considerations.

Estimating the directional characteristics

Each spectrum was divided into one or more regions according to the scheme described above. Directional characteristics were ascribed separately to each in the following way.

Wind sea

As stated previously, the form adopted for each portion of the directional spectrum was that described in Equation D.1. In the case of the wind sea portion, values were determined for s by reference to an empirical formulation due to Mitsuyasu et al (1975) viz.

$$s = 11.5\,\tilde{f}^{-2.5} \quad ; \quad \text{for } \tilde{f} > \tilde{f}_m \tag{D.10}$$

and

$$s = 11.5\,\tilde{f}_m^{-7.5}\tilde{f}^{5.0} \quad ; \quad \text{for } \tilde{f} \leq \tilde{f}_m \tag{D.11}$$

where $\tilde{f}$, the non-dimensional frequency is defined by

$$\tilde{f} = \frac{2\pi f U}{g} \tag{D.12}$$

where f is wave frequency

U is wind speed

f_m is spectral peak frequency

The mean direction is taken to be that of the wind.

Old wind sea

The value of the spreading index for the old wind sea portion of the spectrum, where this category exists, was fixed at s = 6 for all frequencies. This fairly wide distribution is probably appropriate to a decaying sea of this nature. It is equavalent to the $\cos^2(\theta - \bar{\theta})$ distribution often used in the literature.

Swell

The form of the swell portion of the directional spectrum was again that of Equation D.1. In this case the value of s depends on the geometry of the meteorological situation. In particular it was necessary to identify the area of strong winds responsible for generating the swell observed on a particular occasion.

The angle subtended by a wind field of width, W, and at distance, D, from the wave measuring site may be calculated.

This angle may then be equated to a characteristic width of the $\cos^{2s}\frac{1}{2}(\theta - \bar{\theta})$ distribution, thus allowing s to be determined as a function of W and D. The characteristic distribution width chosen was the width of a rectangle of the same height and area. This results in

$$s = \frac{\pi}{(\tan^{-1}\frac{W}{2D})^2} \qquad (D.13)$$

The mean direction was taken to be the bearing of the centre of the wind field. In the case of the South Uist data the search for the generating region, or regions, was aided by the quantity and continuity of the wave data. The spectral data collected during the first year have been presented as a contoured time series of spectral density values, Fortnum et al (1979), and a short section is illustrated in Figure D.2. On the working sheets, Figure D.3, the occasion of each of the selected spectra was marked by a vertical line positioned at the appropriate point on the time axis. A section taken along this line through the surface represented by the contours, would produce the spectrum recorded on that occasion. On each of these lines was marked, in the appropriate position, the previously determined cut-off frequency dividing wind sea from swell energy, these are shown as crosses in Figure D.3.

In the present context the features of direct interest are the contour ridges with positive slope, indicating an increase with time of the frequency associated with the energy peak. This is consistent with the observation of the arrival of swell from a distant source; the dispersive property of waves ensuring that the lower frequency waves generated at some distance, D, arrive before those of higher frequency.

Waves of frequency, f, generated at time, t_o, having a group velocity

$$Cg = \frac{g}{4\pi f} \qquad (D.14)$$

arrive at the recording site at time t where

$$(t - t_o) = D\,\frac{4\pi f}{g} \qquad (D.15)$$

whence

$$\frac{df}{dt} = \frac{g}{4\pi D} \qquad (D.16)$$

and

$$t = t_o \quad \text{when} \quad f = 0 \qquad (D.17)$$

The slope of the line defining the ridge peak is therefore inversely proportional to storm distance, and the intercept on the abscissa indicates the generation time, Figure D.1. In principle this information should allow the storm to be identified on the relevant meteorological chart. Similar procedures based on this form of presentation have been used previously for the identification of swell sources, Snodgrass et al (1966), Munk et al (1963), Cartwright et al (1977). In those studies, however, spectra with a higher frequency resolution were obtained by analysing data recorded over longer periods (3 hours, 3½ hours and 1 1/4 hours, respectively) than the relatively short records taken in this long term routine collection programme. Consequently the plots used here are comparatively coarse and not ideally suited to reproduce the fine structure of spectra at low frequencies. This problem was exacerbated by a degree of smoothing introduced by the program used to contour the data. Even so, they offered the best opportunity available to tackle this difficult aspect of the method. The difficulty introduced by the poor definition of the swell ridges was partially overcome by approaching the problem in a manner similar to that employed by Cartwright (1977). Rather than attempting to determine the orientation of the ridges with sufficient precision to allow the ridge lines to be drawn in, meteorological charts covering the entire period were inspected for regions of high winds directed towards the site which could be possible sources of the observed swell. Midday and midnight charts covering the North Atlantic were obtained and individually searched for promising wind fields. A transparent overlay showing the pattern of great circle lines intersecting at the site (along which swell would propagate) was used to aid the search. All windfields with winds of greater than 20 knots directed along these lines were noted; the wind speeds, U_s, being determined either from plotted ship observations or from the geostrophic wind, U_g, determined from the isobar spacing. Surface winds were generally calculated from the approximate expression Pore et al (1969) and Shore Protection Manual (1977).

$$U_s = U_g \times 0.6 \qquad (D.18)$$

Lines were then plotted on the contoured charts consistent with the data and distance of each storm thus identified, Figure D.3. Lines which best matched any discernable ridge features were taken as indicating a link between the windfield and the observed swell. In many cases, however, the swell ridges were indistinct and displayed no clearly discernable orientation or structure; large numbers of storm lines were also often present making the matching of storm line to swell a difficult, and somewhat subjective, task. It was often necessary to re-inspect the meteorological charts to check for over-looked windfields, or to re-assess various interpretations of complex meteorological situations. A choice between contending storm lines could sometimes be made on the basis that the wind strength should be consistent with the wave frequencies present in the swell ridge. Following Cartwright, the approximate expression

$$f_p = \frac{g}{2\pi U_s} \tag{D.19}$$

relating the swell energy peak frequency, f_p, to the wind speed was used.

In an attempt to reduce the subjective element in a sometimes difficult procedure, a flow chart, describing the steps to be followed under the various circumstances encountered, was drawn up. In spite of these efforts, however, there were some cases in which no satisfactory match could be made, and here directional characteristics were ascribed in a more pragmatic manner (see below). On some occasions where the swell conditions showed no distinct ridge structure, two swells from different sources appeared to be contributing to the energy, and both were noted. Such occasions were relatively few in number.

During this detailed inspection of the contour plots it was noted that the previously plotted wind sea cut-off points were largely consistent with the character of the wave energy revealed by the contour plots. Rapidly growing wind seas could be discerned as well defined ridge structures with negative slope, indicating a movement of energy from high to low frequencies with time. On one or two particularly convincing occasions the plotted cut-off points neatly skirted the lower edge of such features, as in the left hand part of Figure D.3. In some cases, however, the position of the cut-off point was apparently in conflict with the evidence of the contour plots. In these cases the meteorological charts and the hourly mean wind time histories were re-inspected to determine whether adjustments in the cut-off frequency were justified.

In cases where two swells were identified as contributing, each swell was allocated its appropriate mean direction and directional width, the total energy in the swell band was shared between the two in proportion to the angle subtended and to the fourth power of the wind speed.

As mentioned before, there were occasions on which it proved impossible to associate observed swell energy with a generating windfield. This usually arose when the swell energy was not associated with a clearly defined ridge on the contour plots. It is probable that, under these circumstances, the observed swell was due to a number of low intensity sources. Consequently it seemed appropriate to ascribe a fairly wide angular distribution in such cases. A value of $s = 6$ was chosen, being approximately equivalent to the $\cos^2(\theta - \bar{\theta})$ distribution which has sometimes been used by other workers. The mean direction was taken to be the same as that identified in the observation immediately preceding the case under consideration. It was hoped by this means to ensure a realistic distribution of mean direction among these difficult cases.

Forming the directional spectrum

The directional spectra were formed by recombining the regions of the spectrum. The final resolution in frequency was identical to that in the original one-dimensional spectra, and the angular distribution functions were evaluated at 10° intervals. At the boundaries between swell, wind sea and old wind sea regions a simple procedure was employed to prevent the occurrence of discontinuities in the final spectrum. The energy in the frequency class within which the boundary fell was spread half according to the directional distribution on one side of the boundary and half according to that on the other.

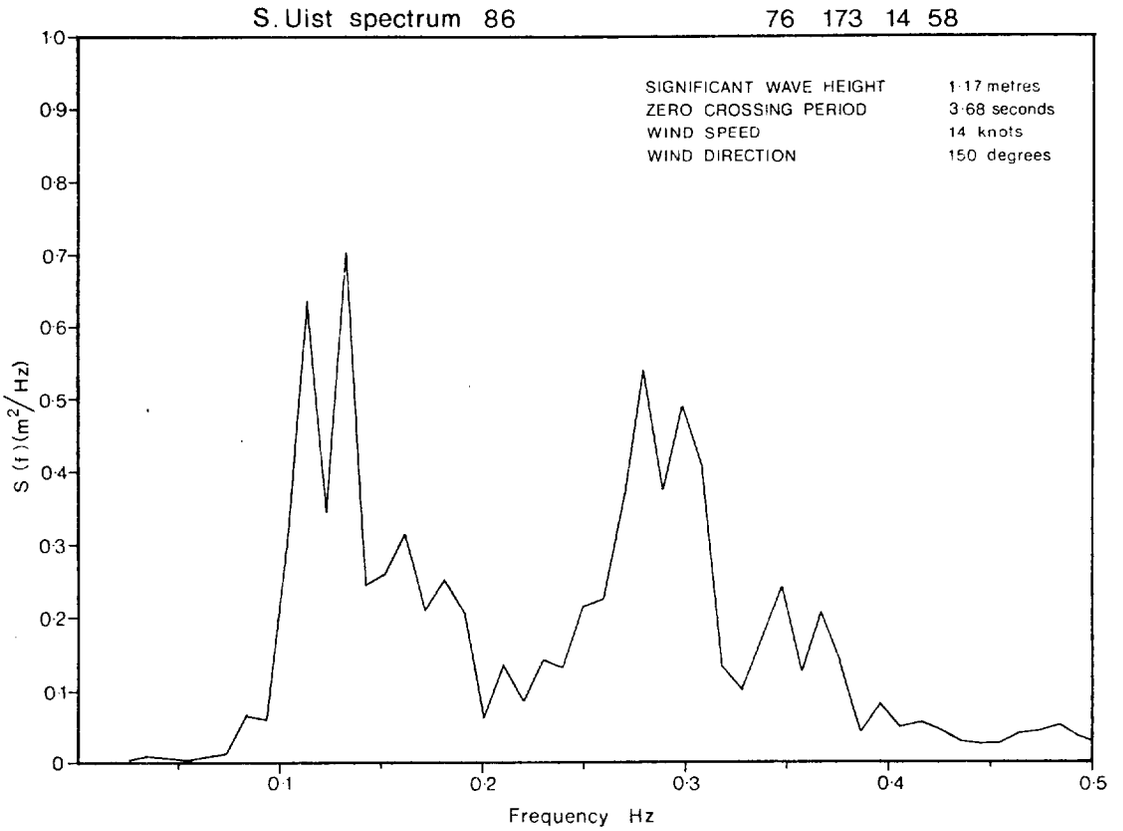

Figure D.1 Example of a bi-modal wave spectrum observed at South Uist offshore (45 m) position.

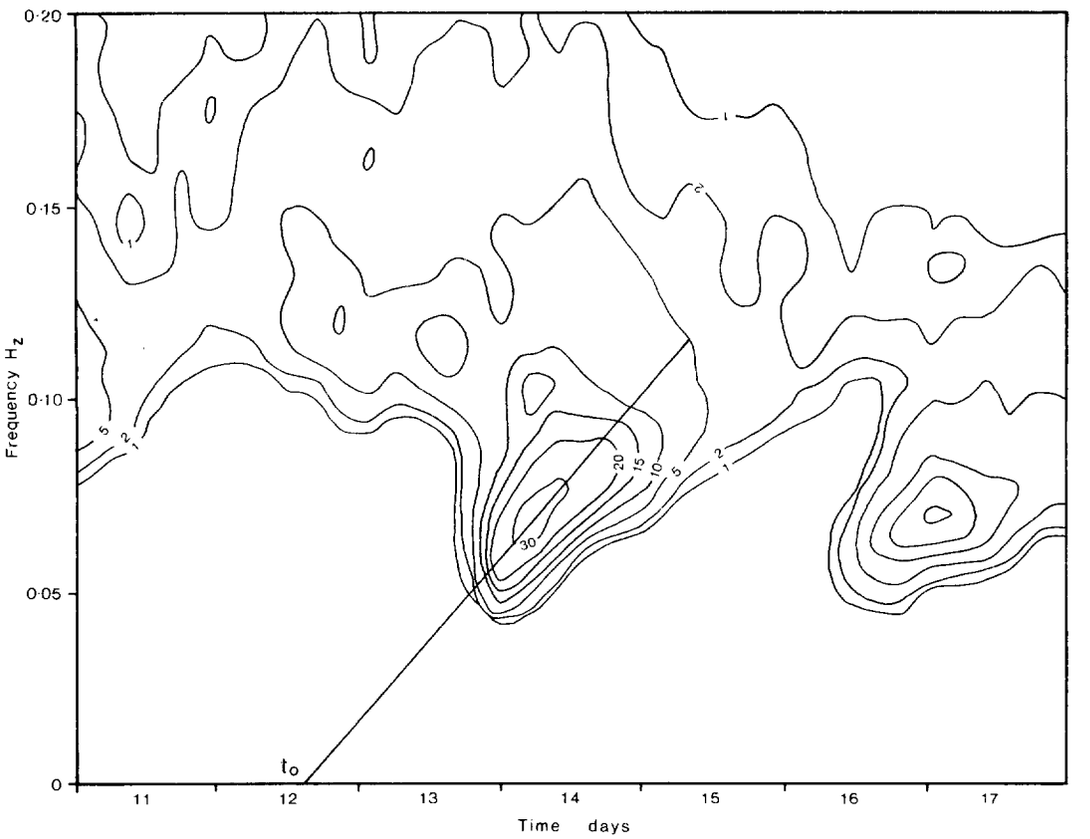

Figure D.2 South Uist offshore (45 m). Contoured time series of spectral values.

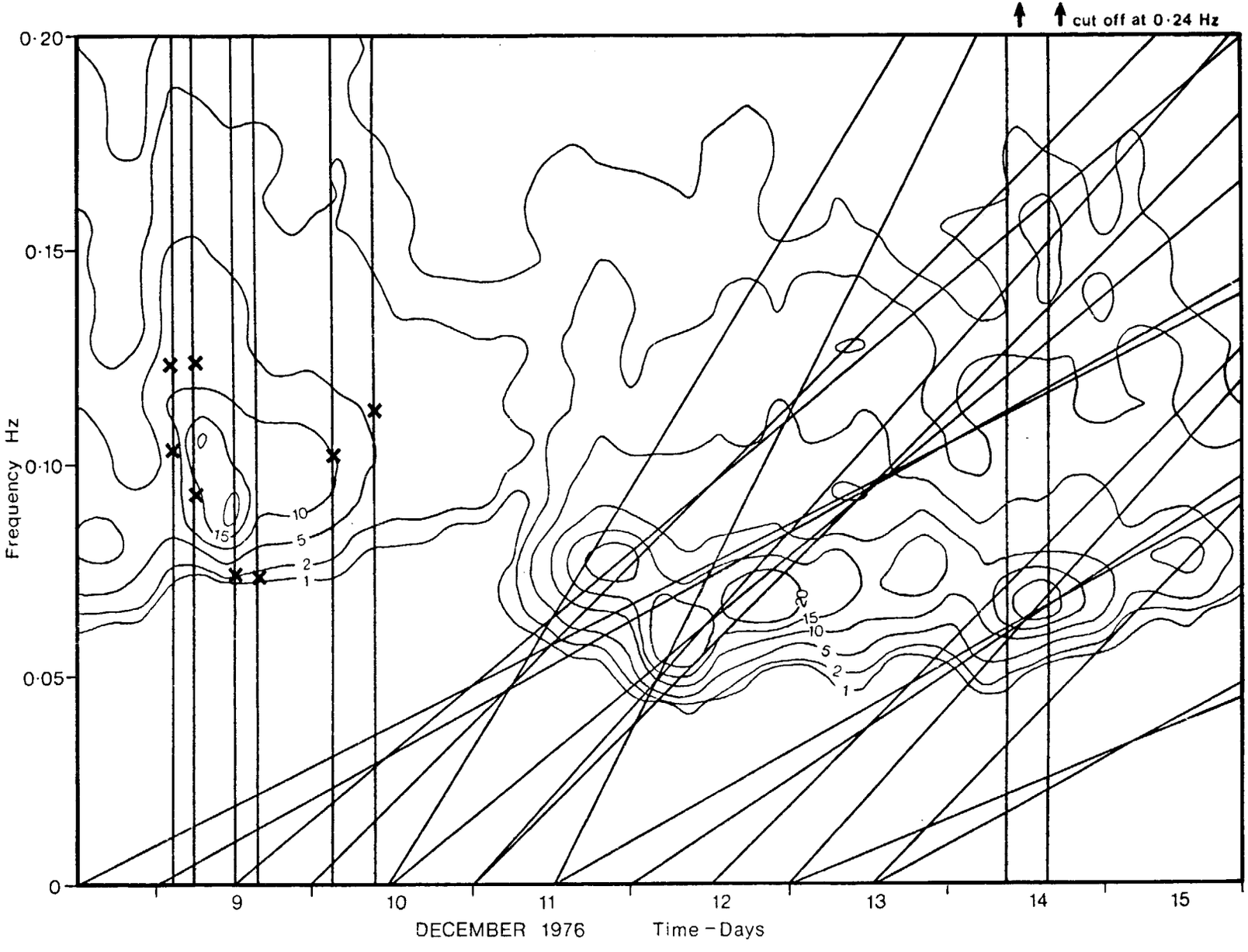

Figure D.3 Contoured time series of spectral values - example of working sheet.

APPENDIX E - Description and results of an experiment conducted to check the reliability of the directional synthesis method

The contents of this appendix are an abbreviated version of a report on this experiment produced shortly after its execution, Crabb (1980).

1. The Measurements

1.1 Waverider

The installation of the Waverider buoy and shore receiving station at the Scilly Isles have been fully reported on by the contractor, Flight Refuelling Ltd (Young 1979). The Waverider measures the instantaneous water surface elevation and transmits this information continuously to shore. At the receiving station the data were recorded for 1044 seconds every three hours, both in digital form and on paper chart roll. The digital logger at this station was fitted with a switch which allowed the routine three hourly recording sequence to be interrupted and a record of arbitrary length to be taken, on both the digital logger and the paper chart roll, at the time of an aircraft measurement.

1.2 Aircraft

A towed target body was fitted with a radar altimeter and attached to the towing winch of a Canberra aircraft by a combined towing and data link cable. The target also carried an accelerometer, and both the vertical acceleration of the target and the target height above the sea surface were recorded on an analogue FM tape recorder aboard the towing aircraft. On a typical sortie over the Waverider buoy the target was towed at an altitude of approximately 15 metres at a speed of 125 metres/sec. An 80 second record of the sea surface profile was taken in each of 8 different directions.

Data tapes were returned to the CI Data Centre for processing along the lines reported by Machin (1974). The accelerometer signal was doubly integrated to yield the vertical displacement of the target, this was subtracted from the target height signal to yield the sea surface profile. Experience with this system had led to the conclusion that some residual target motion still contaminated the signal at this point, and the signal was thus filtered with a digital high pass (W_o = 0.15 Hz) to remove it. Unfortunately, this process undoubtedly removed some legitimate wave energy at the same time. The consequences of this are discussed in a later section. Data were finally presented to IOS as magnetic tape files of sea surface profile digitized at 0.05 second intervals.

A total of 9 successful sorties were made as detailed below:-

Date	Time	Wind Speed knots	Wind Direction	Visually estimated mean wave direction
24.7.78	1206	7	250°	290
14.3.79	1200	24	030°	010
15.3.79	1200	15	030°	020
21.3.79	1120	20	300°	305
26.3.79	1155	20	280°	300
28.3.79	1200	25	340°	350
29.3.79	1500	25	350°	350
23.4.79	1335	20	270°	200
24.4.79	1225	25	330°	300

2. Estimating the Directional Spectra at the Scilly Isles site

2.1 Data available

Three hourly digital recordings of the Waverider signal were obtained routinely during April, but a failure of the digital recorder, not discovered until the tape was read, meant that paper chart records only were available during March. Individual records corresponding to the aircraft sorties were extracted from the charts and rendered into digital form. The record taken on 24 July 1978 was not used, and the record for 29 March 1979 could not be digitized because of an intermittent ink trace. Thus a total of seven from a possible nine measurements were used in this analysis. Because of the lack of routine data for March it was not possible to produce a contoured spectral plot to aid swell identification for this period. One-dimensional spectral data were, however, available from the DB1 location and these were used to produce a substitute plot.

The data available for the analysis are summarised in the following chart

Data Source	Date 5 10 15 20 25 30 5 10 15 20 25 30 March 1979 April 1979
Overflights	– – – – – – – –
Scilly wave data	– – – – – – ———————
Scilly wind data	———————————————
DB1 wave data	——————————— – –
DB1 wind direction	———————————
DB1 wind speed	None

2.2 Forming the directional spectrum estimates

To render the estimation procedure as used at South Uist suitable for use at the Scilly Isles site, it was necessary to 're-tune' the procedure previously used to divide the spectra into wind sea and swell regions. This modification entailed plotting all the one-dimensional spectra from the Scilly Isles buoy for April and using those displaying clearly defined wind sea and swell peaks to adjust the algorithm.

The Waverider records taken at the time of each overflight were divided into 1024 second sections and transformed section by section into energy spectra. These records had been taken by site personnel (HM Coastguard) switching the recorder on when the aircraft arrived in the area and switching it off when it left. Consequently the records were of variable length, comprising from one to three 1024 second sections. All data available for each overflight were used to produce a mean one-dimensional spectrum for each occasion.

Each spectrum was divided into wind sea and swell regions and directional properties ascribed as previously described.

It is unfortunate for the generality of this series of checks that the above procedure revealed that no significant swell component was present on any of the overflight occasions. Although this may be regarded as a significant shortcoming it does mean that the lack of routine wave data for March is not in practice of any importance.

3. The Comparisons

The comparisons made between estimated and measured quantities are presented below

and the results discussed.

It is perhaps worth stating at the outset that a problem common to all these comparisons is the difficulty in establishing the degree of legitimate variation to be expected between separate samples from the same population. That is to say, in establishing whether or not the observed difference between two values of a quantity indicates a significant difference between the underlying processes from which they were drawn.

3.1 Comparison of measured and estimated encounter spectra

The measured sea surface profiles, as supplied by the CI Data Centre, were each plotted on a VDU screen and visually inspected for the presence of spurious spikes. Large amplitude spikes were found in some records and were edited out. It must be accepted that such an inspection procedure could have overlooked other errors which, due to a lack of familiarity with such data, were not recognised. A Fourier spectrum was then calculated for an 80 second section of each profile record. Some records were not as long as this and were consequently not considered. These spectra are the measured encounter spectra.

Estimated encounter spectra for comparison with these measured spectra were then calculated from the directional spectra estimated for the time and date of each overflight.

The encounter spectrum is derived from the directional spectrum (Cartwright 1963) using the fact that each element $E(f_i, \theta_i)$ of the directional spectrum has an apparent frequency to an aircraft flying at speed V and direction $\emptyset$, of:-

$$f_i' = f_i - \frac{V\cos(\theta_i - \emptyset)}{\lambda_i}$$

where λ_i is the wave length calculated according to the dispersion relation.

A computer program was written to transform the energy of each element of the estimated directional spectrum to the appropriate point on the encounter frequency axis. The performance of this program was checked against an analytical solution for the simple case of a Pierson-Moskowitz spectrum spread by a $\cos^2(\theta - \bar{\theta})$ function (Hammond and McClain 1980), and was found to compare well except for a slight excess energy allocated by the program to the lowest encounter frequency. Using this

program, encounter spectra were calculated for each overflight using values of V and $\emptyset$ (corrected for wind drift) reported by the flight crew. In this abbreviated version of the original report Figures E.1 to E.10 show pairs of estimated and measured encounter spectra for each low level run from the first three sorties flown. Note that, for economy in drawing, only the first of these plots is fully annotated but the details are the same for all the remaining figures.

3.2 Initial discussion of the comparison

When originally plotted a consistent discrepancy was apparent between measured and estimated spectral densities at mid and high frequencies. It was assumed that a systematic error in one or both of the measurement systems was responsible. The discrepancy (-1.1dB) is clearly seen in Figure E.11 which plots the average value of the ratio of aircraft to estimated spectral density at each frequency. The average value of this ratio was determined over a range of mid-band frequencies and the aircraft spectra were multiplied by a factor of 1.29 to compensate for the discrepancy.

Implicit here is the assumption that the Waverider measurements, on which the estimates are based, provide a more reliable indication of wave height than do the altimeter results. Figures E.12 and E.13 show how the mean square waveheight (m_o) measured on each aircraft run compares with the same quantity measured simultaneously by the Waverider.

Figures E.1 to E.10 which incorporate the adjustment to the aircraft spectra, show a fairly consistent deficiency in the aircraft spectra at low frequencies, this again is clearly seen in Figure E.11. It was mentioned in Section 1.2 that a high pass filter was used to remove residual target motion from the aircraft data. The empirically determined shape of the filter response is shown superimposed upon the data points of Figure E.11*, and it appears probable that the application of this filter was largely responsible for the observed deficiency.

---

* The filter response curve as actually determined was displaced by +0.68dB relative to the curve shown in Figure E.11. The curve did thus not level out at 0dB as might be expected, but at -0.42dB. The filter was therefore a contributing factor to the overall -1.1dB discrepancy noted above, the remainder being presumably due to a calibration inconsistency. The comparison of the filter response and the data is correctly shown in the Figure, since the curve position chosen is equivalent to eliminating the effect of the supposed calibration error. The shape of the filter response was initially determined empirically by evaluating its effect on the specrum of a random number series. Confirmation of the shape was later obtained analytically by my colleague Dr G N Crisp.

The presence of the spurious target motion which the filter was intended to remove is also apparent at the two lowest frequencies, where the measured to estimated spectral density ratios exceed those which would be predicted by the filter response alone. The low frequency region of the measured encounter spectra appears then to contain both wave energy and energy due to residual target motion, both of which have been reduced by the application of the filter. Some of the increased variability, as evidenced by the width of the error bars, at low frequencies may be due to this fact. It is not possible under the present scheme to separate these two components. Given this difficulty it is not possible to determine the true degree of agreement between the estimated and measured encounter spectra at low frequencies. An improved scheme for removing target motion from the measured profiles has recently been suggested (Salmond 1979) and this could be applied to the raw data. It would appear, however, that the difficulty is fundamental and any comparison of encounter spectra is bound to be as much a test of the procedure used to remove target motion as of the procedure used to estimate one of the compared quantities. At frequencies outside this lower frequency range the agreement is seen to be generally good. Confidence limits are readily calculable for the aircraft spectra and are marked on the first of the plots. They are not so readily determined for the estimated spectra and this point will be more fully discussed later. The significance which may be attached to the degree of agreement obtained was investigated by a series of calculations designed to demonstrate empirically the sensitivity of the encounter spectrum to changes in various properties of the associated directional spectrum, the results of these calculations are described in the following sections.

3.3 Effect of errors in estimating mean wave direction

An estimated directional spectrum was chosen at random for this test and encounter spectra corresponding to ten different profiles at 10° intervals were calculated. A selection of these is plotted in Figure E.14. The result of wrongly estimating the mean wave direction would be to ascribe a direction to each estimated encounter spectrum which did not correspond with the true surface direction. Each encounter spectrum measured by the aircraft, where the true direction is known, would then be compared with an estimated spectrum calculated for a different direction. The likely effect of such a discrepancy may be seen by inspecting the difference between encounter spectra for different directions. It is apparent that the difference between spectra separated by 20° is not great, and consequently it must be concluded that, in this example at least, the estimated encounter spectra are

not very sensitive to the accuracy with which the mean wave direction is estimated.

The effect of deviating from the mean direction is to move energy progressively to lower frequencies. The effect on spectral shape is not great when the spectra are initially rich in low frequency energy. The effect would be more marked if the encounter spectrum in the mean direction contained little energy at these frequencies.

3.4 Effect of errors in estimating directional spread

The effect of errors in the estimated width of the angular distribution of wave energy were investigated by producing a simple model directional spectrum; in this case a Pierson-Moskowitz one-dimensional spectrum spread by a $\cos^n\theta$ function, where n was given values from 2 to 20. The resulting encounter spectra for a range of n values, at a fixed direction of 60° from the mean, are shown in Figure E.15. Again it may be seen that the encounter spectrum is not very sensitive to the angular spread of wave energy.

3.5 Effect of variability in the measured Waverider spectra

A further source of possible disagreement between measured and estimated encounter spectra is to be found in the statistical variability of the Waverider spectra used as the basis for the estimates. As described in Section 1.2 the original Waverider records were not of a fixed length and were divided into a number of 1024 second sections for the calculation of the spectra. Up to three such spectra were available for each flight and a mean of all those available was used. Using the component spectra individually, however, led to differences in the resulting encounter spectra as shown in Figure E.16. Thus the sampling variability in the Waverider spectra is to a certain extent manifest in the estimated encounter spectra, and in considering the plots an allowance must be made for possible legitimate differences from this cause.

3.6 Discussion

Inspection of the plots of Figures E.1 to E.10 reveals that over the mid and high frequency ranges, the agreement between estimated and measured encounter spectra is generally good within the limits of the expected statistical variability. In the light of the simple sensitivity test previously described, it must be said that this degree of agreement does not reveal a great deal concerning the accuracy of the estimated directional spectra from which the encounter spectra were derived.

The difficulty involved in interpreting the results at low frequency has already been discussed in Section 1.2. In view of the inconclusive nature of these comparisons other ways were sought to establish the accuracy of the estimated directional spectra; these are described in Sections 4 and 5.

The results of the encounter spectra comparisons and the sensitivity tests do, however, indicate that the encounter spectrum is probably a very robust quantity and not oversensitive to moderate changes in the directional properties of the waves. If, as indeed seems likely, the encounter spectrum and the closely related wave number spectrum prove to be important quantities for device design, we may expect to be able to measure or estimate its form to a relatively high degree of accuracy using simple techniques. In this sense the insensitivity of the encounter spectrum to the detailed directional properties of the waves is advantageous as far as its use in engineering design is concerned. The questions which remain to be addressed are, which properties of the encounter spectrum are relevant in this application and are these suitably stable also?

4. Comparisons with DB1 data

A separate attempt to determine the quality of the estimated directional spectra was made by comparing mean wave directions and directional spreads with those measured by DB1. Although DB1 is moored some 260 km to the south west of the Scilly Isles site, it is reasonable to expect that, under suitable meteorological conditons, directional properties there would be a reasonable indication of those likely to be experienced to the west of the Scilly Isles. This would not be the case when an incoming swell train had arrived at DB1 but not reached the Scillies. Likewise a meteorological front positioned between the two sites would imply different wind and thus wave directions. Wave conditions resulting from winds blowing from the arc 60° to 90°, where the fetch at the Scillies is very limited, would also be dissimilar at the two sites. There is no indication that any of the above limitations apply on the occasions for which the comparisons were made.

Figures E.17 and E.18 show comparisons between the mean wave directions measured at each frequency by DB1 and those estimated at the Scillies site. The region within which the majority of the spectral energy lies is marked on these plots by dashed vertical lines. It may be seen that the agreement is generally good to within 20° or 30°. It is relevant to note that the sensitivity test described in Section 3.3 would indicate that even if this degree of discrepancy represented

actual errors in estimated mean wave direction, and not just a real difference in conditions at the two sites, the effect on the encounter spectra would be small.

Figures E.19 to E.24 show comparisons between the spreading index, s, estimated at each frequency for the Scilly Isles spectra, and those measured by DB1. Again, the region of significant energy is marked.

In this series of plots the values of s for the Scilly Isles have been estimated as previously described. The analysis of DB1 data, however, gives rise to two separate quantities, s_1 and s_2. Both are functions of the coefficients of the angular harmonics of the directional distribution (Longuet Higgins et al 1963). If the unimodal $\cos^{2s}\frac{1}{2}(\theta - \bar{\theta})$ model, adopted in both the standard DB1 analysis and in the present procedure, is a good representation of the actual directional distribution these two quantities should be equal. Both s_1 and s_2 are shown in the figures, and it is the mean of these two quantities which should be compared with the estimated s, though for higher values of s, s_2 is generally the more reliable value.

In considering these comparisons it is again not clear what degree of similarity one may expect at these diverse locations. A complicating factor is the fact that wind speed is used to determine the value of s in the estimated case and, during the period considered, the wind speed sensors on DB1 were inoperative. The quantity s is a sensitive function ($\propto u^{-2\cdot5}$) of wind speed (Mitsuyasu et al 1975), and for these comparisons it would have been more appropriate to use wind speeds measured at DB1 rather than those at the Scilly Isles in its determination. Part, if not all, of the observed discrepancy may be due to the difference in wind speeds as measured onshore and those actually experienced at sea. Ewing (1980) has found that offshore winds in the region of the Hebrides were greater than those measured at Benbecula by an average factor of 1.29. Since the uncorrected shore based winds were actually used in the estimation of wind sea directional widths in the main Hebrides study, the discrepancies apparent in the plots presented here may also be inherent in the spectra of the selected set. There is then, some reason to suspect that the values of wind sea directional spreads incorporated in this set may be too narrow.

Furthermore, the simple way in which directional properties were ascribed to the swell portions of the selected set spectra may also give rise to over narrow

estimates of directional spread. This is because such relevant factors as the movement of generating storms whilst transmitting swell to the site, and the possibility of the presence of a number of low intensity sources on any given occasion were ignored.

The simplest way to at least partially compensate for this unquantifiable tendency to narrowness, would appear to be to abandon the directional resolution of 10° to which the spectra were originally evaluated in favour of a 30° resolution. The smoothing effect of this procedure renders the directional distributions less narrow in appearance. Preliminary discussion with some potential users indicated that this would in any case be their preferred resolution.

5. Discussion

The main conclusions drawn from the comparisons previously presented are firstly that the intended prime test quantity, the encounter spectrum, has not proved to be a sufficiently sensitive function of the directional properties of the wave spectrum. This, combined with the difficulties experienced with the measurements at low frequencies, has meant that no conclusive statement on the quality of the estimated directional spectra can be made on the basis of these comparisons alone. Secondly, comparisons made with the DB1 measurements suggest that the estimated mean wave directions would be in good agreement with those which might have been measured at the site, but that the procedure has resulted in a tendency towards over narrow distributions of energy with direction. A simple strategy whereby the worst effects of this error may be mitigated has been suggested.

The one obvious shortcoming in this evaluation procedure has been the lack of observed swell. This means that the ability of the procedure to estimate the directional properties of this most significant portion of the wave spectrum remains largely untested. A separate consideration of a 'swell ridge' appearing in the DB1 contoured spectral data on the 16 and 17 March produced an estimated mean direction of 270° compared with 273° obtained from the low frequency DB1 measurements. The estimated directional width on this occasion was 15° compared with a measured width of 58°. This isolated example is of course not a reliable general indication of a trend but, in so far as it goes, tends to reinforce the previous conclusion regarding wind sea mean directions and widths.

A separate approach to the evaluation of the selected set as an indicator of the

main properties of the South Uist directional wave climate is to compare it with estimates from other sources. Comparisons with the results obtained from the Meteorological Office wind-wave model presented in Section 2a indicate very close agreement on annual average power, and an encouraging similarity in the shape of the directional distribution of power.

A further broad confirmation of the representativeness of these results was obtained from a consideration of data from OWS Lima (Crabb 1979), which suggested that the mean annual average power at South Uist should lie in the range 45.7 to 54.0 kW m^{-1}.

Such evidence as is available points to the selected set being an acceptable first estimate of the long term wave characteristics at the South Uist site. This is not to say that, on every occasion, individual spectra reproduce exactly the conditions which might have been measured but that, given the in-built constraints of the procedure, each spectrum is an inherently reasonable possible outcome of prevailing conditions.

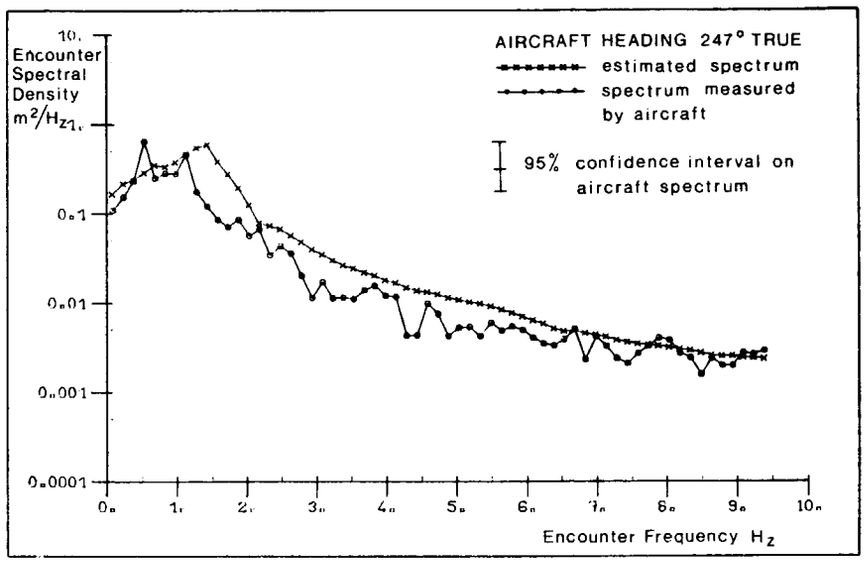

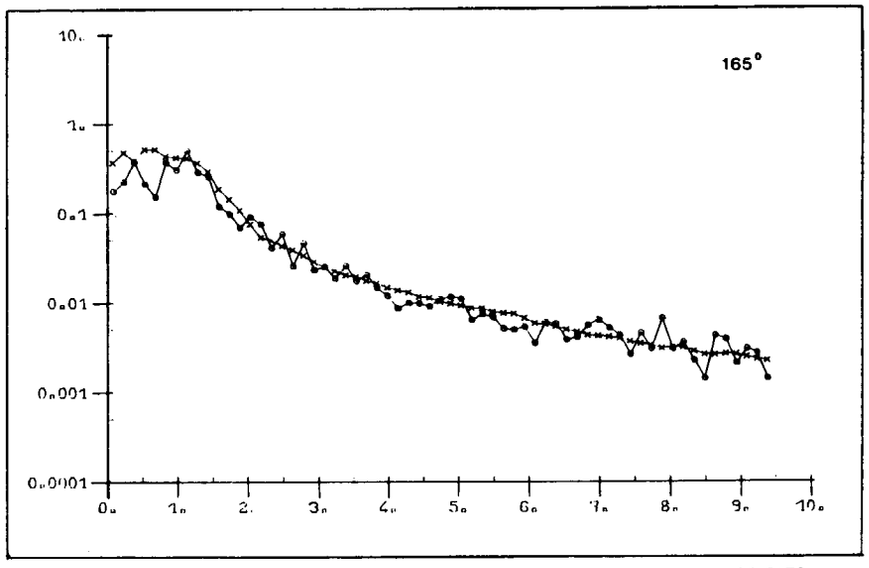

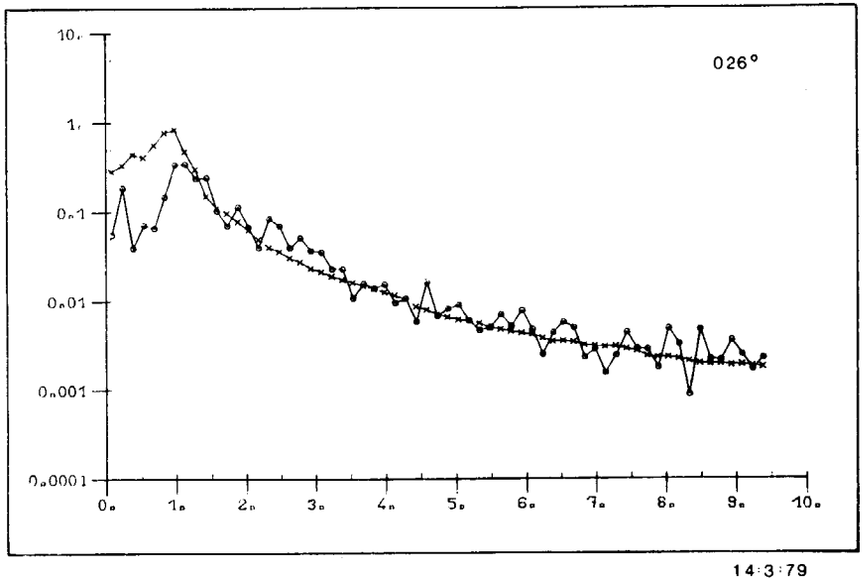

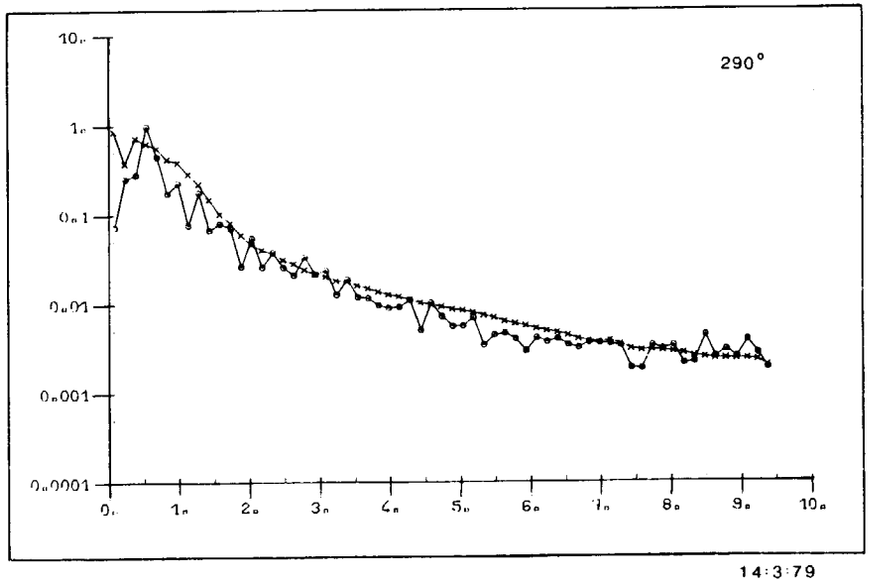

Figure E.1-2 Comparison of predicted and measured encounter spectra (details as figure E.1)

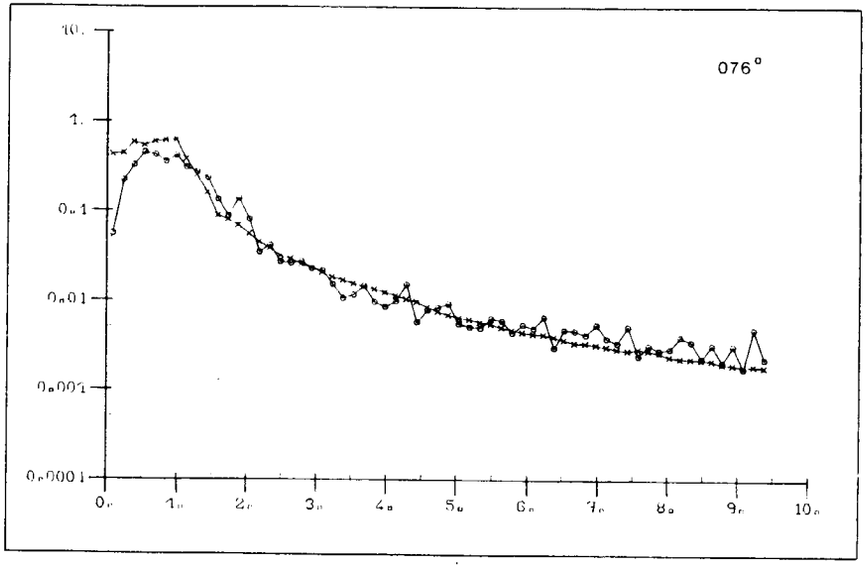

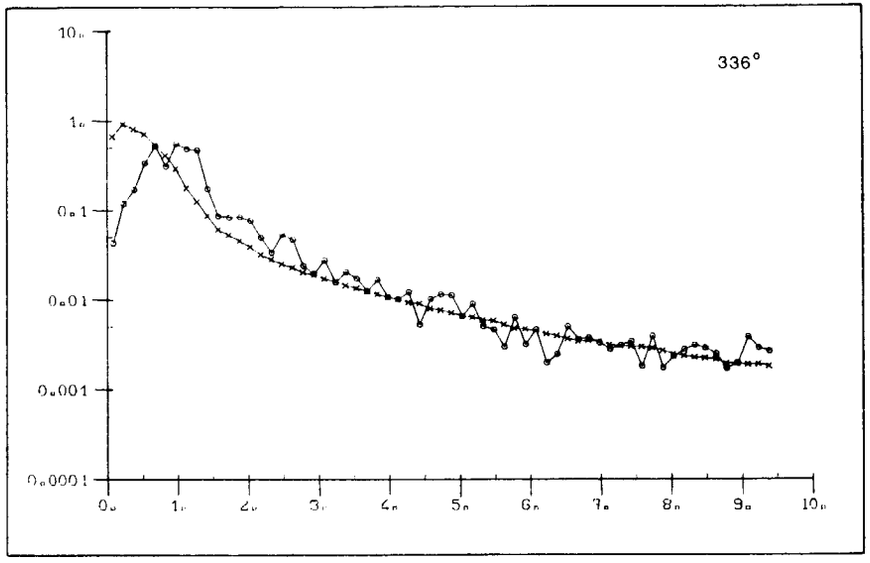

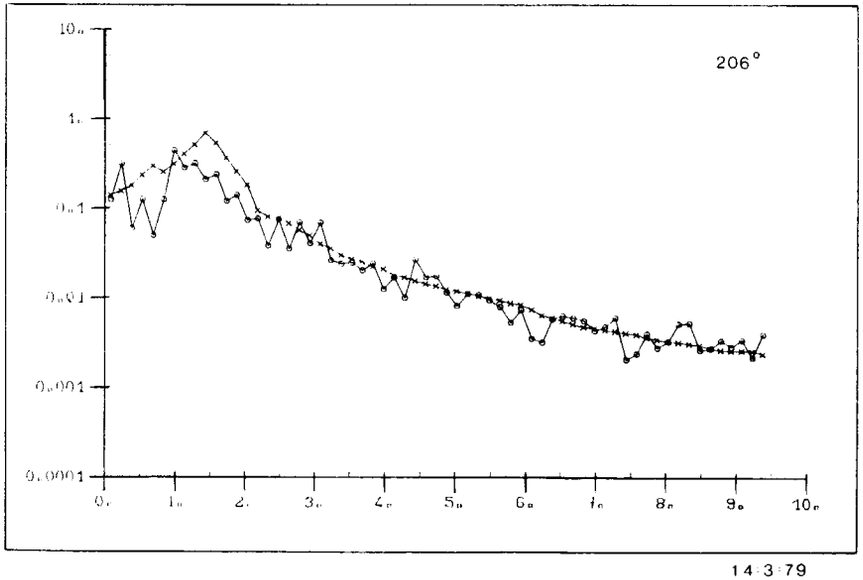

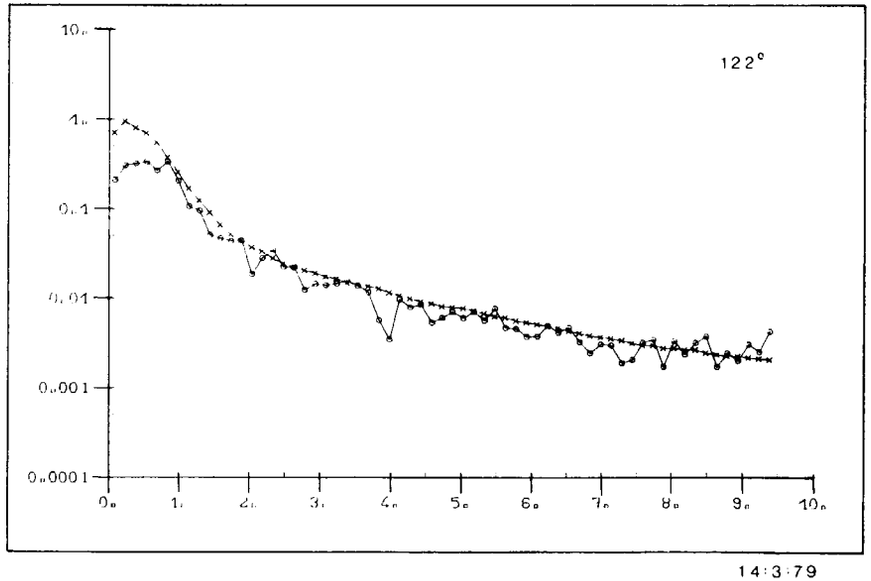

Figure E.3-4 Comparison of predicted and measured encounter spectra (details as figure E.1)

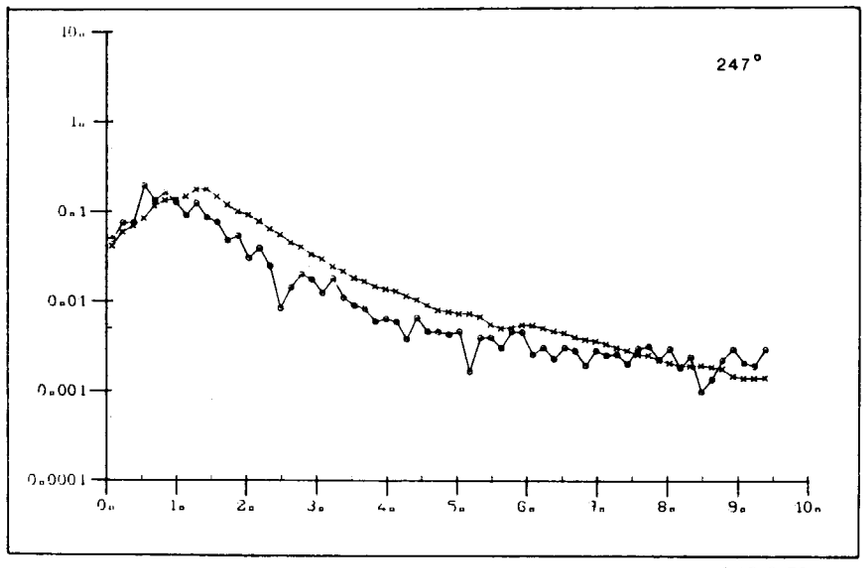

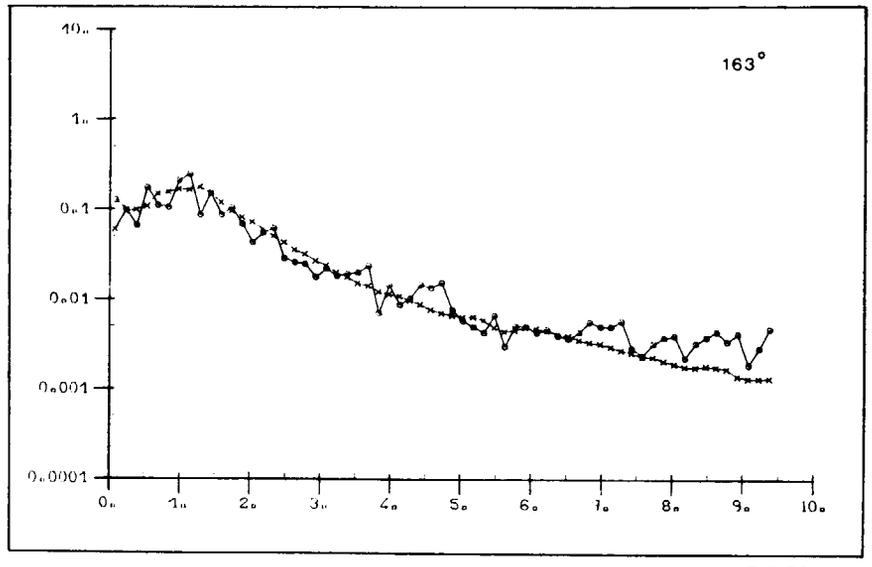

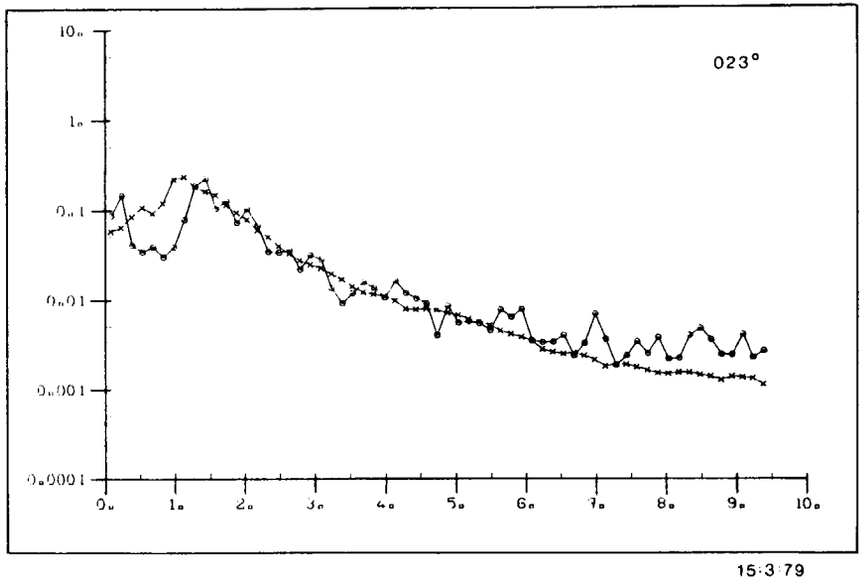

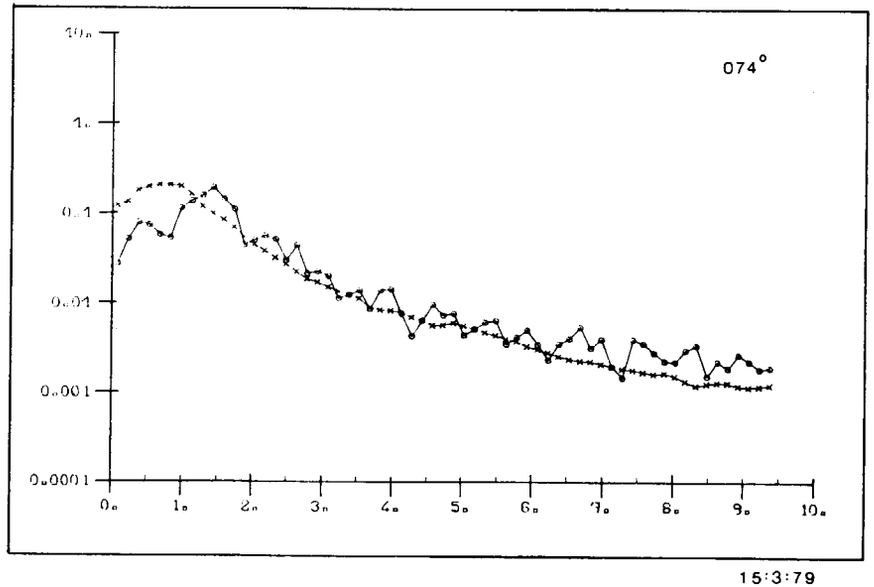

Figure E.5-6 Comparison of predicted and measured encounter spectra (details as figure E.1)

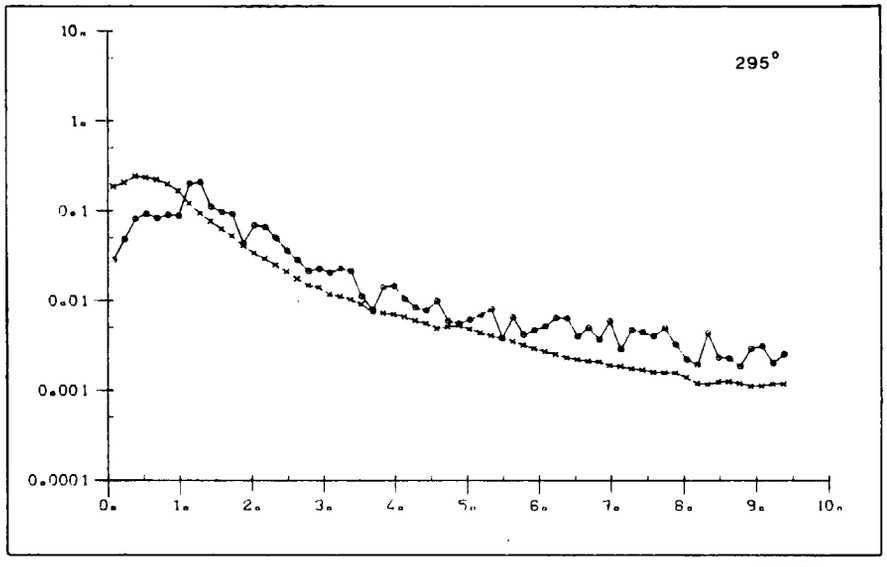

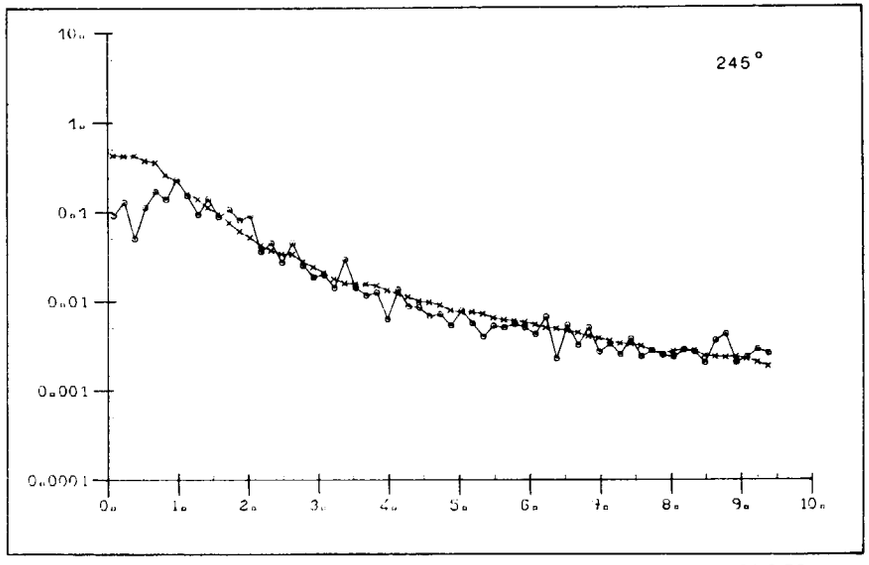

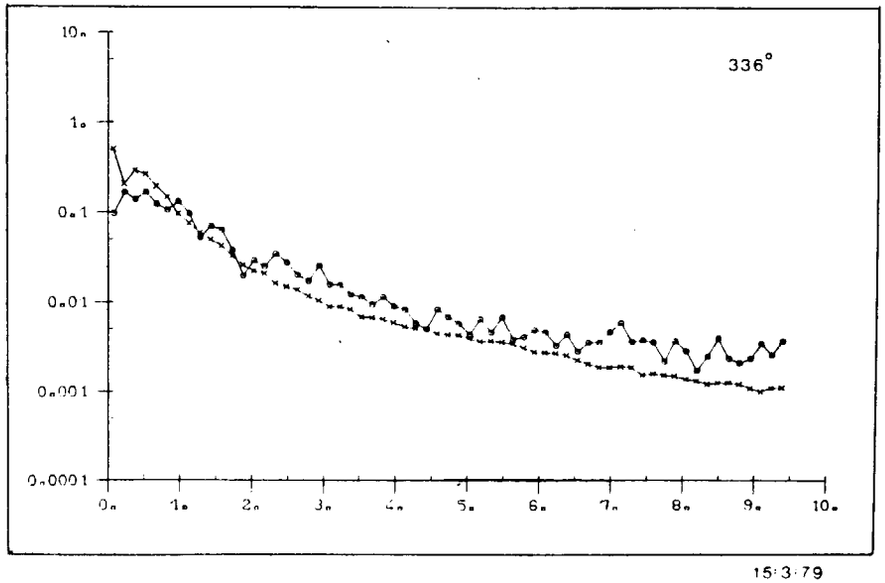

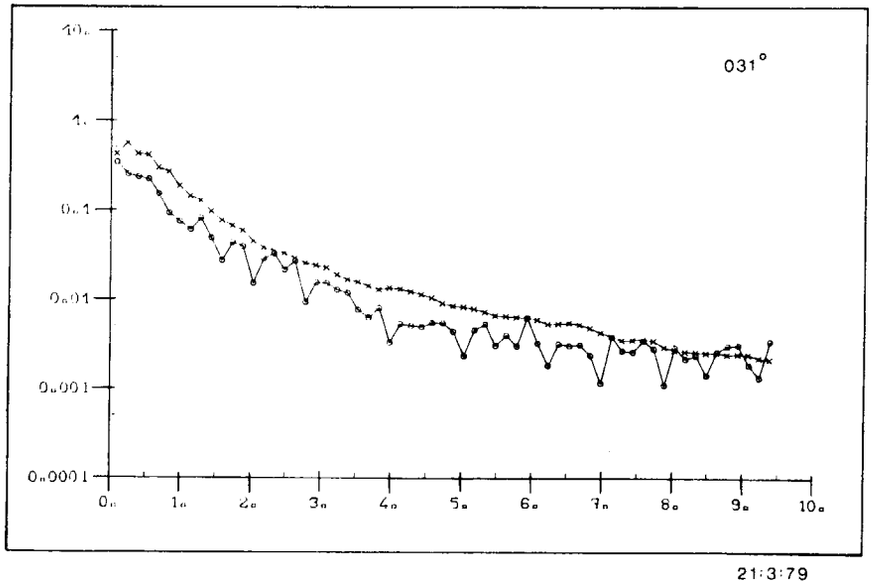

Figure E.7-8 Comparison of predicted and measured encounter spectra (details as figure E.1)

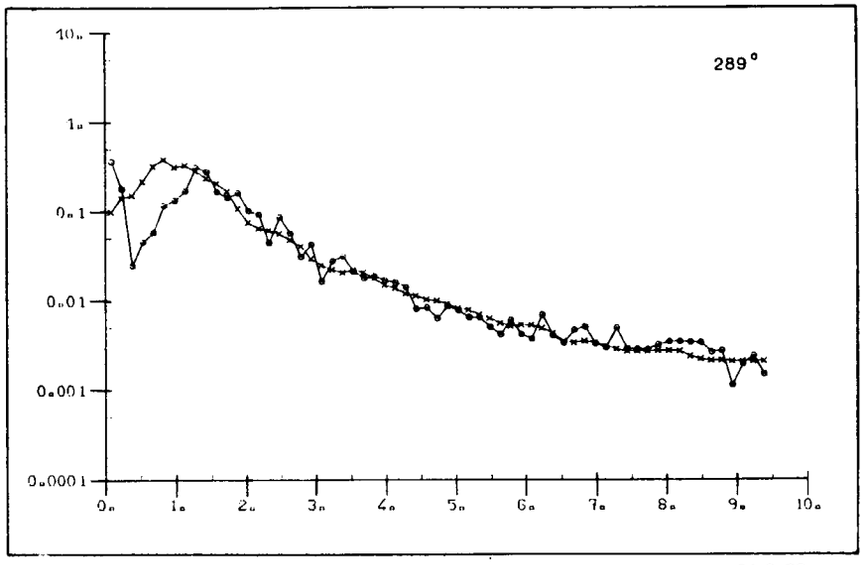

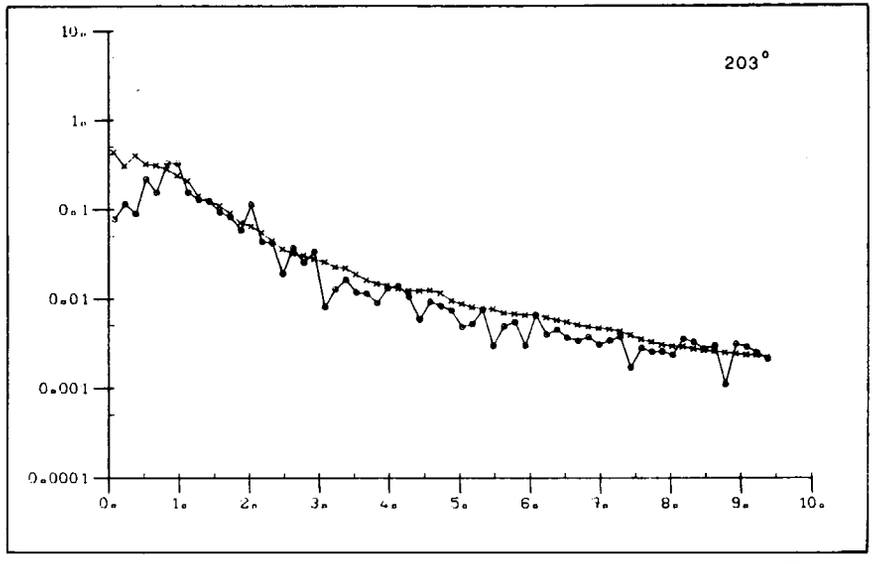

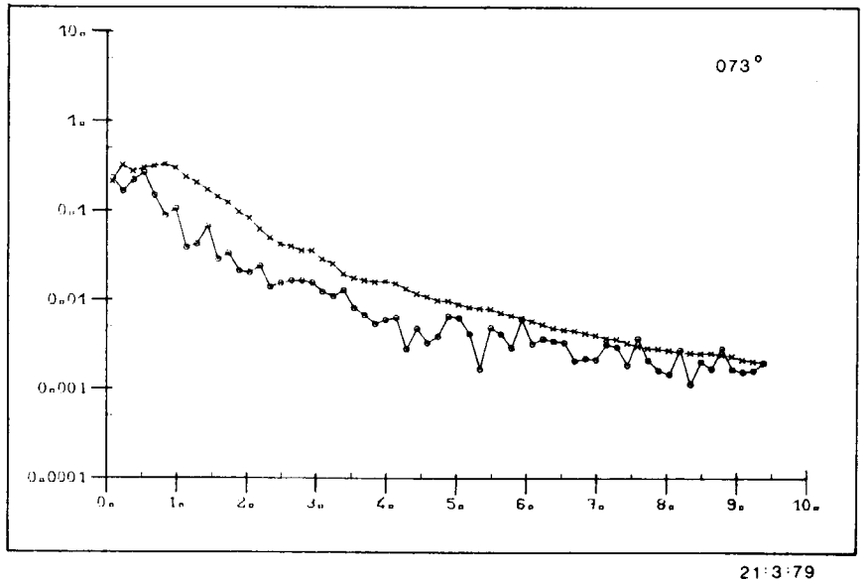

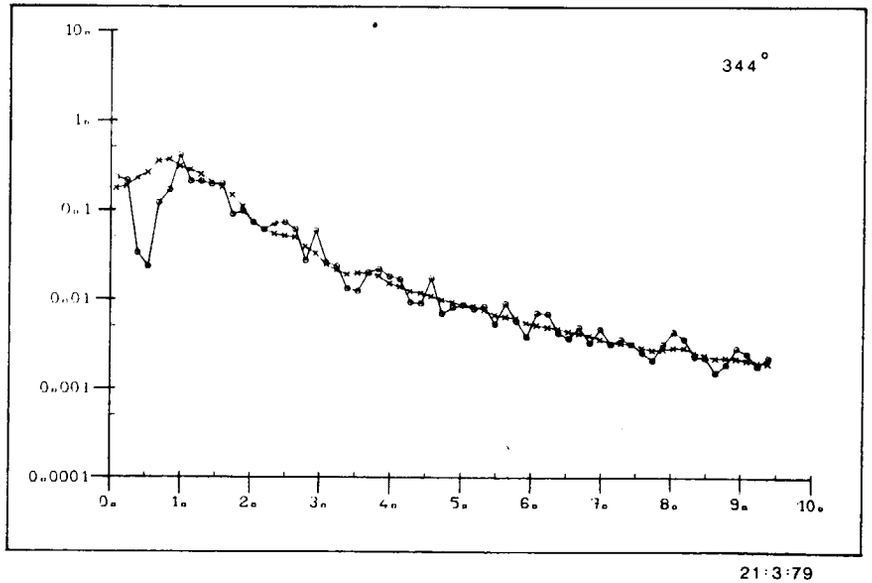

Figure E.9-10 Comparison of predicted and measured encounter spectra (details as figure E.1)

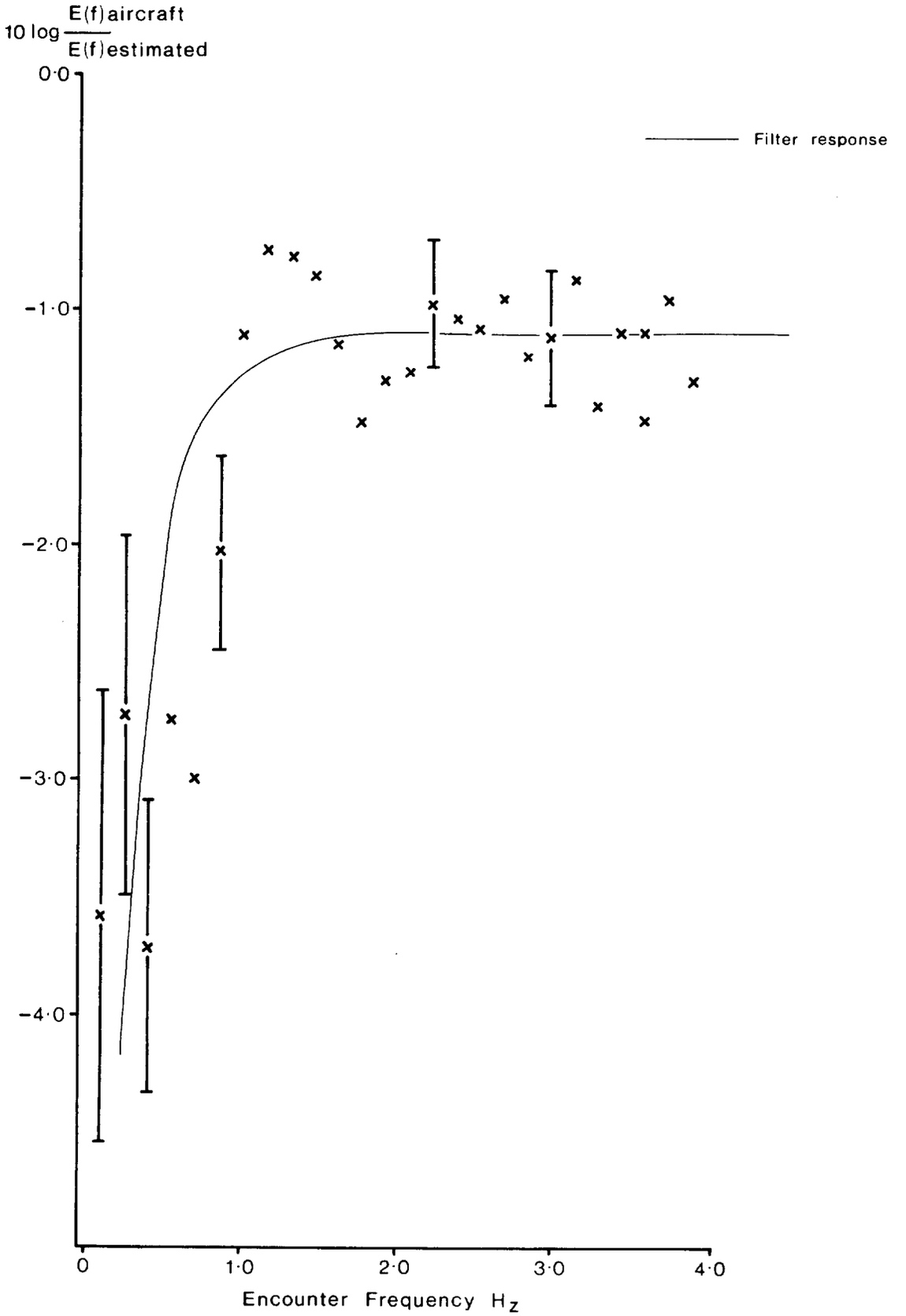

Figure E.11 Average ratio (dB) of encounter spectral densities derived from aircraft measurements to those derived from the estimated directional spectra. Some typical standard error bars are shown.

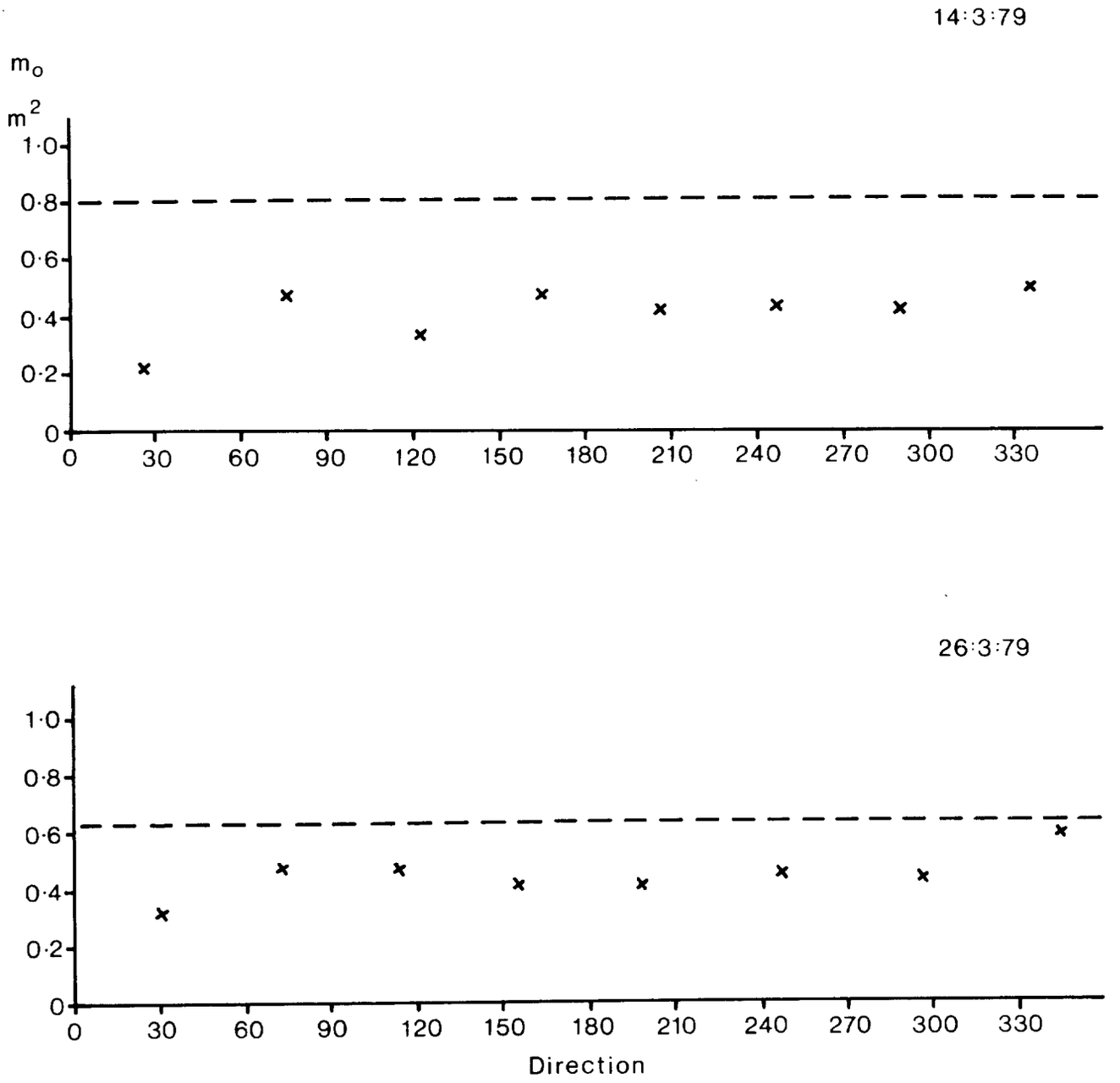

Figure E.12 Mean square wave height (m_o) measured on each aircraft run (x) compared with m_o measured at the same time by the Waverider (----).

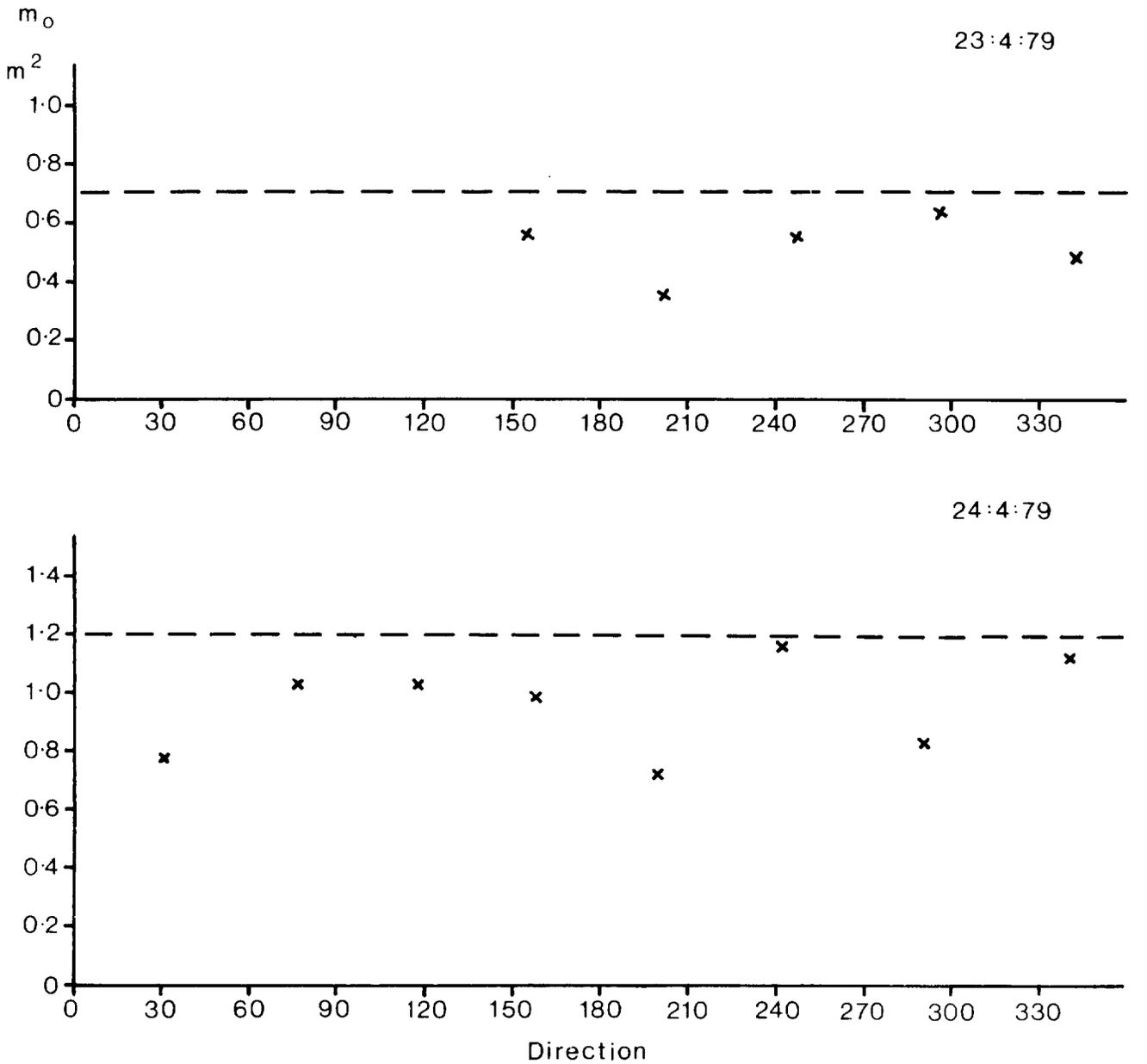

Figure E.13 Mean square wave height (m_o) measured on each aircraft run (x) compared with m_o measured at the same time by the Waverider (----).

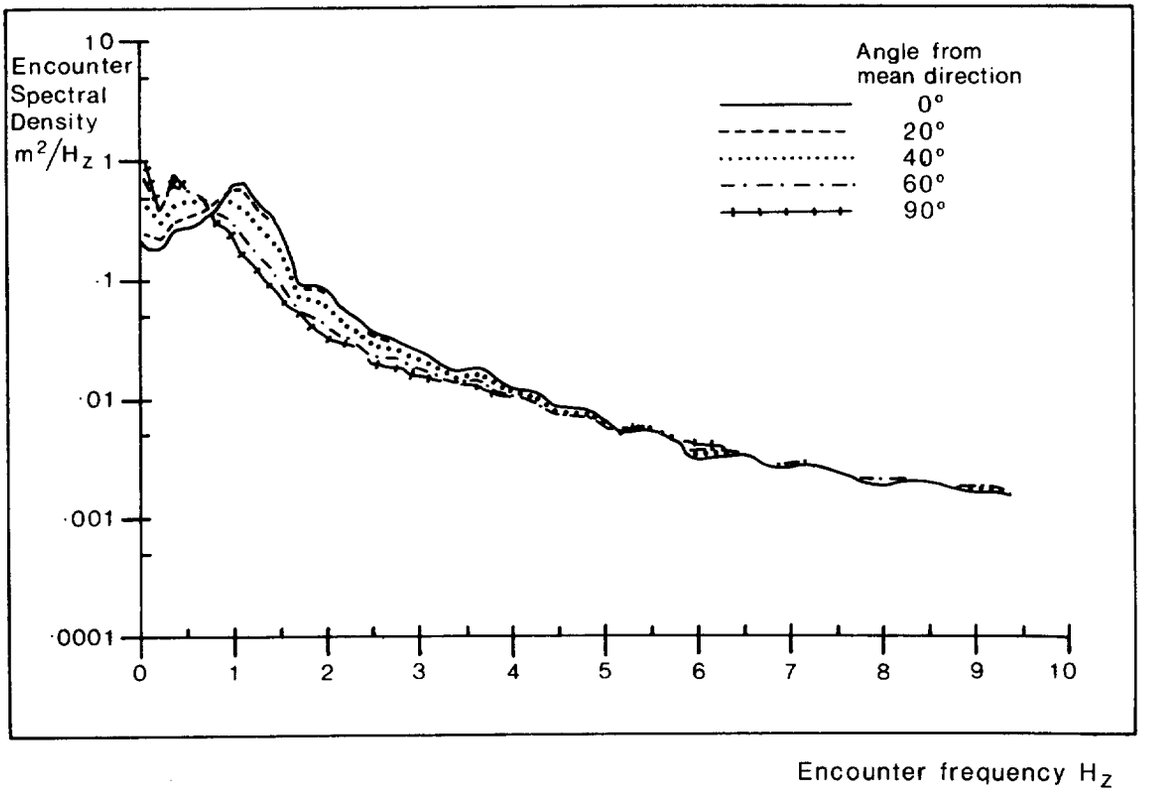

Figure E.14 Encounter spectra calculated at various angles from mean direction to show effect on spectral shape of errors in estimating mean direction.

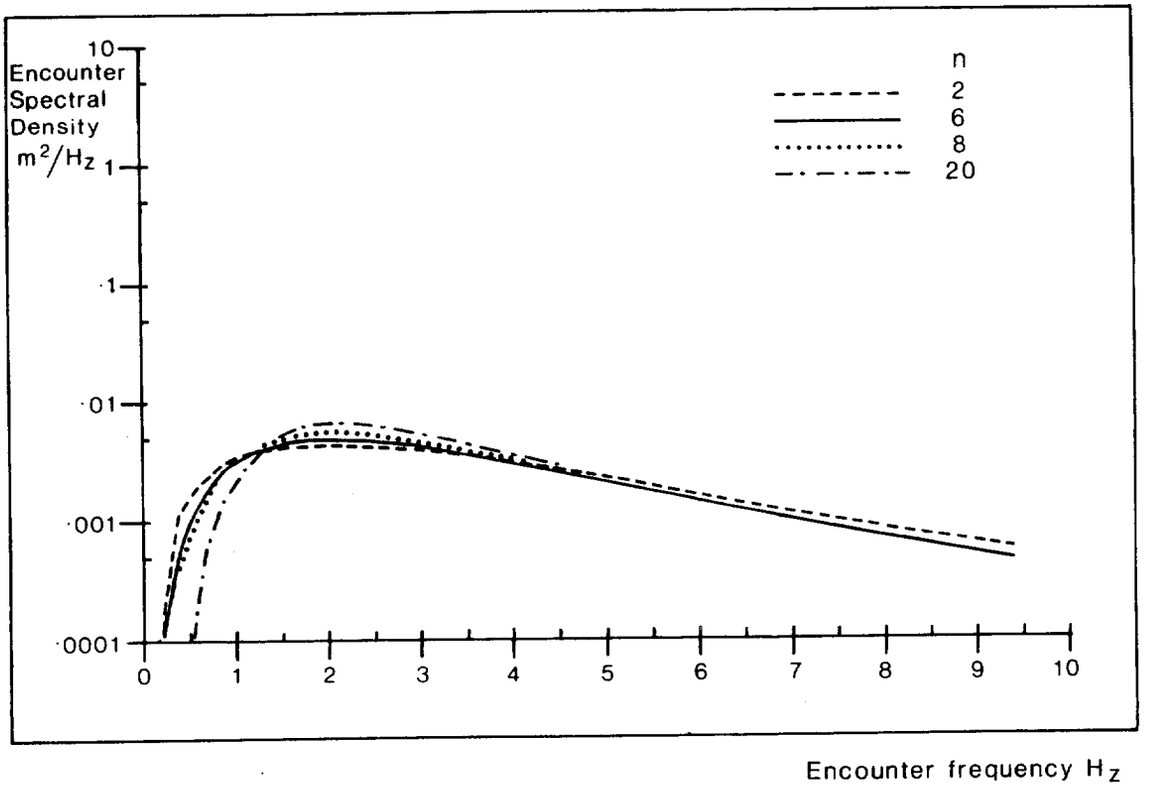

Figure E.15 Encounter spectra at 60° mean direction derived from a model directional spectrum with various values of spreading index n to show effect of errors in estimating n.

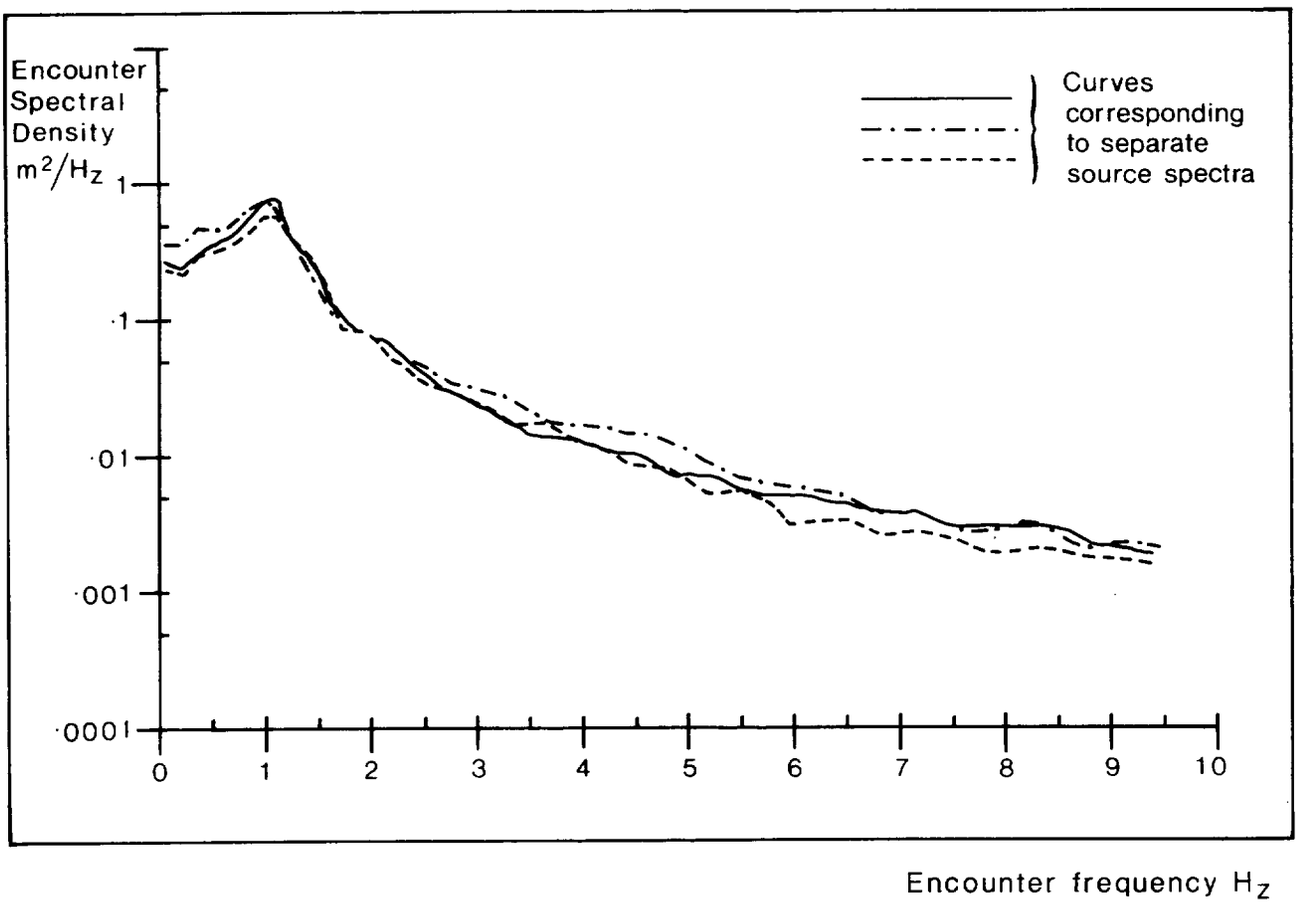

Figure E.16 Encounter spectra at 60° to mean direction derived from consecutive 1024 second Waverider records.

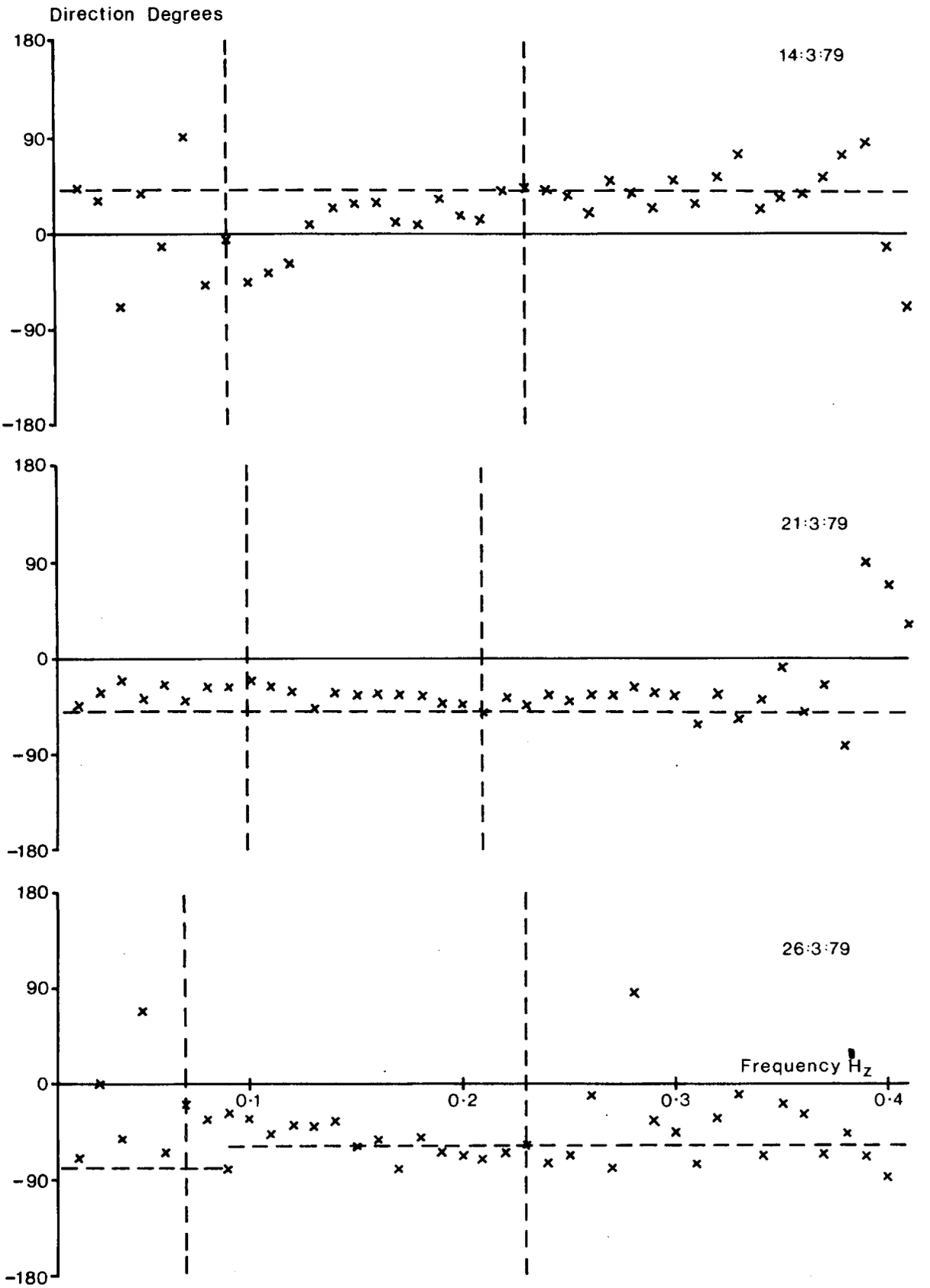

Figure E.17 Mean wave directions (x) at each frequency measured by DB1 compared with mean directions estimated at the Scilly Isles Buoy (----). Vertical dashed lines demark region of significant spectral energy.

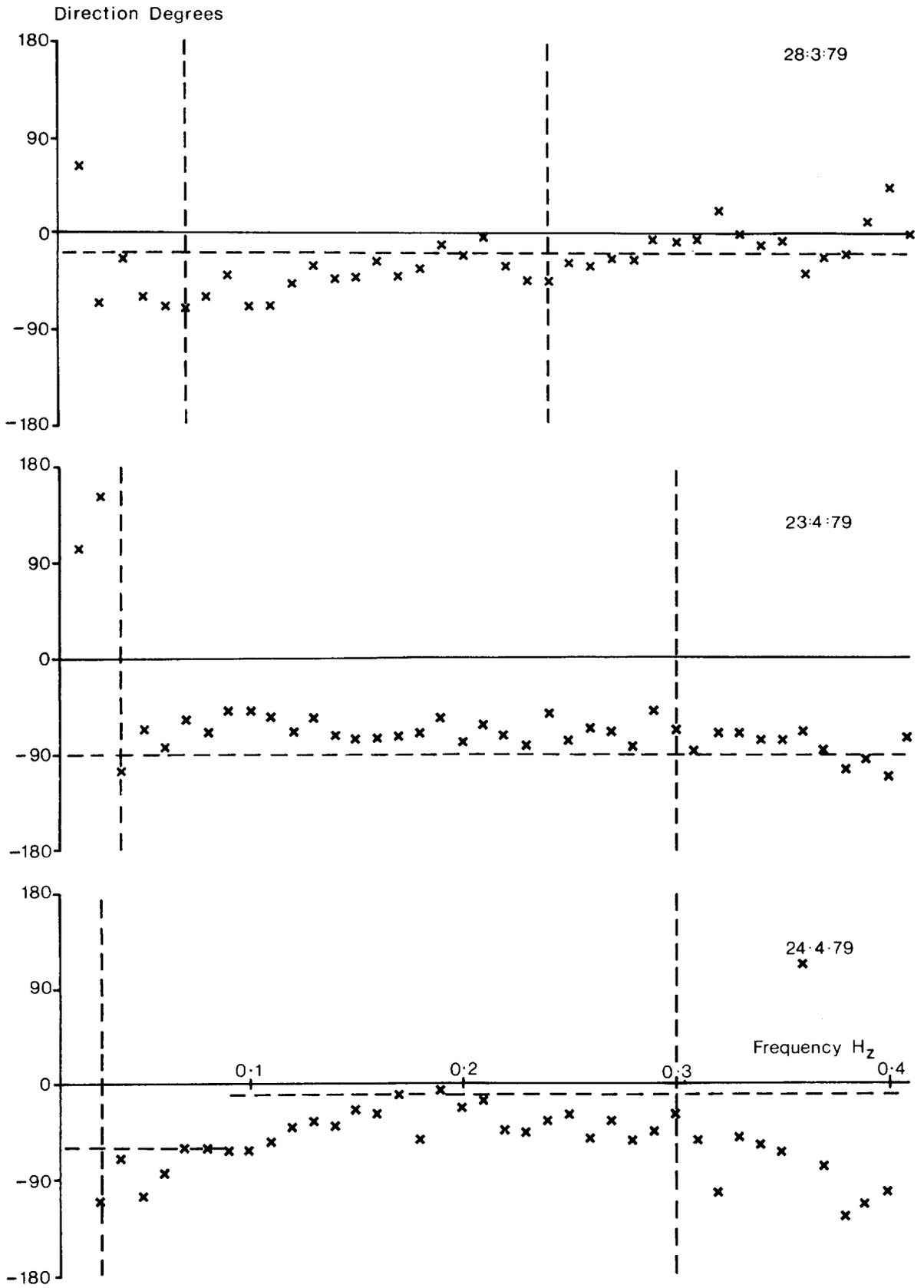

Figure E.18 Mean wave directions (x) at each frequency measured by DB1 compared with mean directions estimated at the Scilly Isles Buoy (----). Vertical dashed lines demark region of significant spectral energy.

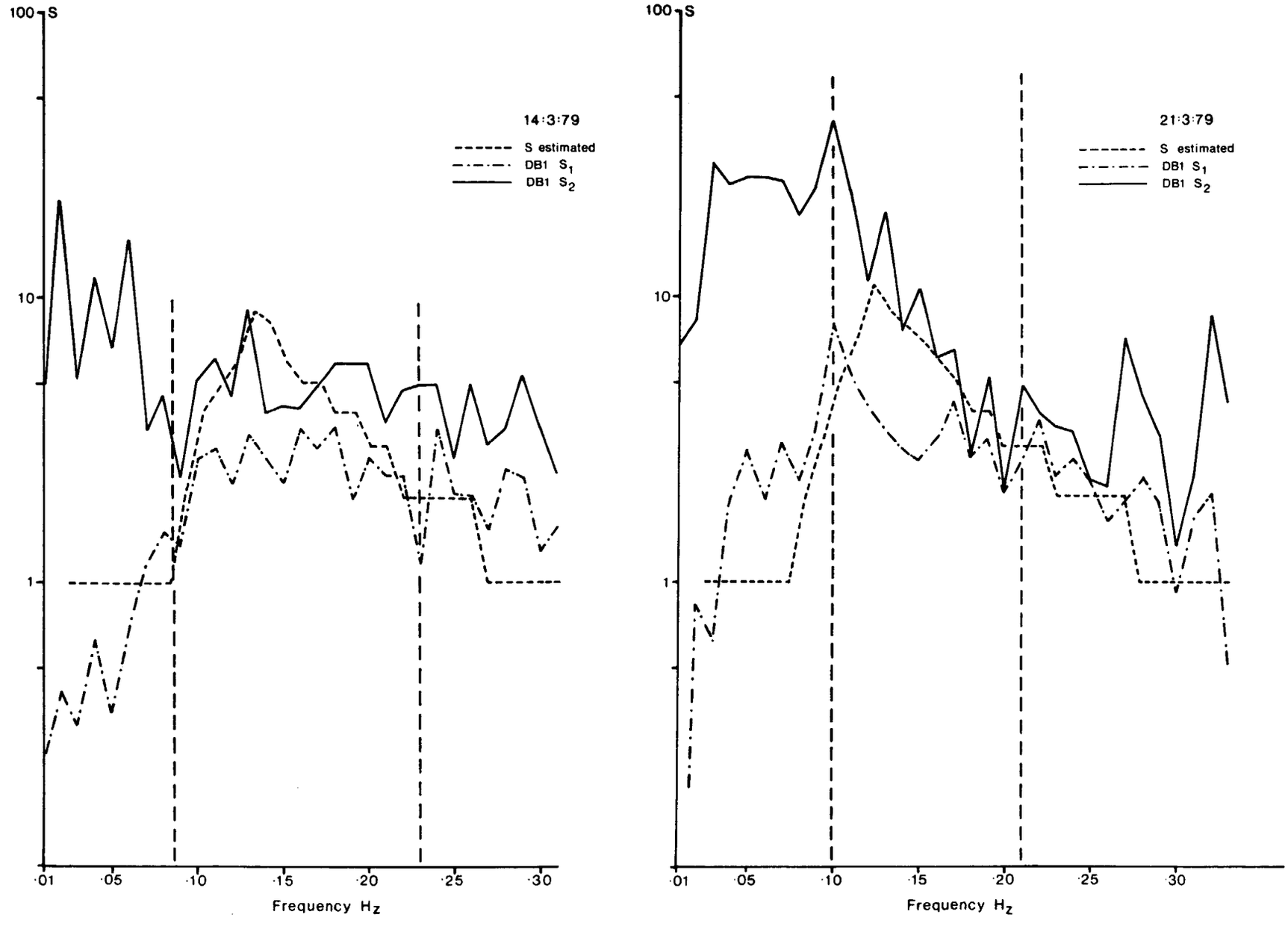

Figures E.19-E.20 Estimated angular spreading index S compared with S_1 and S_2 measured by DB1. Vertical dashed lines demark region of significant spectral energy.

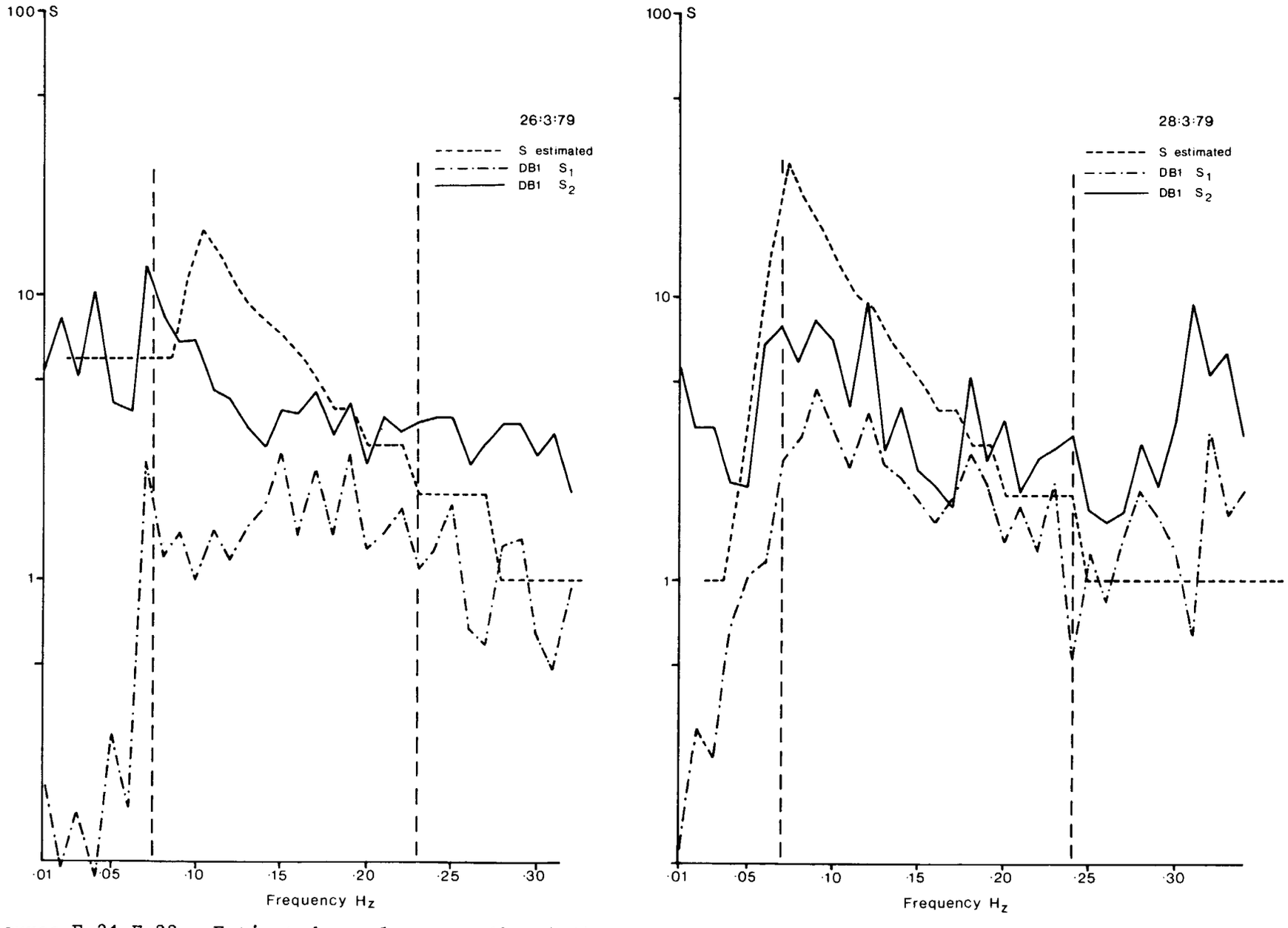

Figures E.21-E.22 Estimated angular spreading index S compared with S_1 and S_2 measured by DB1. Vertical dashed lines demark region of significant spectral energy.

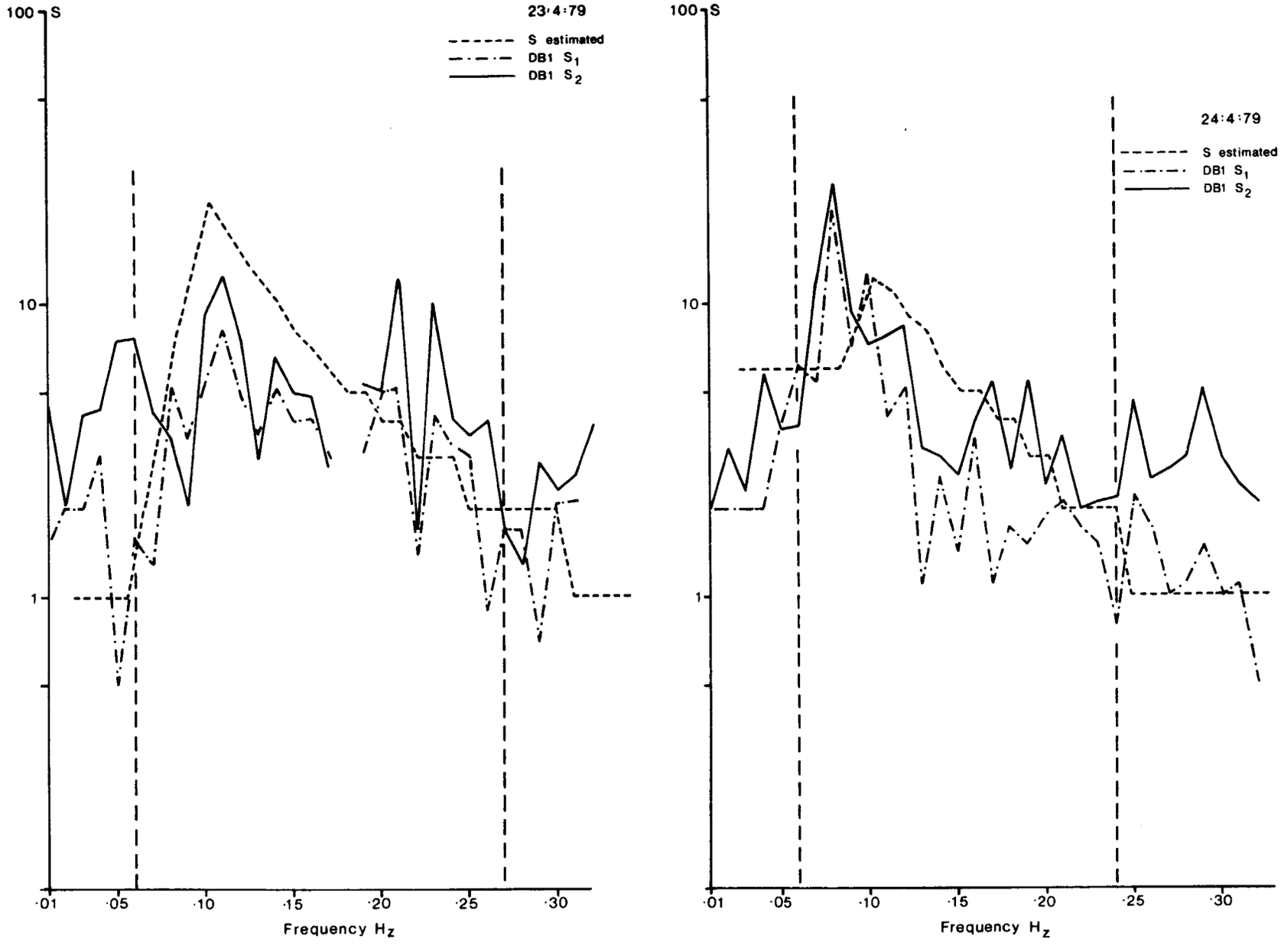

Figures E.23-E.24 Estimated angular spreading index S compared with S_1 and S_2 measured by DB1. Vertical dashed lines demark region of significant spectral energy.

APPENDIX F - Classification of the directional spectra and selection of a working subset

Values of each of the five parameters P, Te, FW, DW and DP (defined in Section 1e of the main report) were calculated for each spectrum and the spectra were sorted into classes according to the values of the three parameters DW, Te and FW. Within each of these classes the spectra were subdivided into classes of power. The spectra were not further subdivided by DP.

At this point it was apparent that the range of spectral types was too great to be adequately represented in a subset of some 40 spectra. Even by effectively excluding one of the parameters (DP) and using moderately broad class widths for the remainder, some 165 occupied classes resulted requiring a minimum of one spectrum to represent each.

The only practical way round this difficulty appeared to lie in setting a number of limited objectives and attempting to select spectra to satisfy these separately. The objectives defined were:

1. To produce a set of approximately 40 spectra covering as wide a range as possible of the three parameters DW, T_e and FW, whilst deliberately restricting the ranges of P and DP as described later.

2. To produce a set of approximately 40 spectra covering as wide a range as possible of the four parameters DW, T_e, FW and P associated with those spectra which contribute the bulk of the energy arriving at South Uist (DP again restricted).

The process whereby these spectra were selected is detailed in the following section.

It is hoped that the first set will allow device performance figures already established as functions of the non-directional parameters Hs and T_e to be extended to encompass a realistic range of spectral 'shapes' in both frequency and direction, and that the second set will allow a direct estimate of the annual productivity of each device to be made.

It has proved possible, by making the necessary compromises, to arrange a substantial overlap between the two sets, enabling both objectives to be realised with a total of 63 spectra.

Set 1

The 399 spectra were sorted according to the values of the three chosen parameters into the following classes:

DW - four classes

Class No	1	2	3	4
Degrees	30	60	90	>120

FW - four classes

Class No	1	2	3	4
Hz	<0.0294	0.0295 - 0.0587	0.0588 - 0.0881	>0.0882

T_e - five classes

Class No	1	2	3	4	5
Secs	<6.00	6.01-8.00	8.01-10.00	10.01-12.00	>12.01

For each range of DW all those spectra jointly occupying a given class of FW and T_e were listed along with the values of P and DP associated with each. The spectra so listed are the occupants of one cell of a frequency histogram in the three dimensions DW, FW and T_e. The average power of all the spectra in each occupied cell was calculated. One spectrum was then selected to represent each cell, subject to the additional constraints that

1. It should have a DP value of either 240° or 270° (75% of all the spectra fall in this range).

2. It should have a power close to the mean power for the cell.

A total of 38 spectra resulted from this procedure. The weight to be attached to each is determined by the population of the cell which it represents.

The three dimensional histogram is set out in Table F.1. This presentation is expanded in Crabb 1981 where the occupants of each of the 38 classes are listed by serial number with the values of each of the five parameters.

Set 2

Each cell of the DW, T_e, FW histogram was further subdivided into classes of power 10 kW m^{-1} wide; as previously mentioned this resulted in a total of 165 occupied classes. This number was reduced to 107 by regrouping the classes as follows:

Power - nine classes

Class No	1	2	3	4	5	6	7	8	9
kW m^{-1}	<10	10-30	30-50	50-70	70-90	90-110	110-200	200-300	>300

A further reduction was effected by restricting consideration to those conditions under which the majority of the total annual energy is transported to the site. The distribution of total energy with Hs and T_e, Figure F.1, marked with approximate power contours, was inspected and those sea states which contribute relatively little to the total energy were identified and excluded.

The following categories of sea state are consequently not represented in Set 2 (the percentage of the total annual energy thereby excluded is marked against each category).

Excluded classes are those with:

Power < 10 kW m^{-1} (excludes 2.4% of total energy)
Power > 300 kW m^{-1} (" 8.5% " " ")
T_e < 7 seconds (" 0.7% " " ")
T_e > 12.5 seconds (" 0.8% " " ")

as well as spectra with unusual combinations of P, FW, DW and T_e (ie classes in the four dimensional histogram occupied by one spectrum only). A further 11.1% of the total energy was associated with such spectra.

By this means it was possible to reduce the number of occupied classes to 46. The spectrum selected to represent each had a power as close as possible to the mean power of the class and a DP value of either 240° or 270°. The 46 spectra selected represent 267 of the original 399 synthesized spectra and, as shown above, these spectra account for 76.5% of the total energy in the set and thus, by projection, of the total energy arriving at the site. When each of the 46 spectra is weighted according to the number in the class which it represents, the set has

an average power of 55.2 kW m^{-1}.

It is envisaged that the use of this set will allow the annual productivity of a device to be estimated. The weighted average power output of a device run against this set expressed as a fraction of the 55.2 kW m^{-1} available, is a direct estimate of the device efficiency over this range of conditions and thus determines what portion of the 76.5% of the total annual energy represented may be retrieved. The ability of the device to capture power in those conditions excluded from the set, and which account for the remaining 23.5% of the annual energy, must be estimated separately. This may be effected by considering the device performance as established against Sets 1 and 2 in conjunction with the statistics of the excluded sea states presented in Table F.2.

Formal justification for the selection procedure

The 399 spectra of the selected set are taken to be representative of the 2920 spectra which might be recorded in an average year. Each spectrum of the selected set therefore represents approximately 7 spectra in the hypothetical whole year set or, alternatively, each spectrum is representative of conditions which would be experienced for 1/399 of the year, ie 21.95 hours.

The distribution of the selected set properties is thus a coarser representation of the supposed annual distribution.

If the ith spectrum has a power Pi, then the average power of the selected set is

$$\bar{P}_{399} = \frac{\sum_{i=1}^{399} P_i}{399} \qquad \text{F.1}$$

The result of this calculation is 47.8 kW m^{-1} and this is taken to be the mean power which would be measured over the average year.

The total energy arriving at the site per metre of wavefront is therefore estimated as

$$E_A = 47.8 \times 365 \times 24$$
$$= 418{,}728 \text{ kWh } m^{-1} \qquad \text{F.2}$$

Now consider the selection of a smaller number of spectra (Set 2) for the purpose of estimating device productivity. As explained in the text, a number of spectra were excluded at the outset leaving 267 which then represent the range of conditions supposed to occur for 267/399 of the year. The average power of this set

$$\bar{P}_{267} = \frac{\sum_{i=1}^{267} P_i}{267} \qquad \text{F.3}$$

was 54.5 kW m^{-1}. The total energy in one year associated with such conditions is then

$$Ep = 54.5 \times \frac{267}{399} \times 365 \times 24$$

$$= 319{,}476 \text{ kWh } m^{-1} \qquad \text{F.4}$$

$$= 0.763 \times E_A \qquad \text{F.5}$$

As previously described the 267 spectra were divided into classes according to the values of DW, T_e, FW and P associated with each. One spectrum was chosen to represent the n_j spectra in the jth class. The mean power of the spectra in the jth class is

$$\bar{P}_j = \frac{\sum_{l=1}^{n_j} P_{l,j}}{n_j} \qquad \text{F.6}$$

where $P_{l,j}$ is the power of the lth spectrum in the jth class.

The chosen spectrum has a power, P_j, as close as possible to $\bar{P}_j$. A total of 46 classes were represented in this way.

The weighted average power of the set of 46 (Set 2) is

$$\bar{P}_2 = \frac{\sum_{j=1}^{46} P_j \times n_j}{\sum_{j=1}^{46} n_j} \triangleq \frac{\sum_{j=1}^{46} \bar{P}_j \times n_j}{\sum_{j=1}^{46} n_j} \qquad \text{F.7}$$

using D.6 and D.3

$$\bar{P}_2 \simeq \frac{\sum_{j=1}^{46} \sum_{l=1}^{n_j} P_{l,j}}{\sum_{j=1}^{46} n_j} = \frac{\sum_{i=1}^{267} P_i}{267} = 54.5 \text{ kW m}^{-1}$$

Thus the weighted average power of Set 2 (55.2 kW m^{-1}) is approximately equal to that of the set of 267 which they represent. Consequently they represent the same portion, Ep, of the total annual energy.

It is envisaged that the output power of a device in all 46 selected spectra will be determined. If the output power for the jth spectrum is Poj, the weighted average output power for the set is

$$\bar{P}_O = \frac{\sum_{j=1}^{46} P_{oj} \times n_j}{\sum_{j=1}^{46} n_j}$$

and the overall efficiency of the device in this range of conditions is

$$\epsilon = \frac{\bar{P}o}{\bar{P}_2}$$

The productivity of the device during the 267/399 of the year in which these conditions prevail is thus estimated to be

$$Eo = \epsilon \times 0.763 \times E_A \text{ kWh m}^{-1}$$

This is one element of the final productivity figure. The productivity of a device under conditions excluded from the set needs to be determined separately and the resulting energy added to Eo. Approximately half of the excluded power has, however, been excluded on the grounds of being associated with very high or very low power sea states, and the rest of the excluded power is associated with a wide range of spectral types. It may thus, as a first approximation, be permissible to assume that the device efficiency under these conditions is substantially the same as that established for Set 2, and that the annual productivity is simply

$$E = \epsilon \times E_A \text{ kWh m}^{-1}$$

Summary of Appendix F

The starting point for the present work was the set of 399 directional wave spectra which are themselves estimates of the probable directional wave conditions at South Uist. It was originally intended that these spectra would serve in the early stages of the Wave Energy Programme in view of the lack of any other more reliable data. It had been expected that they would, sooner rather than later, be superseded by measured directional data. There is still no immediate prospect of this occurring and it appears probable that a crucial evaluation of individual devices will be undertaken on the basis of the spectra described here. There must be reservations about proceding on this basis.

Given, however, that there is no other reasonable way forward, it is encouraging to note that in those respects where it has been possible to test the respresentative nature of the 399, no serious shortcoming has come to light. Furthermore, although the 399 were seen as a temporary expedient, no conscious compromise on precision was made in the method of their synthesis.

Definite compromises have however been made in the attempts, described here, to further condense the information which they contain. The results presented here have been produced in response to strong pressures arising solely out of practical considerations, and their presentation does not imply that the estimated range of wave conditions at South Uist is sufficiently narrow that it can be adequately represented by a few 'typical' spectra.

Whilst the spectra listed here have been selected by reasonable and well-defined criteria, and as such cover a fairly wide range of conditions against which it is reasonable to check device performance - particularly for comparative purposes - no attempt has been made to cover those conditions which might result in extreme responses from particular devices. The systematic investigation of device performance in 'extreme' conditions must be outside this test set, and it should be borne in mind that the 399 themselves cannot cover the whole range of wave conditions likely at South Uist.

TE \ FW	CLASS NUMBER 1	2	3	4
CLASS NUMBER 1		3	1	
2	4	7	4	
3	15	8		
4	9			
5				

DW CLASS 1

TE \ FW	CLASS NUMBER 1	2	3	4
CLASS NUMBER 1		2	2	
2	28	41	5	
3	56	12	1	
4	30	2		
5	18			

DW CLASS 2

TE \ FW	CLASS NUMBER 1	2	3	4
CLASS NUMBER 1		2		2
2	12	15	2	
3	20	6		
4	18			
5	2			

DW CLASS 3

TE \ FW	CLASS NUMBER 1	2	3	4
CLASS NUMBER 1		1	1	2
2	5	26	4	
3	20	4		
4	8			
5	1			

DW CLASS 4

Distribution of the 399 synthesized directional spectra with the three parameters DW, FW and TE.

Numbers tatulated are total number of spectra in each class.

TABLE F.1

STATISTICS OF SEA STATES EXCLUDED FROM SET 2

NUMBER OF SPECTRA EXCLUDED	CLASS NUMBER IN EACH PARAMETER				NUMBER OF SPECTRA EXCLUDED	CLASS NUMBER IN EACH PARAMETER			
	DW	FW	TE	P		DW	FW	TE	P
3	1	2	1	1	2	3	2	1	1
1	1	3	1	1	2	3	4	1	1
4	1	2	2	1	6	3	1	2	1
4	1	3	2	1	8	3	2	2	1
1	1	1	3	1	1	3	3	2	1
1	1	1	3	4	1	3	3	2	2
1	1	1	3	5	1	3	1	3	1
1	1	2	3	4	1	3	1	3	7
1	1	1	4	4	1	3	2	3	1
1	1	1	4	5	1	3	2	3	2
1	1	1	4	8	1	3	2	3	3
					1	3	2	3	7
2	2	2	1	1	1	3	1	4	2
2	2	3	1	1	1	3	1	4	3
4	2	1	2	1	1	3	1	4	9
11	2	2	2	1					
1	2	2	2	4	1	4	2	1	1
1	2	3	2	1	1	4	3	1	1
4	2	3	2	2	2	4	4	1	1
9	2	1	3	1	2	4	1	2	1
4	2	2	3	1	1	4	1	2	3
1	2	2	3	4	10	4	2	2	1
1	2	3	3	1	1	4	2	2	4
1	2	1	4	8	1	4	3	2	3
1	2	2	4	2	3	4	1	3	1
1	2	2	4	7	1	4	2	3	1
1	2	1	5	1	1	4	2	3	2
1	2	1	5	2	1	4	2	3	3
2	2	1	5	4	1	4	2	3	5
1	2	1	5	6	2	4	1	4	1
1	2	1	5	8	2	4	1	4	9
					1	4	1	5	9

TABLE F.2

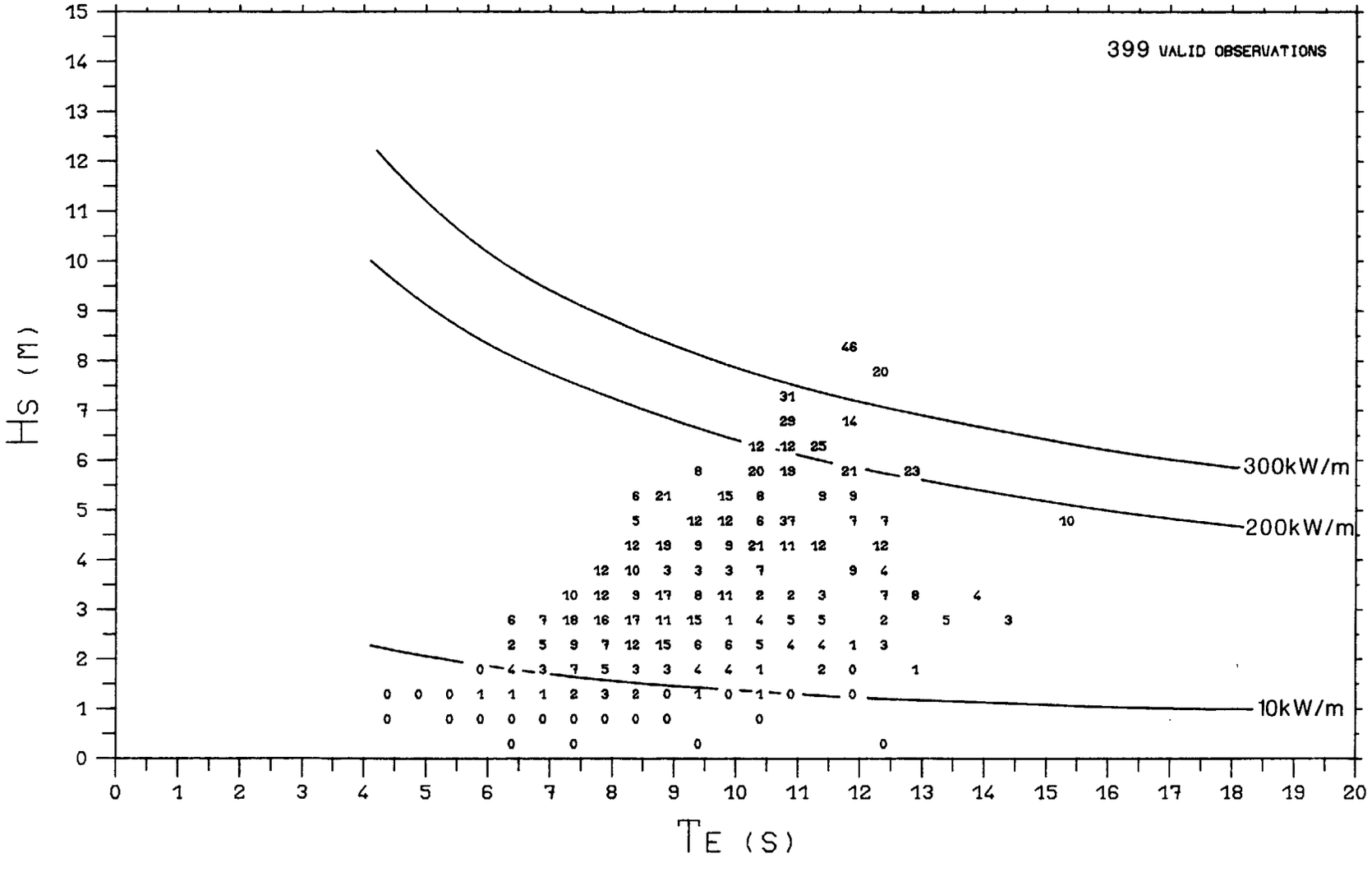

Figure F.1 South Uist selected set. Distribution of total measured wave energy with Hs and Te (parts per thousand).

APPENDIX G

Results based on wave data collected at UKOOA sponsored sites are reported separately in this appendix.

Comparison of long term average powers at Foula (discussion delayed from Section 2a)

Data collected during 1977 and 1978 have been used previously to predict the long term annual average power at this site. The procedure employed was essentially the same as that employed at South Uist, in which a subset of representative wave spectra were chosen from the data series. The method is fully described and discussed in Appendix C.

A value of 45.5 kW m^{-1} was obtained, with a correction of approximately +2 kW m^{-1} being necessary to allow for the effects of missing data.

As noted in Table 3, it was unfortunately not possible to establish the relationship between measured and Met Office model data at this site, due to there being insufficient overlap in the data time series. Thus the only other estimate of long term average power is the figure of 54.89 kW m^{-1} obtained as a straight average of the Met Office model powers.

Discussion of DB1 measured data

The results of the regression analysis performed on the measured DB1 powers and those calculated from the Met Office data are set out below in an extension to Table 2.

No of data points	slope b	intercept a	correlation coefficient	s.e.in b	s.e.in a kW m^{-1}
500	0.655	12.0	0.763	0.025	2.04

When applied to the four year average model power of 56.92 kW/m reported in Table 3, the resulting prediction for the four year average measured value is

49.28 kW m^{-1} with a standard error ± 1.24 kW m^{-1}

This figure exceeds that obtained for the Scilly Isles site by 9%.

As well as recording wave height, the DB1 buoy measured the angles of pitch and

roll experienced, thus allowing some information on wave direction to be deduced. In the discussion that follows the DB1 data have been used to derive the form of the distribution of power with direction on the assumption that, at each frequency, the distribution is unimodal and symmetric. In particular the model

$$E(\theta) \quad \alpha \cos^{2s}\left(\frac{\theta - \bar{\theta}}{2}\right)$$

is employed.

Whilst this is the usual method of interpreting pitch-roll measurements in terms of direction, it has distinct limitations. Most significant of these is the assumption of a symmetric distribution.

The average distribution of power with direction, derived on this basis, is presented in Figure G.1. The previously presented distribution derived from the Met Office model data is also reproduced here for comparison. In this figure the values of measured power have been scaled so that the two curves contain the same area; thus aiding the visual comparison.

The directionality factor calculated from the measured data is 0.56 compared with the value of 0.74 obtained from the model data.

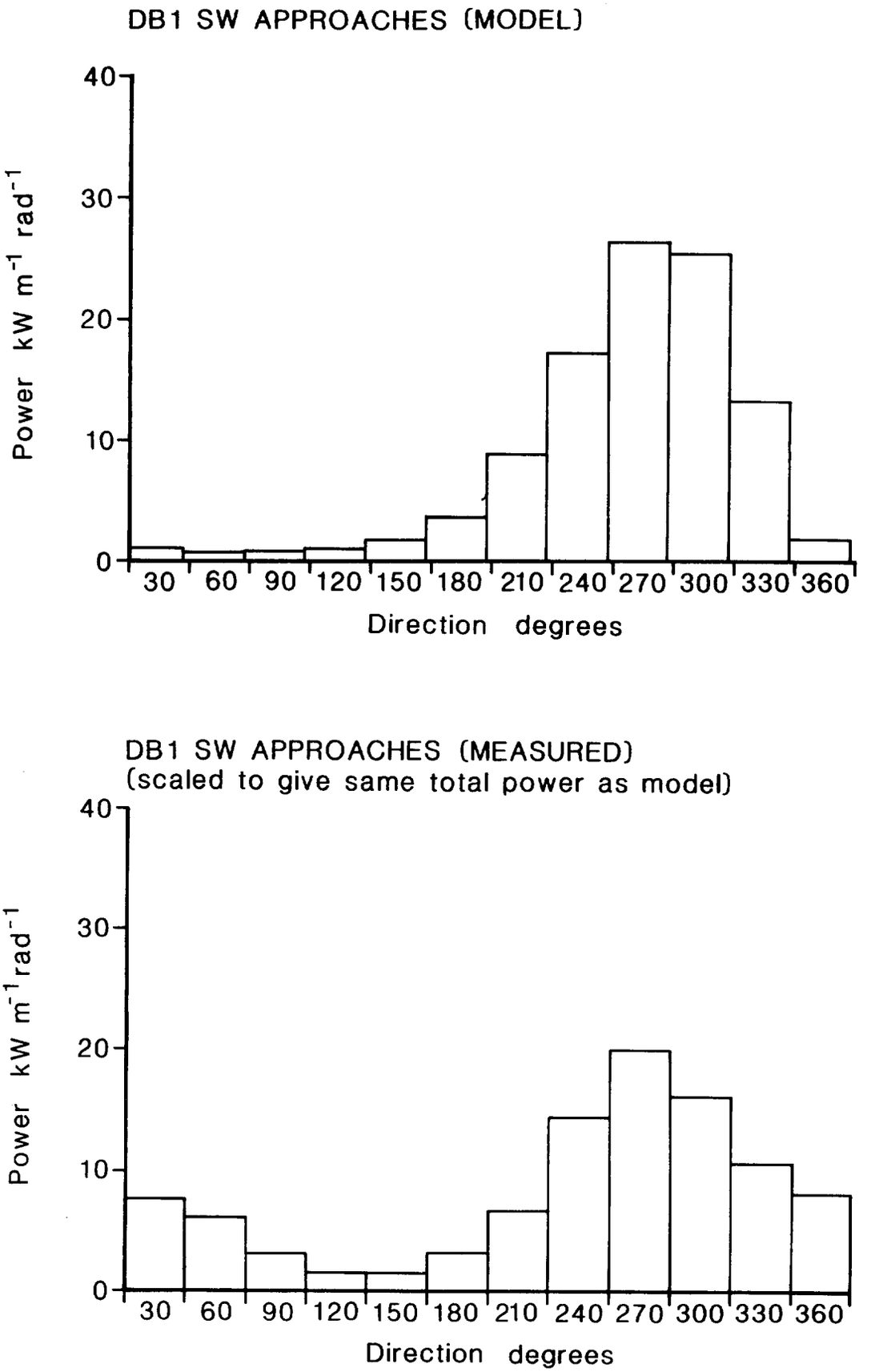

Figure G.1 Distribution of power with direction for the DB1 location. Meteorological Office wave model and measured results.

REFERENCES

Note Documents referenced by WESC serial number are held by the Energy Technology Support Unit, AERE, HARWELL, Oxfordshire, OX11 0RA.

BRAMPTON, A H and BELLAMY, P H, 1982. Study of wave spectra transformation. Hydraulics Research Station report No EX1063, 28 pp.

CARTWRIGHT , D E, 1963. The use of directional spectra in studying the output of a wave recorder on a moving ship. Pp 203-218 in Ocean Wave Spectra. Prentice-Hall N J.

CARTWRIGHT, D E, DRIVER, J S and TRANTER, J E, 1977. Swell waves at Saint Helena related to distant storms. Quarterly Journal of the Royal Meteorological Society, 103, (438), 655-683.

CRABB, J A, 1978. Selected wave records and one-dimensional spectra for South Uist. WESC(78)DA48.

CRABB, J A, 1979. Wave power levels to the west of the Outer Hebrides. WESC(78)DA64b.

CRABB, J A, 1980. An investigation into the reliability of the procedure used to estimate the directional wave climate at South Uist. WESC(80)DA105.

CRABB, J A, 1981. Selected directional wave spectra for use in the assessment of wave energy convertor performance. WESC(81)DA127.

CRISP, G N, 1980. Selected wave records and one-dimensional wave spectra for St Gowan. WESC(80)DA112.

EWING, J A, 1980. Observations of wind-waves and swell at an exposed coastal location. Estuarine and Coastal Marine Science 10 No 5.

EWING, J A and PITT, E G, 1982. Measurements of the directional wave spectrum off South Uist. Wave and Wind directionality: applications to the design of structures. Proceedings of International Conference on ....., Editions Technip, 47-65.

FORTNUM, B C H, HUMPHERY, J D and PITT, E G, 1979. Contoured wave data off South Uist. Institute of Oceanographic Sciences Report No 71.

GOLDING, B W, 1978. A depth dependent wave model for operational forecasting, 593-606, in Turbulent fluxes through the sea surface, wave dynamics and prediction, Edited by A Favre, and K Hasselmann, New York: Plenum Press.

HAMMOND, D L and McCLAIN, L R, 1980. Spectral distortion inherent in airborne profilometer measurements of ocean wave heights. Ocean Engineering 7 pp 99-108.

HOGBEN, N, 1978. Wave climate synthesis for engineering purposes. National Maritime Institute Report NMI R45, 37 pp.

INOUE, T, 1967. On the growth of the spectrum of a wind generated sea according to a modified Miles-Phillips mechanism and its application to wave forecasting, New York University, Physical Sciences Laboratory Report TR-67-5.

LONGUET-HIGGINS, M S, 1957. The statistical analysis of a random moving surface. Philosophical Transactions of the Royal Society A 249, 321-387.

LONGUET-HIGGINS, M S, CARTWRIGHT, D E and SMITH, N D, 1963. Observations of the directional spectrum of sea waves using the motions of a floating buoy, in Ocean Wave Spectra, Prentice-Hall, 1963, Proceedings of a Conference held Easton, Maryland 1961, 111-135.

MACHIN, A C, 1974. Sea wave spectra derived from airborne Radio Altimeter measurements. Royal Aircraft Establishment Technical Memo GW(NEW) 1001.

MITSUYASU, H, TASAI, F, SUHARA, T, MIZUNO, S, OHKUSO, M, HONDA, T and RIKIISHI, K, 1975. Observations of the directional spectrum of ocean waves using a clover leaf buoy, Journal of Physical Oceanography, 5, 750-760.

MOLLISON, D, BUNEMAN, O P and SALTER, S M, 1976. Wave power availability in the NE Atlantic. Nature 263, 223-226.

MOLLISON, D, 1977. Estimation of long term wave power averages using wind data. Edinburgh Wave power report No 47. WESC(77)DA33.

MOLLISON, D, 1979. South Uist as a standard wave power site. WESC(79)DA82.

MOLLISON, D, 1982. Comments on (Brampton and Bellamy 1982). WESC(82)DA147.

MUNK, W H, MILLER, G R, SNODGRASS, F E and BARBER, N F, 1963. Directional recording of swell from distant storms, Philosophical Transactions of the Royal Society, A, 255, 505-584.

PITT, E G and SCOTT, M T G, 1982. A preliminary study of the effect of the direction of waves at South Uist on the relative power levels at the offshore and inshore sites. WESC(82)DA142.

PORE, N A and RICHARDSON, W D, 1969. Second interim report on sea and swell forecasting, US Weather Bureau, Technical Memorandum No TDL-17.

SALMOND, D J, 1979. Sea profile estimation by Kalman filtering. Royal Aircraft Establishment Technical memo AW34

SALTER, S M, 1974. Wave power. Nature 249 720-724.

SCOTT, M A and CRABB, J A, 1981. An estimate of the one-dimensional spectral wave climate west of the Shetland Isles. WESC(81)DA125.

SHORE PROTECTION MANUAL, 1977, in Shore Protection Manual, Volume 1, Fort Belvoir, Virginia: US Army Coastal Engineering Research Center, 3-27.

SILVESTER, R, 1974, in Coastal Engineering, 1, Amsterdam Elsevier, 98.

SNODGRASS, F E, GROVES, G W, HASSELMANN, K F, MILLER, G R, MUNK, W H and POWERS, W H, 1966. Propagation of ocean swells across the Pacific, Philosophical Transactions of the Royal Society, A, 259, (1103), 431-497.

YOUNG, M R A, 1979. Sea state measurement from an airborne altimeter and a Waverider buoy in an area west of the Isles of Scilly. Flight Refuelling Ltd, Wimborne, Dorset, Report MS/ENG/MRAY/P.9/18.